

Laboratory Investigation into Soundless Chemical Demolition Agents for Rock Breakage in Underground Mines

Kelly-Meriam Habib

Department of Mining and Materials Engineering

McGill University, Montreal, QC, Canada



February 2019

Thesis submitted to McGill University in partial fulfillment of the requirements of the degree of

Master of Science

© Kelly-Meriam Habib 2019

Abstract

The method of drilling and blasting with explosives is widely used in the mining industry for mine development and ore production. However, the use of explosives is associated with rigorous safety and environmental constraints as blasting creates toxic fumes, ground vibrations and dust. The following study is conducted on Soundless, Explosive-Free Chemical Demolition Agents (SCDAs), a more environmentally friendly method for the fragmentation of rock as a potential replacement of explosives. SCDAs are powdery materials similar to Portland cement, which when mixed as a slurry and poured into blind drilled holes, an expansive pressure is produced upon curing and eventually breaks the material apart. Given that SCDAs are commercially available, there is proof of workability in civil engineering applications for the breakage of concrete foundations. SCDAs are commonly used in the demolition of concrete foundations as well as in stone quarries where the use of explosives is either restricted or prohibited. An interest is drawn towards SCDAs due to its environmental advantages which mitigate the risk of explosives. This study is a step in investigating its workability in hard rock mine development and production where the rock is subjected to high in-situ confinement pressure which would make rock breakage cumbersome.

A drawback of the SCDAs is that the time needed to develop the full expansive pressure is too long for practical mine development applications. The primary goal of the study is to accelerate the expansion rate of SCDAs as one of the steps towards development of a feasible method of rock breakage in underground mines. The SCDA used in this investigation is Betonamit, a commercially available expansive cement. The experimental investigation was conducted in the Rockbolting Lab of the Mine Design Laboratory. This study is an extension of the work previously conducted by Musunnuri & Mitri (2009) and Dessouki & Mitri (2011) in the Mine Design Laboratory of McGill University.

The factors investigated are: the expansive pressure, expansive pressure rate, and fractural growth on concrete blocks. The effect of chemical additives on expansive pressure is investigated with the goal to reduce the time of expansion. Common concrete accelerators including calcium chloride, sodium chloride, calcium formate, and sodium were investigated.

Résumé

Le forage et dynamitage avec explosifs est largement utilisé dans l'industrie minière pour le développement minier et la production de minerai. Par contre, l'utilisation des explosifs est associée à des contraintes rigoureuses de sécurité et d'environnement tel qui crée de la fumée toxique, de la vibration au sol et de la poussière. Cette recherche est basée sur le ciment expansif comme un remplacement plus écologique parmi les méthodes conventionnelles de fragmentation des roches. Le ciment expansif est un matériau en poudre similaire au ciment de Portland qui lorsqu'il est mélangé sous forme de suspension et versés dans des trous forés, produisent une pression expansive lors du durcissement et brise le matériel environnant. De plus, il existe une preuve de maniabilité dans les applications de génie civil sur la fondation de béton. Le ciment expansif est souvent dans la démolition de fondation de béton ainsi que dans les carrières de pierre où l'utilisation d'explosifs est restreinte ou interdit. Le ciment expansif présente un intérêt en raison de leurs avantages environnementaux qui atténuent le risque d'explosifs. Cette étude est une étape dans l'étude de son ouvrabilité dans le développement et la production de d'une mine de roche dure où la roche est soumise à une haute pression de confinement in situ rend la rupture de roche encombrante. Un inconvénient est que le temps nécessaire pour développer la pression expansive complète prend trop de temps pour des applications pratiques de développement minier. L'objectif principal de l'étude est d'accélérer le taux d'expansion du ciment expansif pour en faire une méthode réalisable de rupture de roche dans les mines souterraines. Le ciment expansif utilisé dans cette enquête est le Betonamit, un ciment expansif disponible dans le commerce.

L'investigation expérimentale a été menée dans le laboratoire Rock Bolting du Mine Design Laboratory à l'Université de McGill. Cette étude est une extension des travaux menés précédemment par (Musunnuri & Mitri, 2009 et Dessouki et Mitri, 2011) dans le Mine Design Laboratory à l'Université de McGill. Les facteurs étudiés sont la pression expansive, le taux expansif et la propagation fracturaire sur des blocs de béton. L'effet de divers additifs chimiques sur la pression expansive est testé pour réduire le temps d'expansion. Les accélérateurs de béton courants, y compris le chlorure de calcium, le chlorure de sodium, le formiate de calcium ont été étudiés.

Acknowledgments

I would like to first and foremost thank my thesis supervisor Prof. Hani Mitri of the Department of Mining and Materials Engineering at McGill. I am sincerely thankful for his constant support, professional advice and guidance which enabled me to complete this investigation successfully. My project was financially supported by National Sciences and Engineering Research Council of Canada (NSERC) which I greatly appreciate. I would also like to thank Louis Laroche, Technician in the Rockbolting Lab, and John Bartczak, Technician in the Structural Engineering Lab of the Department of Civil Engineering, for their technical assistance. Finally, special thanks to all my colleagues in the Mine Design Lab for their cooperation and friendship.

Contributions of the author

The author performed each experiment and reported the results as is.

Table of Contents

Abstract.....	II
Résumé.....	III
Acknowledgments.....	IV
Contributions of the author.....	V
Chapter 1.....	12
Introduction.....	12
1.1 Background to soundless chemical demolition agents.....	12
1.2 Scope and objectives.....	12
1.3 Thesis structure.....	13
Chapter 2.....	14
Literature Review.....	14
2.1 Introduction.....	14
2.2 Potential alternative to blasting.....	14
2.3 SCDAs overview.....	15
2.4 Procedure for the use of SCDAs.....	17
2.5 Applications.....	17
2.6 Commercially available expansive cement.....	17
2.7 Chemical Composition SCDAs.....	18
2.8 Mechanism for the generation of expansive stress.....	22
2.9 Volumetric expansion theories.....	23
2.10 Factors affecting the expansive rate in SCDAs.....	28
2.11 Analysis Tools.....	33
2.12 Chemical Admixtures.....	35
2.13 Previous related work.....	38
2.15 Conclusion.....	45
Chapter 3.....	46
Experimental Program.....	46
3.1 Introduction.....	46
3.2 Specimens.....	47
3.3 Admixtures.....	47

3.4 Equipment.....	48
3.5 Experimental Procedure	49
3.5 Specimen Preparation	51
Chapter 4.....	56
Experimental Results	56
4.1 Introduction	56
4.3 Discussion.....	63
Chapter 5.....	76
Conclusion	76
5.1 Experiment Results.....	76
5.2 Future Testing.....	77
References.....	78
Appendix I : Table of Data Findings	83
Appendix II: Qualitative Results	98

List of Figures

Figure 2-1: Volume change in shrinkage compensating cement, self-stressing cement and Portland cement (Taylor, 1997)	15
Figure 2-2: Fractural Propagation in a borehole (Harada, 1989).....	16
Figure 2-3: Hexagonal ettringite crystal structure (Heikal, 2004).....	23
Figure 2-4: Proposed expansion mechanism of Type K paste (Shallom,1974).....	25
Figure 2-5: Proposed mechanism for unrestrained Type K cement (Cohen,1983)	26
Figure 2-6: Electronic microscopic images of ettringite crystals (Mehta, 1973)	27
Figure 2-7: Effect of different water: cement on expansive pressure (Hinze & Brown, 1994)	29
Figure 2-8: Effect of borehole on expansive pressure (Hinze & Brown, 1994).....	30
Figure 2-9: Effect on ambient temperature on expansive pressure (Natanzi et al.)	31
Figure 2-10: Effect of temperature on expansion (Natanzi et al, 2016) & (Harada et al, 1994).....	31
Figure 2-11: Schematic configuration for the testing of expansive cement in a hollow cylinder (Hinze & Brown, 1994)	33
Figure 2-12: Effect of Sodium Chloride BWOW on curing time (Theodoriu & Assambla, 2015)	35
Figure 2-13: Compressive strength developed with increasing calcium chloride by weight of cement (BWOC) (Michaux et al. 1989)	36
Figure 2-14: Total porosity of Ordinary Portland Cement (Heikal, 2004).....	37
Figure 2-15: Ranya Granite block experiments (Labuz & Dowding, 1985)	39
Figure 2-16: Basic cracking (Gambatese,2003).....	40
Figure 2-17: Experimental set-up for testing SCDA in uniaxially loaded samples (Mitri and Musunuri, 2009)	43

Figure 2-18: Expansive cement under uniaxial loading (Mitri & Musunuri,2009).....	43
Figure 2-19: Expansive cement under free load (Mitri & Musunuri, 2009).....	43
Figure 2-20: Wellbore filled with SCDA parallel to the bedding plane (Guo et al,2009).....	44
Figure 2-21: Wellbore filled with SCDA perpendicular to the bedding plane (Guo et al.,2009)	44
Figure 3-1: Schematic configuration for the testing of Betonamit in a hollow thick- walled cylinder	46
Figure 3-2: Experimental set-up for the testing of SCDA a) Thick wall cylinder configuration b) P-3500 Strain indicator c) Connection for a quarter bridge	49
Figure 3-3: Concrete molds	50
Figure 3-4: Curing of concrete cubes in humid room	50
Figure 3-5: Concrete cube with demic points	51
Figure 3-6: UCS concrete samples	55
Figure 3-7: Brazilian concrete samples.....	55
Figure 4-1: Top view BET-Control-01a showing cracking pattern	60
Figure 4-2: Top view BET-Control-01b showing cracking pattern.....	60
Figure 4-3: Top view of BET- $\text{Ca}(\text{HCOO})_2$ -3%-02a showing cracking pattern	61
Figure 4-4: Top view of BET- $\text{Ca}(\text{HCOO})_2$ -3%-02b showing cracking pattern	61
Figure 4-5: Top view of BET- CaCl_2 -3%-03a showing cracking pattern	62
Figure 4-6: Top view of BET- CaCl_2 -3%-03b showing cracking pattern	63
Figure 4-7: Expansive pressure generated by pure SCDA (Betonamit).....	63
Figure 4-8: Expansive pressure generated by Betonamit and the addition of NaCl by weight of cement	64
Figure 4-9: Expansive pressure generated by Betonamit and the addition of Calcium chloride by weight of water.....	65

Figure 4-10: Pressure at 3 hours of various concentrations of CaCl_2 66

Figure 4-11: Pressure at 6 hours of various concentrations of CaCl_2 66

Figure 4-12: Expansive pressure generated by Betonamit and the addition of Calcium formate by weight of water..... 64

Figure 4-13: Pressure at 3 hours of various concentrations of $\text{Ca}(\text{HCOO})_2$ 65

Figure 4-14: Pressure at 6 hours of various concentrations of $\text{Ca}(\text{HCOO})_2$ 68

Figure 4-15: Expansive pressure of Betonamit + 3% of CaCl_2 BWOW and Betonamit +3% of $\text{Ca}(\text{HCOO})_2$ BWOC..... 69

Figure 4-16: BET-Control-01a crack growth over a period of 6 hours 70

Figure 4-17: BET-Control-01b crack growth over a period of 6 hours 71

Figure 4-18: BET-Calcium Formate-3%-02a crack growth over a period of 6 hours. 72

Figure 4-19: BET-Calcium Formate-3%-02b crack growth over a period of 6 hours. 72

Figure 4-20: BET-Calcium Chloride-3%-03a crack growth over a period of 6 hours. 73

Figure 4-21: BET-Calcium Chloride-3%-03b crack growth over a period of 6 hours. 74

List of Tables

Table 2-1: Performance of different commercially available SCDAs.....	18
Table 2-2: Percent constituents in Portland cement (Bye,1999)	19
Table 2-3: Major complexes in Portland cement.....	20
Table 2-4. Expansive pressure generated by Bristar-100S (Hanif,2007)	38
Table 3-1: Specimen Specifications of pure Betonamit	52
Table 3-2: Specimen Specifications with the addition of Sodium Chloride	52
Table 3-3: Specimen specifications with the addition of Calcium Chloride.....	53
Table 3-4: Specimen specifications with the addition of Calcium Formate.....	53
Table 3-5. Specimen specifications for Test #2.....	54
Table 4-1: Expansive pressure as a function of time	57
Table 4-2: Crack width of specimens at time of fracture initiation	59
Table 4-3: Crack width of specimens at 6 hours.....	59

Chapter 1

Introduction

1.1 Background to soundless chemical demolition agents

The conventional approach to demolish concrete structures or fragment a large structure into smaller blocks, for example the fragmentation of rock in underground mines, has typically included the use of explosive (Hinze & Brown, 1994). However, the use of explosives usually results in obvious safety and environmental risks. Due to those risks, there is a growing interest in transitioning from explosives-based rock fragmentation to rock fragmentation with Soundless, Explosive-Free Chemical Demolition Agents (SCDAs). SCDAs are a type of hydraulic cement which after mixing and curing in a confined borehole, exert significant internal pressure to break the material in which the borehole is made. Expansion is attributed to the chemical reaction that occurs during the moist curing process (Mather, 1970). SCDAs also known as expansive cement, have been commercially used as a substitute to explosives to break concrete. SCDAs are commonly used in the demolition of concrete foundations, in stone quarries where the use of explosives is restricted or prohibited. SCDAs are also used to fill steel tube to provide high strength, high ductility, and high stiffness (Hanif et al., 2017).

1.2 Scope and objectives

The novelty of this technology is owed to its environmentally safe advantages which mitigate the complications of explosive blasting. Such application would be well suited for the fracturing of rocks in underground mines. The knowledge gap lies in the SCDAs' workability in high in-situ stresses such as in underground mines.

The objectives of this investigation conducted in the Mine Design Lab are:

- 1) Test #1: Finding chemical admixtures to accelerate the expansion SCDAs to achieve the required expansive pressure to break hard rock
- 2) Test # 2: Assess the time and growth of fracture generation on concrete blocks using appropriate wt. % admixtures from results obtained in Test #1.

The experimental investigation was conducted in the Rockbolting Laboratory of the McGill Mine Design Laboratory. The experimental parameters investigated are expansive pressure, time of rock breakage and growth of fracture generated by the SCDA and the modified SCDA. Common accelerators are investigated in attempt of increasing the rate of expansive pressure and reduce the time of breakage.

1.3 Thesis structure

The thesis is divided in five chapters as follows. Chapter 1 is an introduction to the thesis topic and it highlights the scope and objectives of the study. Chapter 2 presents a comprehensive review of literature of SCDA and their applications, chemical compositions and the underlying expansion mechanisms. Chapter 3 describes the sample preparation and experimental procedure developed for this study. The results of the experiment are presented in Chapter 4. Pressure-time curves are obtained for all specimens in Test #1. Crack width- time graphs are presented to depict the fractural growth of the SCDA and modified SCDA. Results are analyzed considering the parameters affecting the expansive pressure and rate. Finally, Chapter 5 provides a summary of the conclusion's suggestions for future work

Chapter 2

Literature Review

2.1 Introduction

The purpose of this literature review is to provide an understanding of the chemical composition and physical behaviour of Soundless Chemical Demolition Agents (SCDAs) in preparation for enhancing its performance. The reviewed contents are the physical and chemical properties of SCDAs, physical mechanism of expansive stress, volumetric expansion mechanism, factors affecting expansive rate, effect chemical additives on expansive rate of SCDAs, and previous related work. Enhanced optimization of SCDAs is necessary to develop an applicable and feasible method for rock fragmentation in underground mines where high in situ stress is present.

2.2 Potential alternative to blasting

In the mining industry, blasting with explosives energy is an essential part of the mining cycle where rock is most conventionally fragmented by drilling and blasting. Commonly used explosives in the mining industry are ammonium nitrate fuel oil (ANFO), black powder, and to a lesser extent dynamite. Ammonium nitrate is an oxidizing agent that not only supplies oxygen to initiate and support combustion of the fuel, but it is also an explosive where on occasion ammonium nitrate can self-detonate posing a higher risk to workers. Certain rock types contain sulphide minerals, and these can react with ammonium nitrate - the primary ingredient in commercially available explosives (ANFO). Such rocks are commonly referred to as 'reactive ground'. These reactions have frequently led to fires or premature detonation of the ammonium nitrate-based explosives (AEISG Code of Practice, 2012). This brings about a serious safety hazard when using ammonium nitrate-based explosives in underground mines. Ideally, the gaseous detonation product of explosives would consist of water, carbon dioxide, and nitrogen. Due to kinetics of the chemical reaction, the detonation of explosives in a blasting operation also produces toxic nitrogen dioxide, nitric oxide and carbon monoxide (Farnfield et al., 2004). The danger lies in the release of these fumes in the gas remaining in the ground after the blast. These fumes have the potential to migrate hundreds of meters through the ground and collect in confined spaces, which can be released during subsequent blast loading operation thus posing serious health and safety risks (Özmen,2013).

Consequently, there is a great importance in developing a safe method to fracture rocks in underground mines when blasting is not the most desirable route for fracturing. SCDA, a soundless chemical demolition agent, is a cementitious powdery substance that expands upon contact with water resulting in high expansive pressure in a confined space such as in a borehole. This material volumetrically expands in the confined area over a period of several hours and produces destructive forces by generating expansion forces without producing shock waves. An attraction to SCDA is attributed to its environmentally friendly features which include the elimination of noise, fly rock, vibration and toxic fumes. Thus, SCDA can eliminate the drawbacks of blasting with explosives energy (Taylor, 1997).

2.3 SCDA's overview

SCDA also known as expansive cement can be divided into two categories shrinkage-compensating cement and a self-stressing cement where both contain Portland cement. Portland cement is the most common type of cement for general applications around the world as the basic ingredient in concrete. A common property of Portland cement is that upon setting of the cement, cracks may be created due loss of water; this results in a slight loss of volume or shrinkage. As shown in Figure 2-1, shrinkage-compensating cement can counteract such shrinkage by expanding just enough to offset the shrinkage thereby preventing cracks from forming.

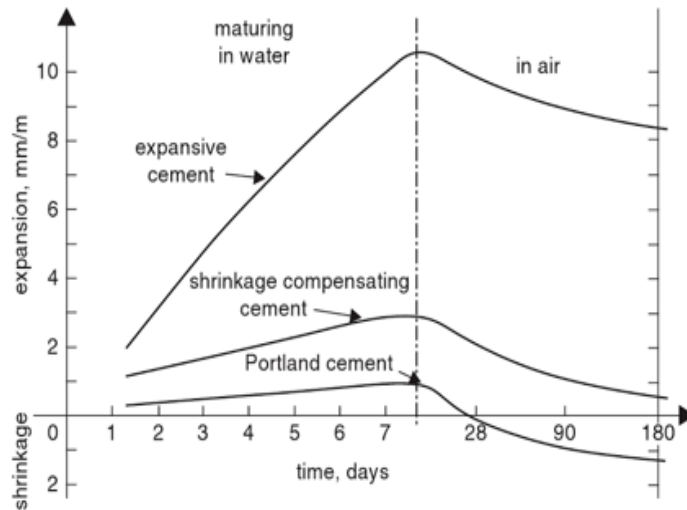


Figure 2-1: Volume change in shrinkage compensating cement, self-stressing cement and Portland cement (Taylor, 1997)

As shown in Figure 2-1, self-stressing cement can produce enough tensile stress to the compressive stress generating a larger expansion causing the breakage of rock or concrete (Taylor, 1997). With that self-stressing cement is of interest to generate destructive forces to intentionally break the surrounding material.

Within a confined hole, expansive cement develops circumferential stress in the radial direction along with tensile stress tangential over a period of time . As shown in Figure 2-2, a fracture is created at the weakest section along the inside surface of the hole; this is at a point where this surface intersects the free surface which is the hole boundary (Harada, 1989). The initial generation of the crack will only propagate when the tensile stress exceeds the tensile strength values of the rock. The stress generated by the SCDA is reduced in proportion to the square of the distance from the edge of hole boundary. Therefore, the tensile stress generated by the SCDA expansion is responsible for the fracturing of the rock as demonstrated in Figure 2-2 (Harada, 1989). Tensile strength is the most important property in determining whether the rock around the hole with expansive cement will break (Hanif, 2007).

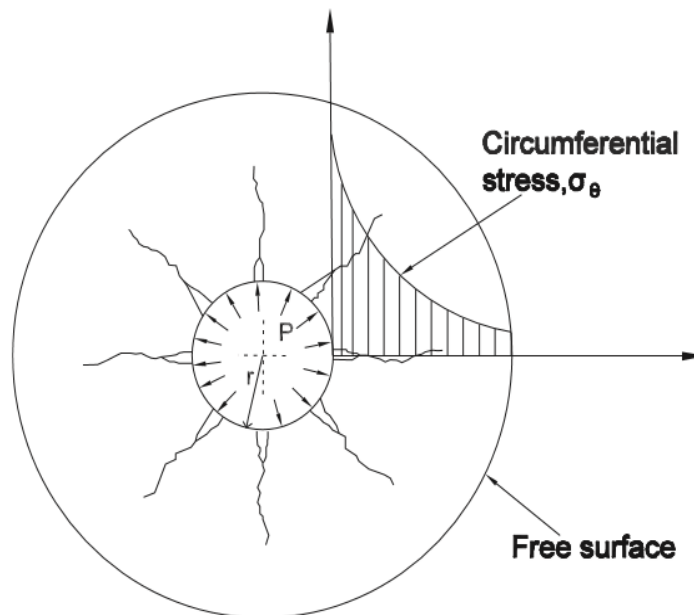


Figure 2-2: Fractural Propagation in a borehole (Harada, 1989)

2.4 Procedure for the use of SCDA's

The use of SCDA's follows a simple procedure in such way that only limited training is required. There are three steps involved as follows.

Step 1: Drill holes in a specific pattern using the appropriate drill bit specific to rock or concrete (Betonamit Technical Manual, 2016).

Step 2: Add 20-30% water to the powdery material and mixing until it becomes lump free and homogenously a flowable mass (Betonamit Technical Manual, 2016).

Step 3: Pour the slurry into the holes 5-10 minutes after mixing. The cement will start to build up pressure cracking the surrounding structure (Betonamit Technical Manual, 2016).

2.5 Applications

The use of expansive cement as an explosive-free method in on the increase especially considering the need for non-violent and pollution free method of breaking rocks in populated areas (Hanif, 2007). Such application is used to break structure in dimension stone quarries and in the demolition industry for rehabilitation projects or construction. In Saudia Arabia, expansive cement is extensively being used for rock fracturing in urban areas as well as granite and marble granite quarries (Hanif, 1997). There are several brands of commercially available expansive cements where each differs in its physical properties and their recommended conditions. Such brands include Betonamit, Bistar, Dexpan, Expando, and Ecobust. These are used for applications such as building remodelling, reinforced concrete cutting, rock breaking, granite, and marble quarrying, and excavating.

2.6 Commercially available expansive cement

Given that there are several commercially available expansive cements, each have different performance, usage instructions and borehole dimension specifications. In terms of the performance of commercially available expansive cements, they have different maximum pressures, times to reach cracking, as well as recommended ambient temperature, water content, borehole diameter and hole depth. The information shown in Table 2-1 is extracted from the technical user's manuals of the respective manufacturers.

Table 2-1: Performance of different commercially available SCDA's

Product	Time to cracking after injection (hr)	Maximum Pressure (MPa)	Recommended Temperature (°C)	Water content (%)	Diameter, D (mm)	Depth, h
Betonamit	Initiation after 12hr	80	-5°to 35°	20%	32-38mm	4D < h < 3m
Bristar	Initiation after 12hr	30 at room temp. after 16 hr of injection	-5°C to 35°C	30%	36mm <D<50mm	h > 3D
Dexpan	Initiation after 2 to 8 hr	124	-5°C to 40°C	30%	38mm	NA
Expando	Cracking completion 24 h	96	0° to 35°C	30%	28mm < D<40mm	NA
Ecobust	NA	137	-8°C to 35°C	NA	38mm <D< 50mm	h > 2D

2.7 Chemical Composition SCDA's

2.7.1 Portland Cement

Expansive cement is composed of a cementitious component, mainly Portland cement and expansive additive. Firstly, Portland cement is manufactured by heating a mixture of limestone and clay in a kiln to 1400-1600°C where the raw ingredients chemically interact to form a new phase-clinker. These raw ingredients are mainly composed of oxide constituents as shown in Table 2-2.

Table 2-2: Percent constituents in Portland cement (Bye,1999)

Oxide	Percentage
CaO	60-67%
SiO ₂	17-25%
Al ₂ O ₃	3-8%
Fe ₂ O ₃	0.5-6%
MgO	0.1-4.0%
SO ₃	0.6-4.0%
Na ₂ O + K ₂ O	1.3-30%

The oxides constituents shown in Table 2-2, are subjected to higher temperatures where clinker complexes are formed and become the major complexes or clinkers in Portland cement. The cement clinker contains 4 major phases, alite (C₃S), belite (C₂S), tricalcium aluminate (C₃A) and ferrite (C₄AF) as shown in Table 2-3. Based on the oxide percent composition, the major Portland cement complex can be estimated using Bogue's equations below. The percent composition of the oxide can be obtained by multiplying the percentage of the oxide constituent by a factor to obtain an estimate of the percent composition of major complexes in Portland cement (Bye,1999).

$$C_3S = 4.07 (CaO) - 7.60 (SiO_2) - 6.72 (Al_2O_3) - 1.43 (Fe_2O_3) - 2.85 (SO_3) \quad (2.1)$$

$$C_2S = 2.87 (SiO_2) - 0.754 (3CaO.SiO_2) \quad (2.2)$$

$$C_3A = 2.65 (Al_2O_3) - 1.69 (Fe_2O_3) \quad (2.3)$$

$$C_4AF = 3.0432 Fe_2O_3 \quad (2.4)$$

Table 2-3: Major complexes in Portland cement (Bye,1999)

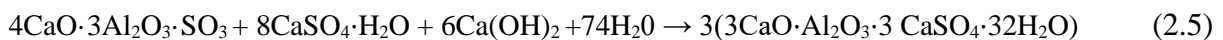
Name of compound	Formula	Abbreviated Formula	Mineral name
Tricalcium silicate	3 CaO·SiO ₂	C ₃ S	Alite
Dicalcium silicate	2 CaO·SiO ₂	C ₂ S	Belite
Tricalcium aluminate	3 CaO·Al ₂ O ₃	C ₃ A	Tricalcium aluminate
Tetracalcium aluminoferrite	4 CaO·Al ₂ O ₃ ·Fe ₂ O ₃	C ₄ AF	Ferrite

2.7.2 Types of expansive cement

Based on the expansive additive, there are three types of expansive cements that are defined by *ASTM C 845 Standard Specification for Expansive Hydraulic Cement*: Type K, Type M, and Type S. Although each type differs in the source of the aluminate component, they all commonly generate ettringite crystals which is one of the driving forces of its expansive ability (ASTM, C. 845 Standard). Type G is another type of expansive cement where the expansive ability is driven by the generation of Portlandite (Arshadnejad, 2011).

Type K

Type K cement is an expansive cement containing anhydrous calcium aluminosulfate (4CaO·3Al₂O₃·SO₃), calcium sulphate (CaSO₄) and uncombined calcium oxide (CaO) (ASTM, C. 845 Standard).



Calcium sulfoaluminate clinker is produced by the burning of raw material containing limestone, bauxite and anhydrite in a rotary kiln at maximum temperature of 1300°C. The calcium sulfoaluminate clinker was obtained by a submitting a mix of gypsum (50%), bauxite (25%), and calcium carbonate (25%) to such higher temperature. The latter mix is subsequently mixed with Portland cement and with a granulated slag as a stabilizer. The mix proportions are 20% calcium sulfoaluminate, 5% of ground granulated slag, and 75% of Portland cement (Ribeiro,1998).

Type M

Type M is an expansive cement containing calcium aluminate (CA) and calcium sulphate (CaSO₄). (ASTM, C. 845 Standard).



Mikhailov (1973) describes self-stressing cement in proportions of 66% Portland cement, 20% CAC (calcium aluminate cement) and 14% gypsum. There is an initial cure in air followed by hot water to allow strength to be developed without comprising the performance with the formation of ettringite. Subsequent cure in cold water is where ettringite formation occurs resulting in expansion. Slag is used as an additional source of aluminum oxide (Al₂O₃) (Mikhailov, 1993).

Type S

Type S cement is an expansive cement composed of tricalcium aluminate (C₃A) and calcium sulphate (CaSO₄) (ASTM, C. 845 Standard).

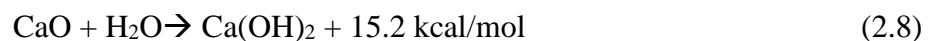


Type S is prepared using Portland Cement and tricalcium aluminate with elevated levels of calcium sulphate. Type S expansive cement is rarely used due to the difficulty in controlling expansion (Ribeiro, 1998).

Type K, M, S expansive additive similarly all contain gypsum (CaSO₄). Gypsum is intentionally added to regulate the setting process. In the absence of gypsum, the tricalcium aluminate in the cements reacts too rapidly with water and the hydration products formed render the cement unworkable. To regulate the setting process, gypsum is intentionally added to the cement clinker at the time of grinder.

Class G

Class G cement is an expansive cement composed of mainly lime, usually 80-90% and SiO₂, and a few substances such as Al₂O₃ and Fe₂O₃ for controlling of the expansion rate. The hydration reaction of lime (CaO) is the source of its expansive force (Arshadnejad, 2011).



2.8 Mechanism for the generation of expansive stress

2.8.1 Source of expansive sources

As discussed in Section 2.7.2, the source of the expansive sources in expansive cement is predominately caused by the generation of hydration products such as Portlandite, $\text{Ca}(\text{OH})_2$, and ettringite crystals, $3\text{CaO}\cdot\text{Al}_2\text{O}_3\cdot 3\text{CaSO}_4\cdot 32\text{H}_2\text{O}$. Both create a gradual development of expansive pressure under confinement (Soeda & Harada, 1994).

2.8.2 Generation of Portlandite

The mechanism responsible for efficient restrained expansion may also be affected by the use of pozzolanic material (Folliard, 1994). The high content of calcium oxide is on the main cause of volumetric expansion in expansive cement. The volumetric change of CaO during hydration can generate up to 1.9 times the original volume (Soeda & Harada, 1994). A hydration reaction occurs between calcium oxide and water generating calcium hydroxide. The lime (calcium oxide) originates from the Portland cement component and from Type K additive. The expansive pressure developing in SCDA is dependent on the degree of hydration of CaO. As shown in Equation 2.8, the hydration of lime is an exothermic reaction generating 15.2 kcal/mol of energy. Due to its exothermic property, lime-based expansive cement can reach a heat of hydration up to 150°C such that boiling water for curing can potentially cause blow outs. Although, the expansive pressure is independent of ambient temperature, temperature has a direct effect on $\text{Ca}(\text{OH})_2$ generation, which in turn controls the degree of expansive pressure (Soeda & Harada, 1994). The optimal amount of calcium oxide is 3-4% in Type K expansive cement for an expansion increase to take place. The addition of CaO to cement creates an increase of the calcium ion concentration in the liquid phase which shows that the calcium hydroxide released by alite (source of alite; Portland cement) hydrolysis does compensate the rapid Ca^{2+} ions consumption for ettringite formation from calcium sulphoaluminate in Type K cement. It is important to notice that ettringite requires calcium ions for its formation stability (Soeda & Harada, 1994).

2.8.3 Generation of Ettringite crystals

In addition to Portlandite, ettringite crystals are another hydration product which further contribute to volumetric expansion as shown in previous chemical equations in Section 2.7.2. Ettringite is the mineral name for calcium sulfoaluminate ($3\text{CaO}\cdot\text{Al}_2\text{O}_3\cdot 3\text{CaSO}_4\cdot 32\text{H}_2\text{O}$) which is normally

found in Portland cement concrete as shown in Figure 2-3. The structure consists of hexagonal columns of $\text{Ca}_3\text{Al}(\text{OH})_6 \cdot 12 \text{H}_2\text{O}$. Each column contains four sites per formula unit with six calcium. For each 4 sites; three are occupied by sulphate groups and one is occupied by two water molecules (Cody, 2004).

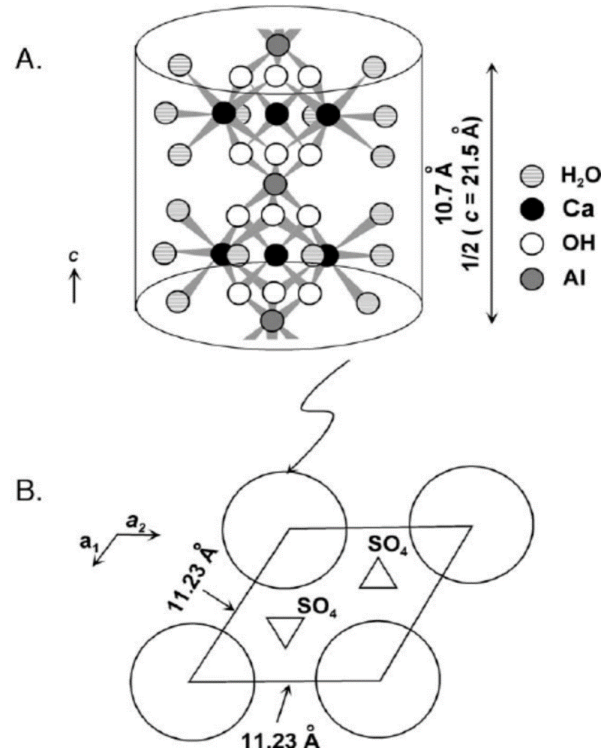


Figure 2-3: Hexagonal ettringite crystal structure a) structure of ettringite column b) circles represent ettringite columns (Cody, 2004)

2.9 Volumetric expansion theories

There are numerous theories aimed at explaining the mechanism of expansion due to the formation of the expansive particles; Ettringite and Portlandite. These theories can be divided into two main schools of thoughts to explain the volumetric expansion in expansive cement:

1. Crystal Growth Theory

2. Swelling Theory

The Crystal Growth theory is caused by the growth of expansive particles on the aluminate particles. The growth of these particles results in the generation of crystals which are referred to hydration products. Subsequent recrystallization results in the generation of expansive stress (Shallom, 1974). The Swelling theory is caused by water adsorption and the swelling characteristics of the ettringite gels which form by a through-solution mechanism. The expansion is owed to the swelling of ettringite particles that are of colloidal size. These particles are often referred to as a gel which are considered to have a large specific surface area. According to the second school of thought, the gel takes up water to produce an overall expansion caused by swelling (Mehta, 1973). These modes of mechanism are both used to explain expansion but do not explicitly specify which mode of formation produces expansion.

2.9.1 Crystal growth theory

A model was proposed by Shallom (1974) to account for an unrestrained paste of pure K component (Refer to Section 2.7.2). The proposed model is divided into two elements, a basic unit which consists of the individual expansive particles and the spatial relation between the units in the paste. As shown in Figure 2-4a, the C_4A_3S particles grow due to the formation of ettringite around them until the first contact takes place at the critical degree of hydration. The critical degree formation refers to the first contact between the expanding sphere where they start pushing against each other and start expanding. In Figure 2-4b, the spheres are in contact while the volume of solute increases, the dimensions of the cast body does not change, and therefore there is a decrease in the porosity of the paste. A decrease in porosity synergistically indicates an increase in hydration products. In Figure 2-4c, the expanding particles start pushing against each other resulting in the expansion of the body. As a result, the pore volume decreases and more of the unreacted CH (calcium hydroxide) and CSH_2 (calcium sulphate hydrate) are removed from the pores between the deposited as ettringite (Bentur & Shalom, 1974).

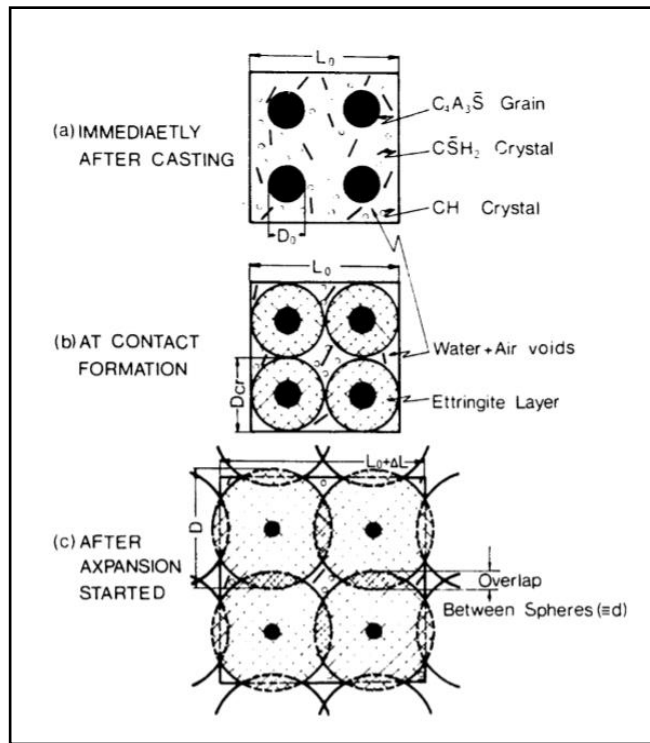


Figure 2-4: Proposed expansion mechanism in unrestrained paste of Type K
(Bentur&Shallom,1974)

Another model is presented by Cohen (1983) which aims to explain the mechanism and kinetics of expansion incorporating the important parameters controlling the expansion process in expansive cement. As shown in Figure 2-5, the model is divided into three sub-systems; the solution, the matrix, and expansive particles. The solution includes the unhydrated particles calcium silicate C_3S and C_2S surrounded by the solution. The main product is the ettringite; the strength producing subsystem (Cohen,1983).

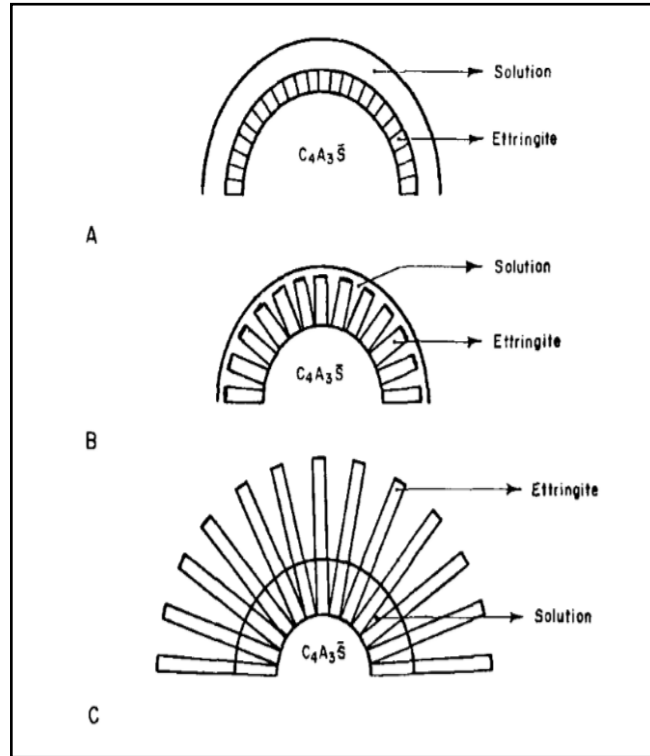


Figure 2-5: Proposed mechanism for unrestrained Type K cement (Cohen,1983)

During the topochemical reaction and the formation of ettringite crystals, the length of the ettringite crystals increases but the thickness remains constant. The formation of ettringite proceeds as long as the necessary reactants are available in stoichiometric quantities. The expansion starts when the crystals become larger than the solution film thickness where it can start exerting pressure against the surrounding matrix. Contradictory to Shallom's model (1974), the volume of the pore will increase as the length of the crystals increases whereas Cohen's (1983) model suggests a decrease in porosity as the formation of spherical ettringite crystals increases. This model shows that the expansion time is inversely proportional to the fineness of the expansive particles and directly proportional to the amount of sulphate source.

2.9.2 Swelling theory

The Swelling Theory was proposed by Mehta (1973). Mehta proposes that colloidal ettringite can attract a large number of water molecules which causes interparticle repulsion between the water molecules and as a result causes expansion. Firstly, Mehta (1973) suggests that the mode of formation for ettringite follows a through-solution mechanism. Secondly, Mehta suggests that in

the presence of calcium hydroxide, the rate of hydration decreases and causes the ettringite crystals to be gel-like and colloidal size. Since colloidal particles have a large specific surface area, water molecules would be absorbed on the surface of ettringite particles generating strong swelling pressure leading to an overall expansion of the system without any change in the crystal lattice of ettringite (Mehta, 1973). Mehta (1973) also performed studies showing that finer blends of ettringite expand significantly more than coarser blends of ettringite. This observation is attributed to the large specific surface of the finer blends absorbing more water (Mehta, 1973). Moore and Taylor (1970) proposed that colloidal ettringite having a crystal structure with a negative net charge is responsible for attracting water molecules. An interparticle repulsion occurs causing an overall expansion of the system (Moore and Taylor, 1970). As shown in Figure 2-6a, in the presence of lime, sulphates and water, ettringite is formed as small crystals and their formation contributes to expansion as opposed to the absence of lime. As shown in Figure 2-6b, long-lathed ettringite crystals are shown due to rapid hydration. These crystals do not produce expansion due to their low specific surface area, absorbing less amounts of water.

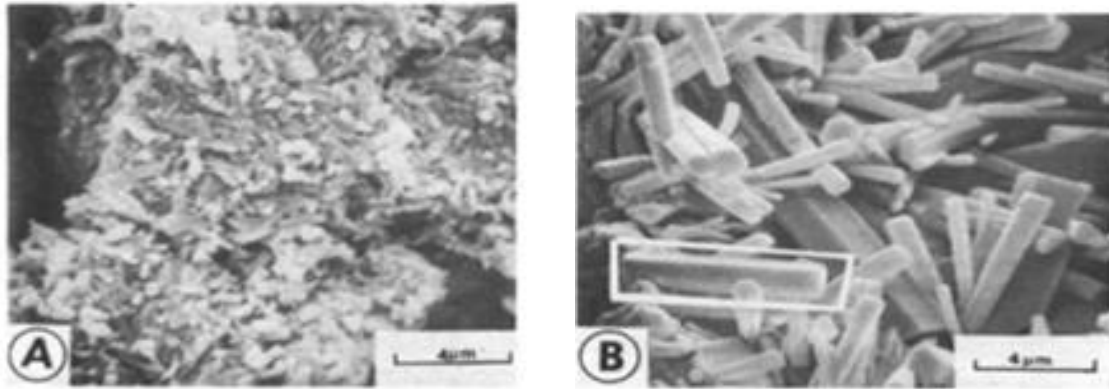


Figure 2-6: Electronic microscopic images of ettringite crystals at 24 hours a) with lime length: 1 μm width: ¼ μm b) without lime length: 6-8 μm width: ½-1 μm (Mehta, 1973)

When lime is present, the OH^- ion concentration increases in the solution. In a saturated lime solution, high concentration of OH^- , Ca^{2+} , and SO_4^{2-} ions will force the crystals of ettringite to be fine and form in close vicinity to the surface of aluminum-bearing particle, just like the pore solution of Portland cement paste (Cohen, 1983). When lime is absent, sufficient $\text{Al}(\text{OH})_4^-$ ions appear in bulk solution due to the low concentration of OH^- and Ca^{2+} ions in the solution to combine OH^- , Ca^{2+} , and SO_4^{2-} ion and generate ettringite crystals. These crystals are formed at

relatively low supersaturated in the bulk solution producing large crystals distributed through an extensive region. It is concluded that it is the concentration of hydroxyl ions that determines the mode of ettringite formation (Cohen, 1983).

Since ettringite crystals are much coarser than the poorly crystallized C-S-H (Calcium-Silicate-Hydrate) gel and the fact that they can easily be identified in SEM (Scanning Electronic Microscope), classifying ettringite as a “gel” is a debate between the two schools. Authors will use the argument that a crystalline structure cannot absorb water molecules within the crystal lattice and therefore it cannot swell by absorption (Cohen, 1983).

The following has been demonstrated by two schools:

1. The size of ettringite crystals and the presence of lime affect expansion
2. In the presence of lime, sulphates, water, and expansive particles, ettringite is formed as small crystals and its formation contributes to expansion
3. In the absence of lime, sulphates, and water hydrates react with expansive particles to give large ettringite crystals which do not contribute to expansion.

2.10 Factors affecting the expansive rate in SCDA

The rate of expansion appears to be dependent upon the amount of readily available aluminate and lime, and proportional to the amount of sulphate. Increasing the content of lime slows down the rate of ettringite formation and supports the formation of monosulphate (AFm, a variation of ettringite that does bring expansion). However, this phase can be transformed afterwards into ettringite during the hardening process. This process may produce better expansion effect because of better transfer of expansive stress after the setting of the cement paste (Opravil et al., 2013). Apart from the chemical composition affecting expansion, there are other parameters to be taken into consideration for the rate such as the water-to-cement ratio, borehole size, ambient temperature, fineness of expansive particles, and mixing time. The latter is discussed in the following sections.

2.10.1 Water-to-cement ratio

According to studies conducted by Hinze and Brown (1994), the water content is inversely proportional to the expansive pressure generated in demolition agents inside a confined volume. The recommended range of water content to be used with the SCDA tested was 30-34% as shown in Figure 2-7. Presumably, this occurs because a smaller water to cement ratio result in a large agent particle density and hence smaller distance between the neighbouring particles. This means that a lower degree of hydration will bring them into contact.

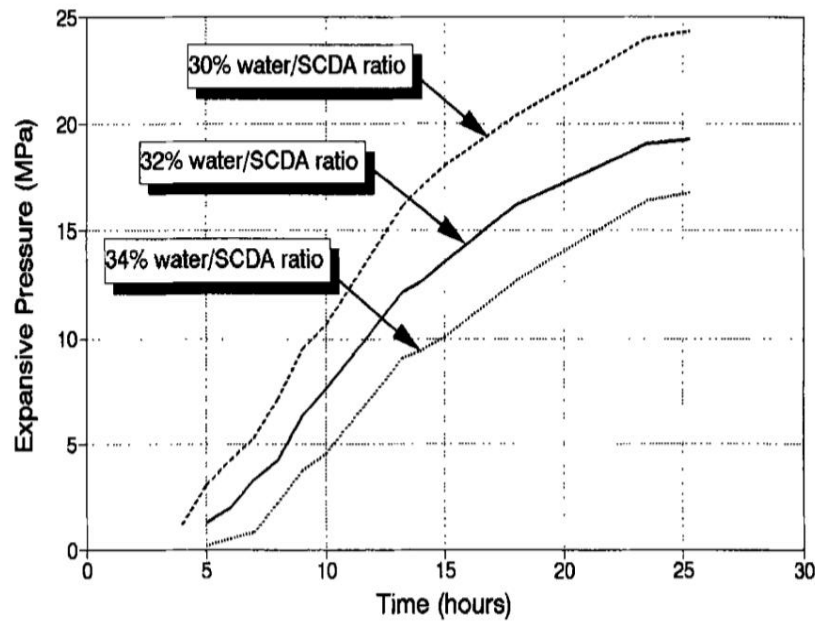


Figure 2-7: The effect of different water-to-cement ratios on expansive pressure
(Hinze&Brown,1994)

If too little water is used, there will be insufficient water to properly hydrate all the SCDA. If the excess amount of water is used, free water will remain and this may compromise the SCDA performance (Hinze& Brown, 1994).

2.10.2 Borehole size

Expansive pressure rate is also affected by the borehole size. The rate of expansive pressure with increasing borehole diameter as shown in Figure 2-8. This can be explained by the hydration reaction of CaO into Ca(OH)_2 . A large diameter provides more space for free lime to be hydrated in the borehole. As mentioned in Section 2.8.2 , this hydration reaction is an exothermic reaction

that releases heat which increases the temperature which is related to the increase in the rate of hydration, one of the main sources of expansion development (Hinze and Brown, 1994). This relationship is also demonstrated by tests carried by Onada cement company in Japan. Onada tested the expansive pressure generated by Bristar, a commercially available expansive cement, using a thin-walled cylinder with a 10mm and 50mm borehole diameter. The pressure obtained a 10mm diameter was 13MPa and a 50mm borehole diameter obtained a pressure of 31MPa. However, after a period of 24 hours, the expansive pressure based on the diameter becomes insignificant (Hanif, 1997).

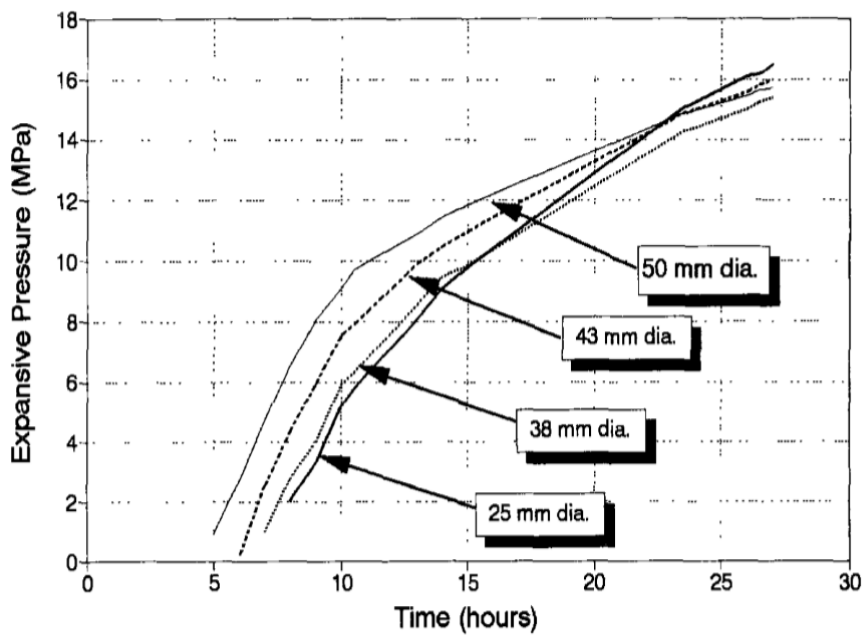


Figure 2-8: The effect of borehole on expansive pressure (Hinze & Brown, 1994)

2.10.3 Ambient temperature

As shown in Figure 2-9, studies by Natanzi and Laefar (2016) have shown that ambient temperature is directly proportional to expansive pressure. The latter is also supported by other studies suggesting that expansive pressure is generated up to a certain threshold value after which a blowout of SCDA may occur (Hinze & Brown, 1994).

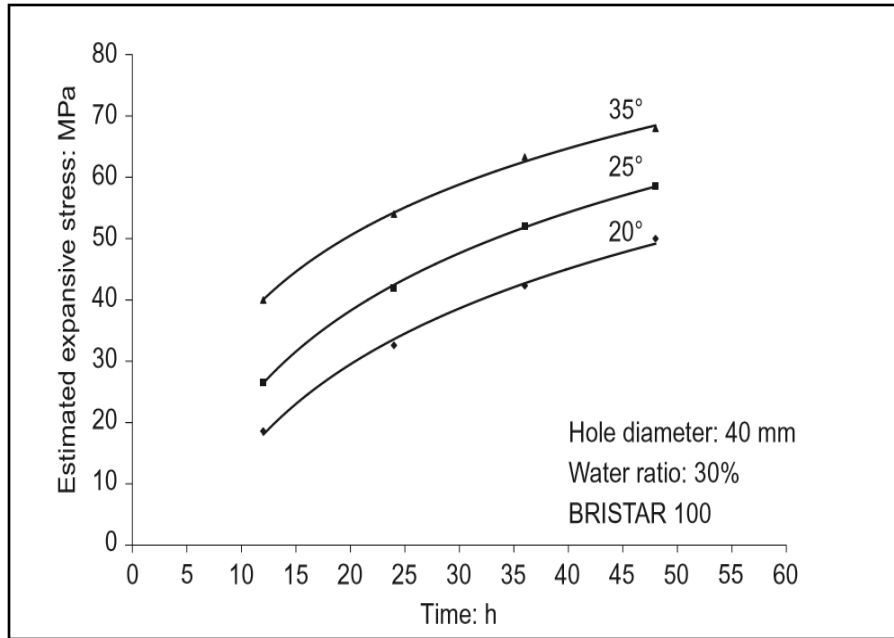
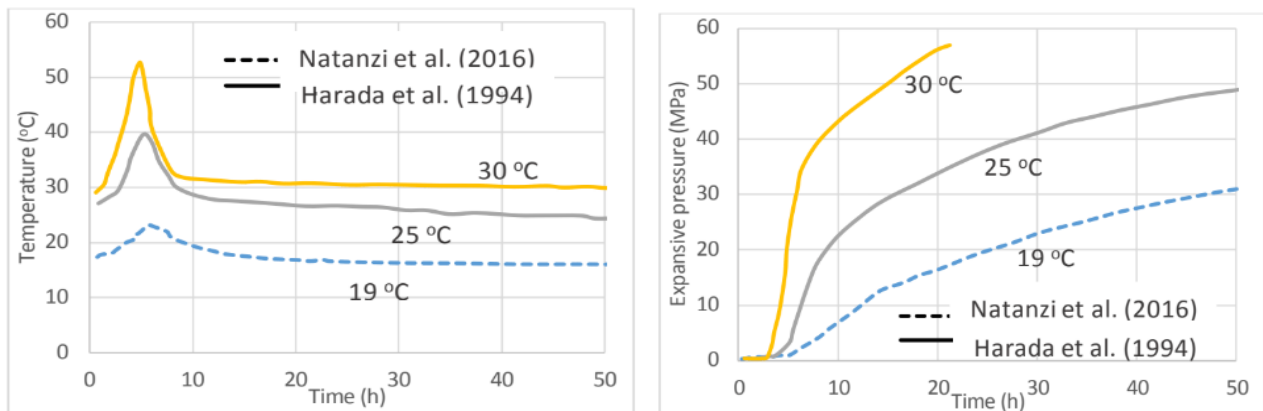


Figure 2-9: Effect of ambient temperature on expansive pressure of Bristar (Natanzi et al., 2016)

The relationship between expansive pressure and temperature is well in accordance with Natanzi et al. (2016) and Harada et al. (1994) who also have reported the effect of temperature on the expansive pressure generated by Dexpan and Bristar. Both report that blow out can occur as a result of elevated hydration heat where at high ambient (19°C to 30°C) noticeable temperature peaks can be generated in SCDA at about 4-5 hours after pouring as shown in Figure 2-10a.



(a) Hydration temperature variation with time

(b) Effect of ambient temperature on expansive pressure

Figure 2-10: Effect of temperature on expansion (Natanzi et al., 2016) & (Harada et al., 1994)

2.10.4 Fineness of expansive particles

The fineness of cement is measured as a specific surface area which is expressed as the total surface area in square centimeters of all the cement particles in 1g of cement. The higher the specific surface, the finer the cement is. Equation 2.9 indicates the parameters affecting the length of ettringite which in turn affects the expansion (Cohen, 1983).

$$le = \frac{1.25T}{BSSc \rho_c} \quad (2.9)$$

where:

le: maximum length of ettringite can be attained upon 100% yield from a single Type K expansive particle (cm)

T: ratio of total volume of ettringite crystals produced from Type K particles to the volume of C₄A₃S particles in 100g of cement

BSSc: Blaine specific surface of Type K particle (cm²)

ρ_c: density of Type K (2.6 g/cm³)

The equation indicates that upon 100% conversion all type K particles to ettringite, the maximum length of single crystals, *le*, is inversely proportional to the Blaine specific surface of the expansive component, *BSSc*, which is assumed to be the same as Type K, the proportionality constant being 1.25/ρ_c. For example, as the fineness of expansive clinker increases, the length of the ettringite crystals decreases. Fineness increases the number of ettringite crystals (Cohen, 1983).

2.10.5 Mixing time

Although it might seem trivial, mixing time has an impact on the degree of expansion and rate. Increasing the time of mixing decreases the expansion of all expansion cements. Mixing accelerates the formation of ettringite and thereby depletes the availability of this hydrate for later expansion. Improper mixing process can reduce the loss of expansion of the expansive cement when admixtures are used. Early ettringite formation does not bring volume increase; whereas late

crystallization of ettringite is the reason of collapse of the paste structure (Sheikh, 1994). The ideal mixing time is specified in the technical user's manuals of the respective manufacturers of the SCDA, i.e. Betonamit specifies at time of 5 minutes to mix and fill the drilled hole.

2.11 Analysis Tools

There have been several methods developed to measure the expansive pressure of expansive cement. In the section below, the three most commonly methods are described.

2.11.1 Thick-Walled Cylinder Method

Using the outer pipe method developed by Hinze and Brown (1994), the expansive pressure can be calculated by pouring the expansive agent using a thick-walled cylinder with one or more strain gauges installed on its outer surface in the tangential direction, at about mid-height of the cylinder. Figure 2-11 depicts the experimental configuration.

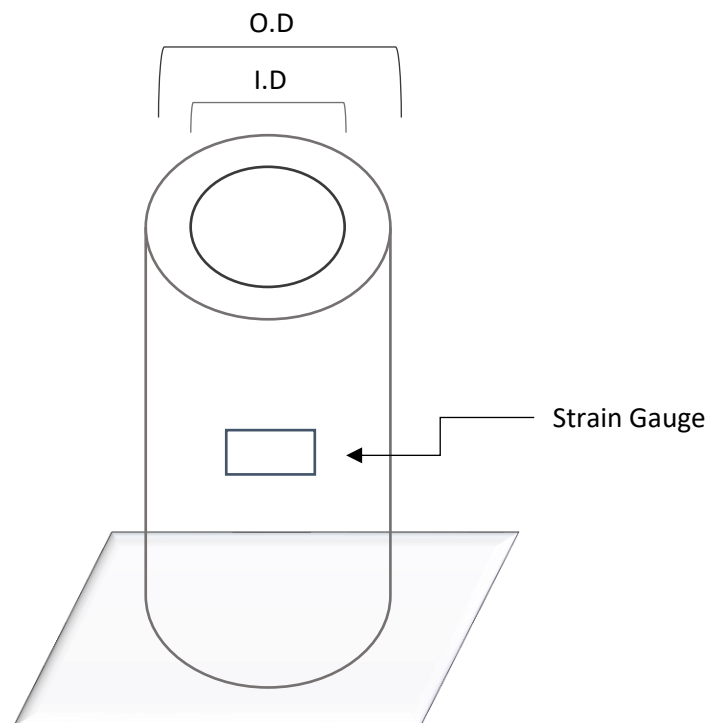


Figure 2-11: Schematic configuration for the testing of expansive cement in a hollow cylinder (Hinze & Brown, 1994)

The following equation is used to determine the pressure in thick-walled cylinder set-up. The tangential microstrain of the specimen is used to calculate the circumferential or tangential strain generated by the expansive agent (Timoshenko & Goodier, 1951).

$$p_i = \frac{E\varepsilon_\theta (r_o^2 - r_i^2)}{2r_i^2} \quad (2.10)$$

where:

- p_i : internal pressure, which in this case is the expansive pressure in MPa
- E : modulus of elasticity of the steel cylinder (200 000MPa)
- r_o : outer radius of cylinder (mm)
- r_i : inner radius of cylinder (mm)
- ε_θ : circumferential or tangential strain on the external surfaces of the test cylinder

The strain ε_θ is the output given by the strain gauge placed at mid-height of the cylinder and measured by using a digital strain indicator. The strain measurements are to be taken at the center of a one-meter, hence mid-span of the cylinder.

2.11.2 Thin-Walled Cylinder

If a thin-walled cylinder is used, the expansive pressure can be calculated with the following equation (Timoshenko & Goodier, 1951).

$$p_i = \frac{2\sigma t}{r} = \frac{2E\varepsilon t}{r} \quad (2.11)$$

where:

- p_i : internal pressure (MPa)
- E : Young's modulus of the steel pipe (MPa)
- t : thickness of the steel cylinder (mm)
- ε : tangential strain
- r : pipe radius (mm)

A cylinder is considered thin-walled when $r/t \geq 10$.

2.12 Chemical Admixtures

Reducing the time of setting would require the use of an accelerator. To increase the performance of the expansive cement in mining applications, accelerators may be beneficial rendering an efficient technology. Accelerating admixtures can be used to increase either the rate of stiffening, setting, rate of hardening or early strength (Fu et al.,1995).

2.12.1 Sodium Chloride

Sodium chloride (NaCl) is considered an accelerator for concrete. However, studies have found deterioration of ordinary Portland cement hydration characteristics with increasing content of NaCl (Zhou, et al, 1996). While some report negative effects on the integrity of cement, others have reported 5% of NaCl by weight of water (BWOW) enhanced the hydration of calcium oxide. As shown in Figure 2-12, the addition of 5% by weight of water or BWOW of salt had a quicker start and faster setting with a time gain of 25-30% compared to a salt free sample.

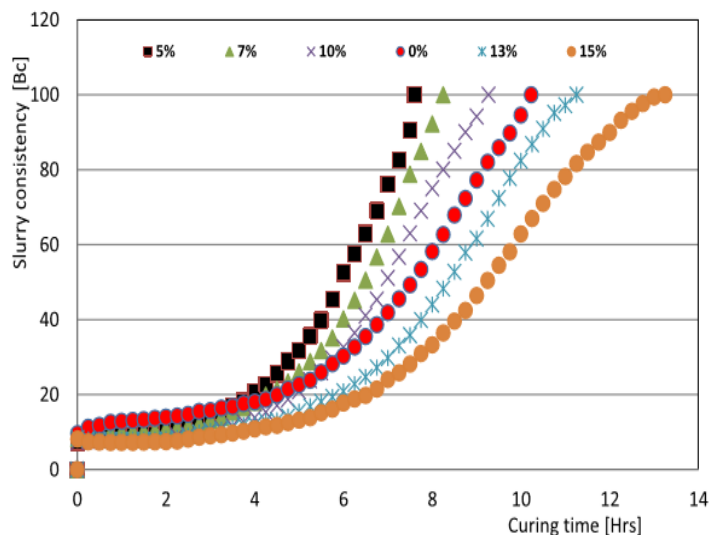


Figure 2-12: Effect of Sodium Chloride BWOW on curing time (Theodoriu & Assambla, 2015)

Similarly, sodium chloride acts as a catalyst for the precipitation of insoluble calcium salt which maintains a low concentration in the solution. Thus, the dissolution of CaO is accelerated which results in calcium hydroxide hydration. Consequently, such concentrations of NaCl could effectively increase the expansive pressure (Teodoriu & Asamba,2015).

2.12.2 Calcium Chloride

One of the most common concrete accelerators is calcium chloride (CaCl_2). Evidence suggests that calcium chloride may increase the permeability calcium-silicate-hydrate (C-S-H), the gel occupying 50% of the paste volume and responsible for most engineering properties of cement paste. As shown in Figure 2-13, calcium chloride is normally added in concentrations of 2-4% by weight of cement (BWOC) (Michaux et al., 1989).

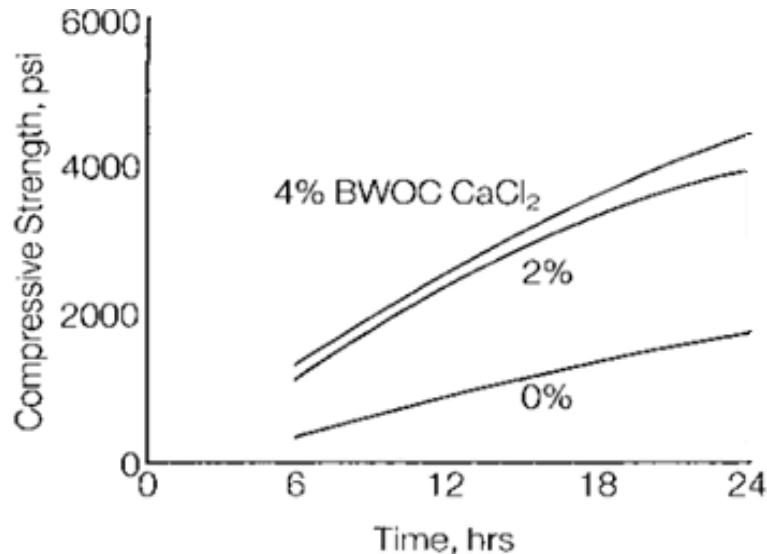


Figure 2-13: Compressive strength developed with increasing calcium chloride by weight of cement (BWOC) (Michaux et al. 1989).

The hydration of the system $\text{C}_3\text{A}-\text{CaCl}_2-\text{CaSO}_4\cdot 2\text{H}_2\text{O}$ shows that calcium chloride primarily accelerates the reaction between C_3A and gypsum. The sulphates react first with calcium chloride followed by the reaction of C_3A and calcium chloride until gypsum ($\text{CaSO}_4\cdot 2\text{H}_2\text{O}$) has been depleted. Results indicate that the addition of 2-4% BWOC of calcium chloride, significantly increases the direct tensile strength and the dynamic modulus of hardened cement paste (Kishar et al., 2013). Abdelrazig et al. (1999) concluded that the addition of calcium salts has a pronounced effect on the calcium hydroxyl and sulphate ion (Ca^{2+} , OH^- , and SO_4^{2-}) concentrations. This is in accordance differential scanning calorimetry showing rapid precipitation of more gypsum and calcium hydroxide within the first 5 minutes of adding calcium chloride in in neat Ordinary Portland cement wastes (Kishar et al., 2013).

2.12.3 Calcium Formate

Calcium formate is also another common accelerator used to reduce setting times. Studies have found that the cement paste produces more ettringite in the presence of calcium formate than in the presence of calcium chloride (Bensted,1978). The effect of calcium formate on pozzolanic cement paste shows that the addition of calcium formate shortens the initial and final setting times. Calcium formate is shown to activate the liberation of $\text{Ca}(\text{OH})_2$, a favourable product for expansion (Heikal,2004).

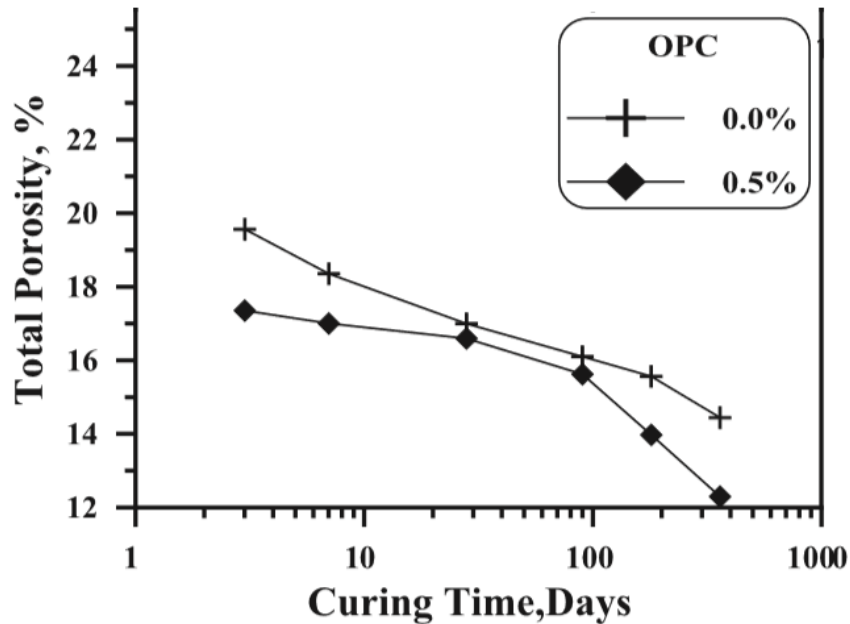


Figure 2-14: Total porosity of Ordinary Portland Cement (Heikal, 2004)

As shown in Figure 2-14, the presence of 0.5% of calcium formate by mass increases the gel: space ratio indicating that a higher degree of hydration products is formed and a decrease in porosity. The production of a dense structure leads to an increase in the rate of hydration. The rapid setting of cement pastes in the presence of calcium formate may be attributed to the crystalline shape of ettringite, which during precipitation would produce fine needles. (Lota et al., 1999). The effect on calcium silicate phases is mainly attributed to the fact that the diffusion rate of HCOO^- ions is much higher than the Ca^{2+} . Consequently, the precipitation of $\text{Ca}(\text{OH})_2$ is accelerated as well as the decomposition of calcium silicates. The influence of calcium formate on the strength of cement pastes may depend on the C_3A content. The acceleration of strength development is more significantly in low concentrations of C_3A (Levitt, 1982).

2.13 Previous related work

2.13.1 Quantifying Pressure

Expansive pressure was measured by using a thick-walled cylinder set-up demonstrated in the schematic configuration in Figure 2-11. The pressure of Bristar-100S, a commercially available SCDA, was measured by a thick-walled cylinder with strain gauges welded midspan to its exterior. The dimensions of the mild steel cylinder are 250mm long with internal diameter of 45mm and outer diameter 80mm. Both ends were constrained with 18mm thick steel plates. The strains were measured by strain gauges to calculate the borehole internal pressure with respect to time. A maximum pressure of 52MPa was obtained over a period of 144 hours as shown in Table 2-4 (Hanif, 2007).

Table 2-4. Expansive pressure generated by Bristar-100S (Hanif,2007)

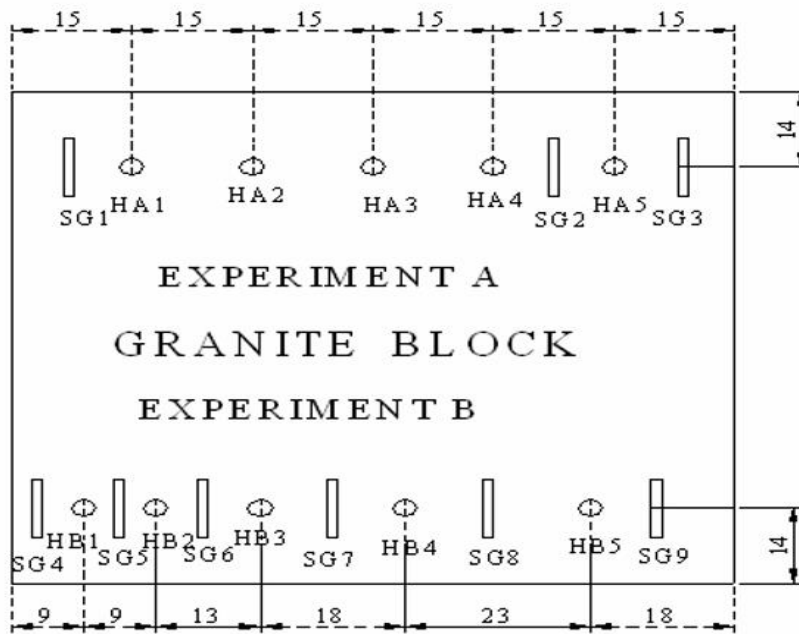
Time (hours)	Pressure (MPa)
24	34
48	41
72	44
96	47
120	50
144	52

A cement company based in Japan, Onoda Cement Co used thin walled cylinder (Section 2.11.2) with strain gauges welded to its their exterior to determine the expansive pressure generated by different grades of Bristar. It was found that stress levels of 1300 t/m² to 3200 t/m² (12.75 to 31.38 MPa) were generated with internal diameters of 10mm and 50mm respectively. These results suggest the hole diameter plays an important role on the resulting expansive pressure. Also, comparing the results of Hanif (2007) in Table 2-4 and those by Onado Cement Co., suggest that higher expansive pressure is generated when the host medium is stiffer. This is because the radial stiffness of 45/80mm thick-walled cylinder is obviously larger than that of the 50/60 mm thin walled cylinder. The radial stiffness of the cylinder is given as EI/r^3 , where I is the moment of

inertia of the cylinder section in mm^2 , and r is the average radius of the cylinder in mm (Timoshenko, 1951).

2.13.2 Borehole Pattern

Few studies have been conducted on the borehole spacing pattern in order to optimize fracture propagation. A study on the deformation behavior and fracture of granite by injecting expansive cement in a set of holes at variable spacing and holes with the same spacing was investigated. As shown in Figure 2-15, two experiments were carried out on a Ranya granite block with two lines of holes on opposite sides, A and B. Both sides have the same number of holes and same depth; however, the HA holes are uniformly spaced out, and the HB holes are gradually spaced out.



a) uniform spacing b) variable spacing

Figure 2-15: Ranya Granite block experiments (Labuz & Dowding, 1985)

In comparison with a line of holes at uniform spacing, the ones with the same number of holes gradually increasing between consecutive holes causes the fracture to be initiated much sooner and propagate at a faster rate starting from the end where the spacing is the smaller (Labuz & Dowding, 1985).

Other studies examined the performance of SCDA using 4.76 mm diameter holes. Results suggest that SCDA can be used on a small scale to create the controlled cracking of concrete. Optimal fracturing of a rock was attempted by introducing non-injected boreholes as shown in Figure 2-16. Results shows that percentage destroyed on concrete is 90% of 6x6 hole grid, 70% in 5x5 hole grid, 40% in 4x4 hole grid, and 10% in a 3x3 hole grid. The presence of noninjected holes was found to be beneficial in all blocks except for the hole grid of 5x5 where cracks did not migrate to the non-injected holes in this block. However, results showed a potential possibility of reducing the amount of SCDA used and incorporate additional boreholes.

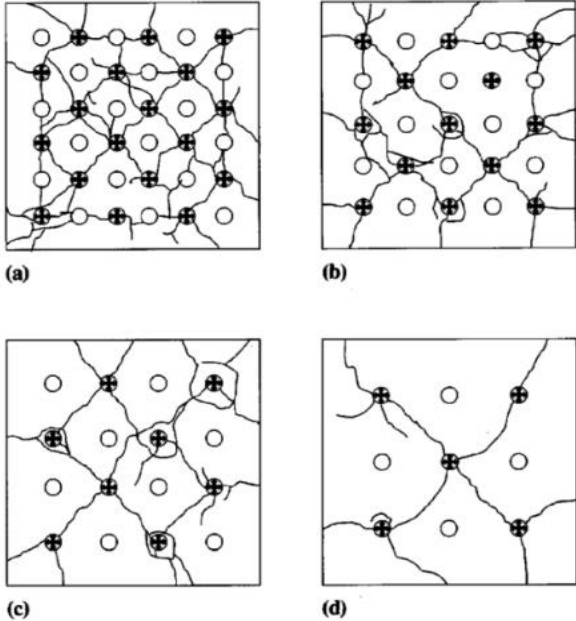


Figure 2-16: Basic cracking with 4.76mm diameter holes with SCDA injected in black a) 6x6 hole grid, 19.1mm spacing b) 5x5 hole grid, 25.4mm spacing c) 4x4 hole grid, 31.8mm spacing d) 3x3 grid, 38.1mm spacing (Gambatese, 2003)

2.13.3 Optimal borehole spacing

Formulas have been developed to determine the minimum spacing required to start cracking. developed a formula to determine the minimum spacing by including a constant, k, dependent on the material to be cracked and the diameter of the hole, d, to be drilled (Gomez & Mura,1984)

$$L = kd \quad (2.12)$$

where:

- L: minimum spacing to start cracking (mm)
- k: constant and dependent on the material to be cracked
- D: hole diameter (mm)

k is an experimental coefficient based on physical properties of different rock types and expansive cement given by the following:

$$k = \frac{\pi}{\sqrt{8}} \left\{ \frac{4\mu\mu^*(1 + \nu^*)\omega}{[\mu(1 - 2\nu^*) + \mu^*]\sigma_c} \right\}^{1/2} \quad (2.13)$$

where:

- σ_c : fracture stress of the rock
- ω : free expansion strain of the SCDA
- μ : shear modulus of the rock material
- ν : Poisson's ratio of the rock material
- μ^* : shear modulus of SCDA filled hole
- ν^* : Poisson's ratio of SCDA filled holes

The experimental value of k is found to be less than 10 for hard rocks, $8 < k < 12$ for medium hard rocks and $12 < k < 18$, for soft rocks (Gomez & Mura, 1994).

Another model to incorporate more parameters was developed to determine appropriate drill hole spacing, the hole diameter, SCDA maximum pressure and surrounding properties (Arshadnejad, 2001).

$$S = \left[-0.0888 \left(\frac{P}{\sigma_t} \right)^2 + 1.0824 \left(\frac{P}{\sigma_t} \right) - 2.1583 \right] \left(\frac{P^2 d^2}{K_{IC}^2} \right) \quad (2.14)$$

where:

- S: the optimum borehole spacing
- P: the expansive pressure
- σ_t : tensile strength of the material to be demolished
- d: drill hole diameter
- K_{IC} : fracture toughness of the material to be demolished

If all is the same, stronger material require closer hole spacing to achieve similar cracking levels. Even though this model incorporates more parameters to determine the borehole spacing, it fails to consider the confining stress acting on the rock mass (Arshadnejad, 2001).

2.13.4 SCDA under load

Laboratory tests were conducted on norite blocks to the test the efficacy of Betonamit SCDA. Norite samples from Vale Inco, Sudbury cut into cubes of 88.9mm with a 11mm borehole diameter each were used to test the efficacy of SCDA under load and under free load. The experimental set-up for testing SCDA under uniaxial load is shown in Figure 2-17 (Mitri & Musunuri, 2009).



Figure 2-17: The experimental set-up for testing SCDA in uniaxially loaded samples

(Mitri & Musunuri,2009)

The results show that under uniaxial compression (64MPa), cracks were observed as shown in Figure 2-18. It was also observed that expansive cement generated stresses up to one week from loading which resulted into further cracks and broke the rock into pieces. Without load, radial cracks were observed, and the cubes were split into halves after 48 hours of filling it with expansive cement as shown in Figure 2-19 (Mitri & Musunuri,2009).



Figure 2-18: Expansive cement under uniaxial loading (Mitri & Musunuri,2009)



Figure 2-19. Expansive cement under free load (Mitri & Musunuri, 2009)

2.13.5 SCDA in shale fracturing for gas recovery

Research was conducted to explore the fracture propagation of SCDAs for gas reservoir stimulation. Results show that using this first-time technology for gas recovery, created radial compressing stress and circumferential tensile strength. As shown in Figure 2-20 and Figure 2-21, the boreholes were injected with SCDA and the results showed that with multiple boreholes, a fracture network is generated (Guo et al,2015).

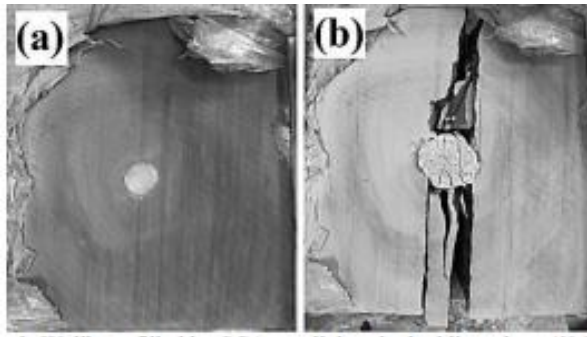


Figure 2-20. Wellbore filled with SCDA parallel to the bedding plane (Guo et al, 2009)

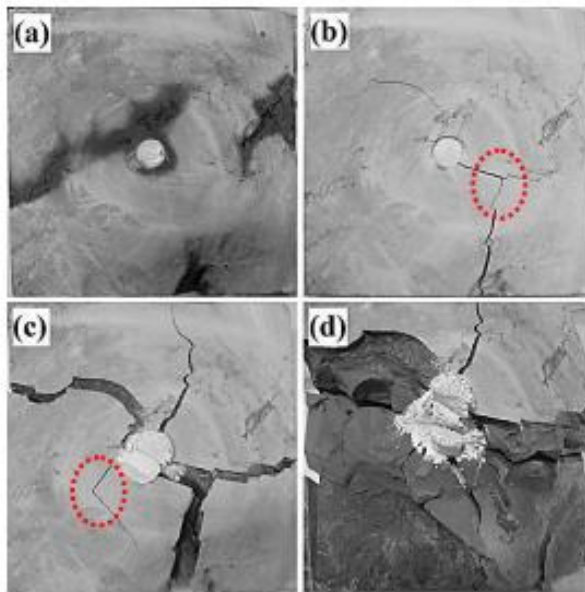


Figure 2-21: Wellbore filled with SCDA perpendicular to the bedding plane (Guo et al.,2009)

2.14 Conclusion

While SCDA's are found to have the potential to be applicable to subsurface mining applications such as underground mines, there is little or no information available in the literature on this topic. Even simple pilot trials have not been reported yet, thus there is a knowledge gap on the mechanical performance of expansive cements in underground mines. This lack of underground trials is more likely attributed to the notion that the in-situ pressure in the rock mass in underground mines is quite high and could limit the initiation and propagation of rock fractures. While this may be true, it poses new challenges, which are the subject of the research investigation currently underway in McGill's Mine Design Laboratory. This study examines the time to achieve rock breakage by investigating the effect of accelerators on SCDA in the aim of increasing the rate of pressure and moving one step forward towards the goal of rock fragmentation with SCDA in underground mines.

Chapter 3

Experimental Program

3.1 Introduction

The goal of the following experimental investigation is to quantify the radial pressure exerted by the SCDA and monitor the crack growth and time of demolition generated by the SCDA selected for this study, which is Betonamit. The manufacturer of Betonamit produces two types namely Type R which is of liquid consistency, and Type S which is of putty consistency. Betonamit Type R was selected for this study. Betonamit is used as a non-explosive cracking agent where after a few hours it develops a high expansive pressure which can break hard rock silently and without vibrations. The aim of this experiment is to increase the rate of pressure increase by the addition of concrete admixtures as one step in optimizing its performance for potential use in the breakage of rocks in underground mines. To monitor the pressure in the SCDA, a thick-walled cylinder configuration is used in this study as shown in Figure 3-1.

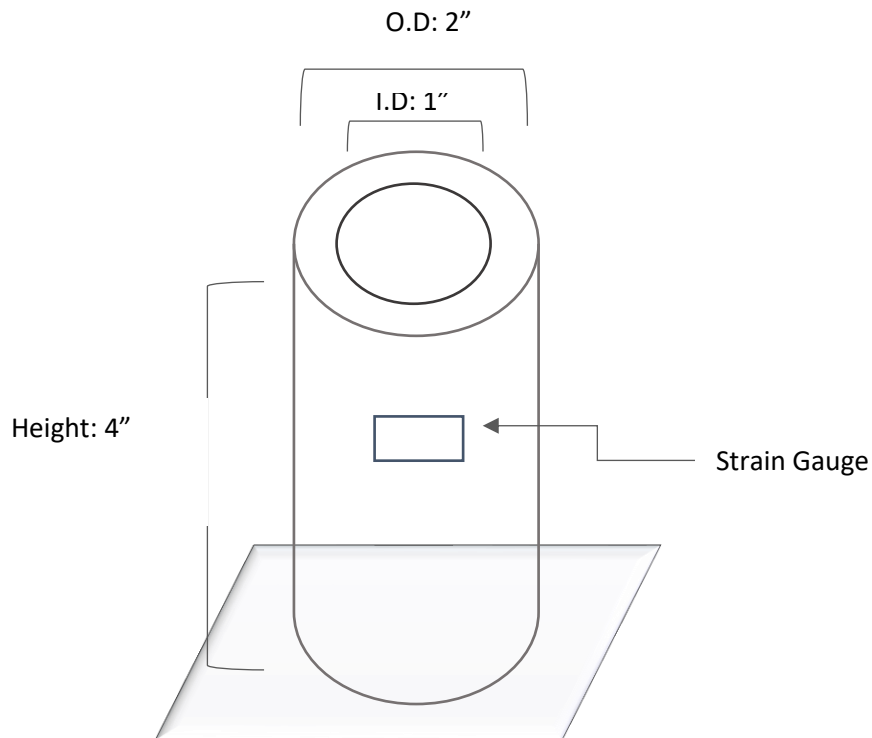


Figure 3-1: Schematic configuration for the testing of Betonamit in a hollow thick-walled cylinder

3.2 Specimens

3.2.1 Test #1

The first part of the experiment consists of injecting the SCDA into the hollow cylinder and recording the tangential strain to determine the pressure over a period of 6 hours. SCDA specimens were confined into steel cylindrical cells to estimate the expansive pressure generated by commercially available expansive cement, Betonamit. The SCDA was prepared and mixed with the guidelines set forth in the Betonamit technical manual. The dimensions of the cylinders are 2” outer diameter (5.08cm), 1” internal diameter (2.54cm), and 4” height (10.16cm). The specimens prepared were to determine if the time of rock breakage could be reduced. The concrete admixtures selected for the first part of the experiment include sodium chloride, calcium chloride, and calcium formate. A thick-walled cylinder configuration was used to measure the tangential strain generated by the cement with and without the chemical admixtures. The tangential measurements from the strain gauges were used to determine the radial pressure generated by the specimen. Pressure-time curves were constructed to study the effect of pressure with the selected additives. Parameters such as water to cement ratio and humidity were kept consistent.

3.2.2 Test #2

The specimens from Test#1 that initiated a higher rate of expansion were investigated on concrete blocks to monitor the time of fragmentation. The fracture growth and time of breakage were examined by filling concrete cubes with SCDA and modified SCDA. The size of the concrete cubical block is 6” (152.4 mm) with a 5” (127 mm) borehole. The concrete blocks were prepared in the Structural Laboratory in the Department of Civil Engineering.

3.3 Admixtures

The selection of additives is based on the chemical composition of the SCDA. Betonamit contains 50-100% of calcium oxide and 2.5-5% of Portland cement and other chemicals (Safety Data sheet according to 1907/2006, Article 31). As shown in Equation 2.8 in Section 2.7.2, the hydration of lime is one of the driving forces contributing to the generation of expansive pressure. Thus, an increase in Ca^{2+} and OH^- ions for the release of $\text{Ca}(\text{OH})_2$ is in favour for an increase in pressure. The selection of sodium chloride, calcium chloride and calcium formate as the additives were

based on literature review. The main hypothesis is that the additives selected will produce an increase in the rate of pressure compared to that of pure Betonamit.

3.4 Equipment

The following tools and instruments are required for the execution of the laboratory experiments.

- P-3500 Digital Strain Indicator
- Pre-Wired Strain Gauges (350 ohms, L, C2A-06-125LW-350)
- Commercial Expansive Agent (Betonamit Type R)
- Steel Cylinders: 4" in Length, 2" in outer diameter, 1" internal diameter
- Humidity (%) and temperature (°C) meter
- Sodium Chloride (NaCl), Calcium Chloride (CaCl₂), Calcium Formate (Ca (HCOO)₂)
- Concrete blocks 6"x 6" x 6", with a 5" deep central borehole
- Demic points
- Vernier

3.5 Experimental Procedure

3.5.1 Test #1

1. Weld a strain gauge in the circumferential direction at mid-height of the steel cylinder as indicated in Figure 3-2a
2. Connect the strain gauge to a quarter bridge configuration to the P-3500 strain indicator as indicated in Figure 3-2b,c

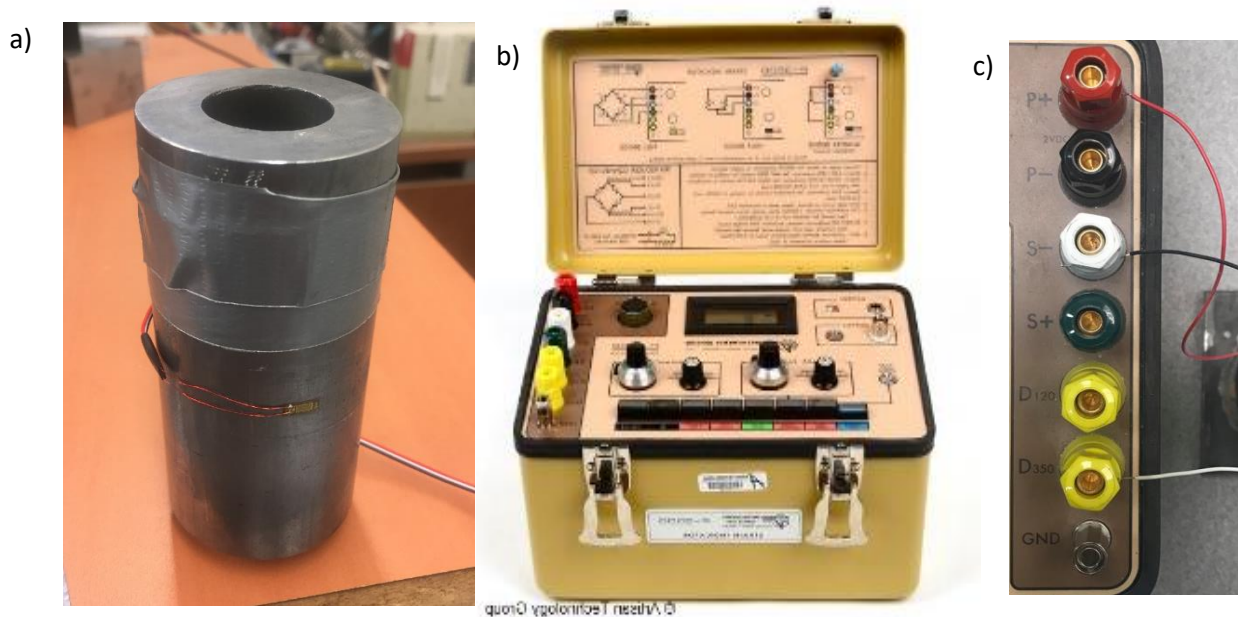


Figure 3-2: Experimental set-up for the testing of SCDA a) Thick wall cylinder configuration
b) P-3500 Strain indicator c) Connection for a quarter bridge

3. Place 100g of Betonamit Type R in a cup and 20% of water by weight of cement.
4. Use using a table top drill press, mix the slurry for 3-5 minutes at low speed, e.g. 600 rpm
5. Mix the additive with 1g of water and add to the Betonamit mix – stir manually for 30 seconds.
6. Pour the slurry into the steel cylinder within 5 minutes of mixing.
7. Record the strain every 15 minutes for a period of 6 hours.
8. Use strain values obtained from the P-3500 indicator to calculate the pressure using Equation 2.10 in Section 2.11.

3.5.2 Test #2

1. Prepare molds for the fabrication of 6" (152.4 mm) concrete cubes (concrete mix meets ASTM C-387 standard) ; see Figure 3-3.



Figure 3-3: Concrete molds

2. Pour concrete mix into the cubes and leave to cure for 28 days; see Figure 3-4



Figure 3-4: Curing of concrete cubes in humidity room

3. Drill a 1" diameter, 5" deep, borehole in the center of a 6" cubic concrete block.
4. Glue demic point using epoxy radially around the borehole as shown in Figure 3-5.

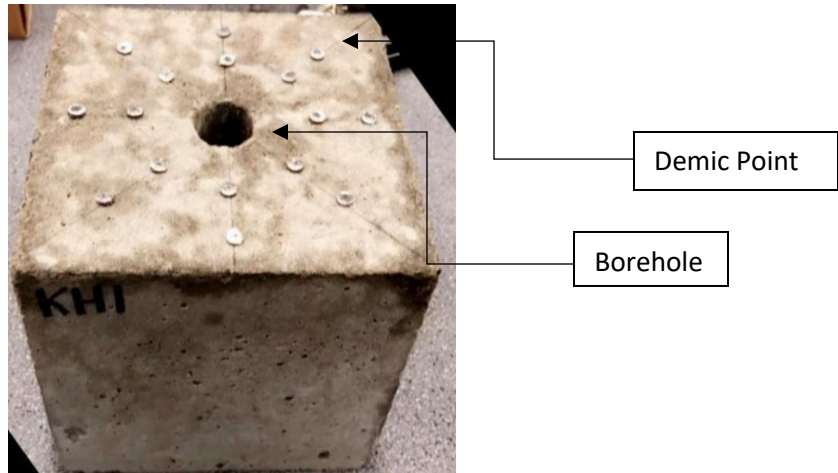


Figure 3-5: Concrete cube with demic points

5. Pour the Betonamit into the borehole of the cube.
6. Estimate crack width by measuring the distance between the demic points using a Vernier every hour.
7. Document test observations with photos every hour to show crack formation and propagation.

3.5 Specimen Preparation

It should be noted that duplicates for each test were done for repeatability and reliability. The specimen ID is as follows: S41-BET- Additive- Test #-a) or b).

where:

- S: Specimen
- BET: Betonamit
- 41: 4" height of cylinder, 1" internal diameter
- Additive: NaCl or CaCl₂ or Ca(HCOO)₂
- a,b: Duplicates

Table 3-1: Specimen Specifications of pure Betonamit

Specimen ID	SCDA (g)	Additive	Water Content (%)	Water Temperature (°C)	Humidity (%)	Temperature (°C)
S41-BET-01a	100	NA	20	4.5	20	25
S41-BET-01b	100	NA	20	4.5	20	25

Table 3-2: Specimen Specifications with the addition of Sodium Chloride

Specimen ID	SCDA ¹ (g)	Additive (BWOC %) ²	Water Content (%)	Water Temperature (°C)	Humidity (%)	Temperature (°C)
S41-BET-NaCl-01a	100	0.25	20	4.5	20	28
S41-BET-NaCl-01b	100	0.25	20	4.5	20	25
S41-BET-NaCl-02a	100	1.0	20	4.5	20	28
S41-BET-NaCl-02b	100	1.0	20	4.5	20	25
S41-BET-NaCl-03a	100	2.0	20	4.5	20	28
S41-BET-NaCl-03b	100	2.0	20	4.5	20	25
S41-BET-NaCl-04a	100	3.0	20	4.5	20	24
S41-BET-NaCl-04b	100	3.0	20	4.5	20	25

¹ SCDA: Betonamit

² BWOC: By Weight of Cement

Table 3-3: Specimen specifications with the addition of Calcium Chloride

Specimen ID	SCDA ¹ (g)	Additive (BWOW%) ²	Water Content (%)	Water Temperature (°C)	Humidity (%)	Temperature (°C)
S41-BET-CaCl ₂ -01a	100	1	20	4.5	20	27
S41-BET- CaCl ₂ -01b	100	1	20	4.5	20	27
S41-BET- CaCl ₂ -02a	100	2	20	4.5	20	25
S41-BET- CaCl ₂ -02b	100	2	20	4.5	20	25
S41-BET- CaCl ₂ -03a	100	3	20	4.5	20	25
S41-BET- CaCl ₂ -03b	100	3	20	4.5	20	26
S41-BET- CaCl ₂ -04a	100	4	20	4.5	20	28
S41-BET- CaCl ₂ -04b	100	4	20	4.5	20	25
S41-BET- CaCl ₂ -05a	100	5	20	4.5	20	27
S41-BET- CaCl ₂ -05b	100	5	20	4.5	20	25

¹ SCDA: Betonamit

² BWOW: By Weight of Water

Table 3-4: Specimen specifications with the addition of Calcium Formate

Specimen ID	SCDA ¹ (g)	Additive (BWOC %) ²	Water Content (%)	Water Temperature (°C)	Humidity (%)	Temperature (°C)
S41-BET-Ca(HCOO) ₂ -01a	100	1.0	20	4.5	20	26
S41-BET-Ca(HCOO) ₂ -01b	100	1.0	20	4.5	20	26
S41-BET-Ca(HCOO) ₂ -02a	100	1.5	20	4.5	20	25
S41-BET-Ca (HCOO) ₂ -02b	100	1.5	20	4.5	20	25
S41-BET-Ca(HCOO) ₂ -03a	100	2.0	20	4.5	20	26
S41-BET-Ca(HCOO) ₂ -03b	100	2.0	20	4.5	20	26
S41-BET-Ca(HCOO) ₂ -04a	100	3.0	20	4.5	20	26
S41-BET-Ca(HCOO) ₂ -04b	100	3.0	20	4.5	20	26
S41-BET-Ca(HCOO) ₂ -05a	100	4.0	20	4.5	20	26
S41-BET-Ca(HCOO) ₂ -05b	100	4.0	20	4.5	20	26

¹ SCDA: Betonamit

² BWOC: By Weight of Cement

Table 3-5. Specimen specifications for Test #2

Specimen ID	SCDA (g)	Additive (%)	Water content (%)	Water temperature (°C)	Humidity (%)	Temperature (°C)
BET-Control-01a	130	NA	20	4.5	20	27
BET-Control-01b	130	NA	20	4.5	20	27
BET-Calcium Formate 3%-02a	130	3% BWOc	20	4.5	20	27
BET-Calcium Formate 3%-02b	130	3% BWOc	20	4.5	20	27
BET-Calcium Chloride-3%-03a	130	3% BWOW	20	4.5	20	27
BET-Calcium Chloride-3%-03b	130	3% BWOW	20	4.5	25	27

BWOC: By Weight of Cement BWOW: By Weight of Water

3.6 Geomechanical properties of the concrete

3.6.1 UCS Test Results

This section is related to the concrete used in the laboratory experiments. The concrete cubes were made in the Department of Civil Engineering Department. In addition to the cubes, cylindrical specimens were poured for mechanical property testing, namely the uniaxial compressive strength (UCS) and the Brazilian test for the determination of the tensile strength. The concrete samples for the UCS and Brazilian test were prepared in compliance to the ASTM C39 Standard. The average UCS is 10MPa and the average tensile strength is 0.98 MPa.



Figure 3-6: UCS concrete Samples

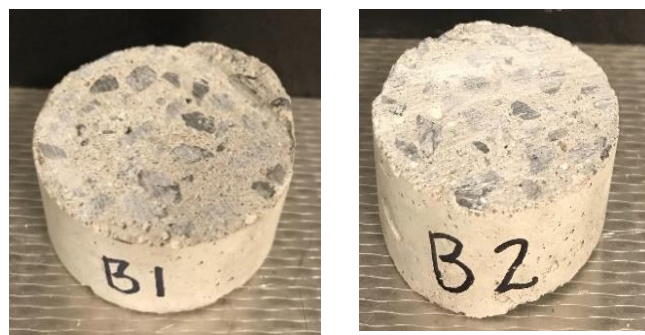


Figure 3-7: Brazilian concrete Samples

Chapter 4

Experimental Results

4.1 Introduction

In this Chapter, the results from Test #1 and Test #2 are reported. For Test #1, the thick-walled configuration was used to measure the tangential strain generated by pure Betonamit, as well as by Betonamit with chemical admixtures which include sodium chloride, calcium chloride and calcium formate (Refer to Appendix A for individual strain values). The strains were recorded from the strain gauge and the average of these values were used to compute magnitude of expansive pressure as it developed over a time period of 6 hours. The use of some of the additives exhibited favorable results towards an increase in expansive pressure rate compared to that of pure Betonamit while some exhibited a decrease in strength. Optimal concentrations of the additives are reported. For Test #2, the fracture growth is examined by monitoring the crack formation generated by both pure Betonamit and Betonamit with the chemical admixtures that gave favourable results in Test #1. For Test #2, photographs were taken to display crack formation of the concrete block and crack-width-time curves are presented.

4.1.1 Test #1

In the comparison of results, two pressure calculations are used, namely t_3 and t_6 , calculated after 3 and 6 hours from the start of the test, respectively. Sample S41-BET-01 is considered be the control sample without any additives. As can be seen from Table 4-1, $P_{t_3} = 10.35$ MPa and $P_{t_6} = 23$ MPa after 3 and 6 hours, respectively from the start of the test, for the control sample. These values are the average obtained from the tests conducted on two control samples “S41 - BET-01a” and “S41-BET-01b” listed as S41-BET-01 in Table 4-1. The individual results are reported in Appendix A. These values will serve as a basis for the comparison of results. The pressure results of four Betonamit samples with Sodium Chloride or NaCl additive are shown in Table 4-1. As can be seen, regardless of the concentration of NaCl, the resulting expansive pressure is inferior to the control sample S41-BET-01. The next series of results in Table 4-1 is for the admixture Calcium Chloride or CaCl_2 . Five samples designated S41-BET- CaCl_2 -01 to -05 were tested with concentrations varying from 1 to 5% BWOW. As can be seen, the results are promising. There appears to be an optimum concentration with the addition of 3% CaCl_2 by weight of water

at which the expansive pressure is superior to that of the control sample. More specifically, sample S41-BET- CaCl₂-03 exhibits expansive pressure of 14.1 MPa after 3 hours, and 28.85 MPa after 6 hours, which are clearly larger than their counterparts for the control sample. Finally, the next series of results in Table 4-1 is for the admixture Calcium formate or Ca(HCOO)₂. Five samples designated S41-BET- Ca(HCOO)₂-01 to-05 were tested with concentrations varying from 1 to 5% BWOC. As can be seen, the results are also promising. There appears to be an optimum concentration with the addition of 3% Ca(HCOO)₂ by weight of cement at which the expansive pressure is superior to that of the control sample. More specifically, sample S41-BET- Ca(HCOO)₂-04 exhibits expansive pressure of 17.4 MPa after 3 hours, and 24.45MPa after 6 hours, whereby a significant increase in pressure is obtained in the early hydration period compared to that of the control sample giving $P_{t3} = 10.35$ MPa and $P_{t6} = 23$ MPa.

Table 4-1: Expansive Pressure as a function of time

Specimen ID	Expansive Pressure (MPa)					
	t ₁	t ₂	t ₃	t ₄	t ₅	t ₆
S41-BET-01	0.75	3.15	10.35	16.2	20.1	23
S41-BET-NaCl-01	0.9	3.9	8.4	12.6	16.2	19.8
S41-BET-NaCl-02	0.45	3	7.8	12.6	16.5	18.5
S41-BET-NaCl-03	0.15	1.35	5.1	9	12.3	15.3
S41-BET-NaCl-04	0.15	0.9	2.7	4.35	6.3	7.33
S41-BET-CaCl ₂ - 01	0.6	2.7	8.53	14.7	18.75	22.62
S41-BET- CaCl ₂ -02	1.05	5.4	13.65	20.55	24.6	28.35
S41-BET- CaCl ₂ -03	0.9	5.1	14.1	20.4	24.95	28.85
S41-BET- CaCl ₂ -04	1.05	4.65	13.95	20.25	24.5	27.8
S41-BET- CaCl ₂ -05	0.6	6	11	12.9	14.7	16.1
S41-BET-Ca(HCOO) ₂ -01	0.6	3.3	10.65	16.5	19.35	20.7
S41-BET-Ca(HCOO) ₂ -02	0	1.35	5.55	8.85	11.4	12.6
S41-BET-Ca(HCOO) ₂ -03	0.45	5.25	12.15	15.3	17.5	18.5
S41-BET-Ca(HCOO) ₂ -04	1.95	11.45	17.4	20.4	22.8	24.45
S41-BET-Ca(HCOO) ₂ -05	2.7	7.5	13.8	15.6	16.2	16.5

4.1.2 Test #2

In the comparison of results, the time of fracture initiation is monitored as well as the degree of fragmentation at the time of fracture initiation and at 6 hours. The aim of this investigation is to draw a comparison with Test#1 and confirm whether the selected admixtures causes a reduction in time of breakage. A total of 6 specimens were investigated such that duplicates for each test were done for repeatability and reliability as follows:

- 1) 2 specimens investigate the effect of pure Betonamit
- 2) 2 specimens investigate the effect of 3% Calcium Formate BWOC
- 3) 2 specimens investigate the effects of 3% Calcium Chloride BWOW

As shown in Table 4-2, BET-Control-01a and BET-Control-01b are the control samples without the addition of additives. The time of fracture and the degree of fragmentation is used as the frame of reference to the specimens of Betonamit with the addition of additives. As can be seen in Table 4-2, the time of fracture initiation for the control samples occurs between 4 and 5 hours. In Table 4-3, the degree of fragmentation is monitored by measuring the crack width generated at 6 hours whereby the control samples exhibited a crack-width between 4.64 mm and 4.86 mm. Photographs displaying crack formation are shown in Figure 4-1 and Figure 4-2 (Refer to Appendix B for results between 0 and 6 hours). These values will serve as a basis for the comparison of results. The next series of results of Betonamit samples with the addition of 3% Calcium Formate or $\text{Ca}(\text{HCOO})_2$ BWOC are shown in Table 4-2 and 4-3 as BET- $\text{Ca}(\text{HCOO})_2$ -3%-02a and BET- $\text{Ca}(\text{HCOO})_2$ -3%-02b. As can be seen in Table 4-2, the time of fracture initiation for BET- $\text{Ca}(\text{HCOO})_2$ -3%-02a and $\text{Ca}(\text{HCOO})_2$ -3%-02b occurs between 4 and 5 hours similar to the control samples. In Table 4-3, the samples with Calcium Formate exhibited a crack-width between 5.44mm and 2.21mm showing a non-significant difference in the degree of fragmentation at 6 hours compared to the control samples. Photographs displaying crack formation are shown in Figure 4-3 and Figure 4-4. The next series of results of Betonamit samples with the addition of 3% Calcium Chloride BWOW are shown in Table 4-2 and 4-3 as BET- CaCl_2 -3%-03a and BET- CaCl_2 -3%-03b. As can be seen in Table 4-2, the time of fracture initiation for BET- CaCl_2 -3%-03a and BET- CaCl_2 -3%-03b at 3.5 and 5 hours respectively. A reduction of 0.5 hours in time of fracture is observed; however, due to lack of repeatability a conclusive statement on the reduction of time of fracture cannot be

made. However, BET- CaCl₂-3%-03a and BET- CaCl₂-3%-03b both exhibited a higher degree of fragmentation compared to the control samples at 6 hours with crack-width of 25.94 mm and 5.53 mm respectively. Photographs displaying crack formation are shown in Figure 4-5 and Figure 4-6. This is indicative of potential usage of calcium chloride as an additive to provide a higher degree of fragmentation earlier on. However, more tests are to be duplicated.

Table 4-2: Crack width of specimens at time of fracture initiation

Specimen	Time of Fracture Initiation (hours)	Crack width (mm)							
		Fracture #1 (mm)		Fracture #2 (mm)		Fracture #3 (mm)		Fracture #4 (mm)	
		a ¹	b ²						
BET-Control-01a	4	0.35	0.21	0.75	0.1	0.24	1	-	-
BET-Control-01b	5	0.16	0.44	1.17	0.8	1	0.05	0	-
BET- Ca(HCOO) ₂ -3%-02a	4	0.78	1.07	-	-	-	-	-	-
BET- Ca(HCOO) ₂ -3%-02b	5	0.69	1.18	1.71	0.4	-	-	-	-
BET- CaCl ₂ -3%-03a	3.5	0.17	1.02	1.47	0.4	2.27	3.35	-	-
BET- CaCl ₂ -3%-03b	5	0.26	0.03	0.9	0.03	1.34	1.22	-	-

¹ Measurements are taken 2" from the edge of the borehole

² Measurements are taken 4" from the edge of the borehole

Table 4-3: Crack width of specimens at 6 hours

Specimen	Crack Width (mm)							
	Fracture #1		Fracture #2		Fracture #3		Fracture #4	
	a ¹	b ²	a ¹	b ²	a ¹	b ²	a ¹	b ²
BET-Control-01a	2.26	1.09	1.9	0.85	1.73	0.8	1.29	4.64
BET-Control-01b	1.27	0.45	4.43	4.86	1.53	0.13	-	-
BET- Ca(HCOO) ₂ -3%-02a	4.22	5.44	0.65	0.11	0.07	0.14	1.09	0.81
BET- Ca(HCOO) ₂ -3%-02b	1.36	2.19	2.31	1.43	-	-	-	-
BET- CaCl ₂ -3%-03a	4-08	5.07	20.17	19.12	23.21	25.94	-	-
BET- CaCl ₂ -3%-03b	2.25	2.28	1.56	0.33	4.12	5.53	3.82	1

¹ Measurement are taken 2" from the edge of the borehole

² Measurement are taken 4" from the edge of the borehole

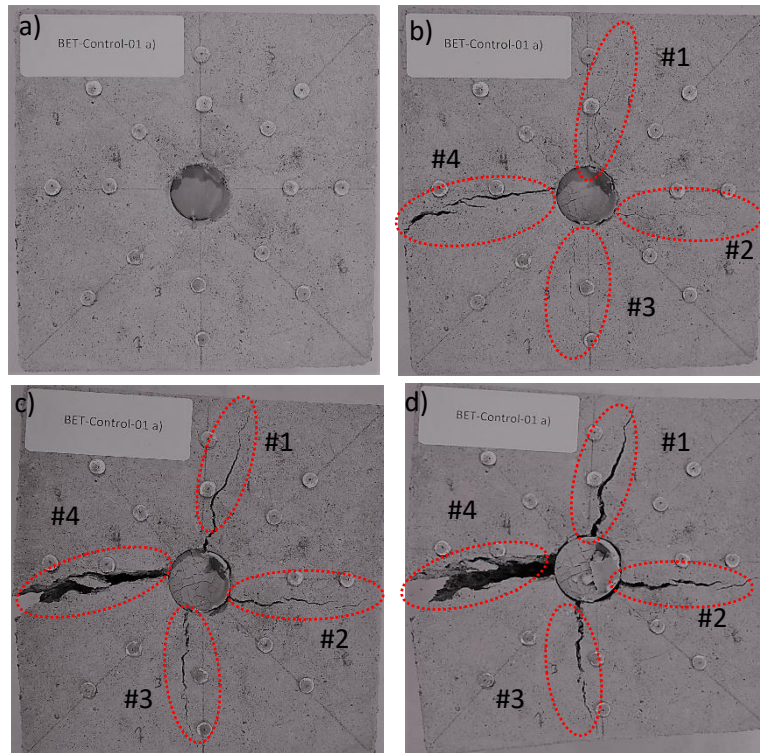


Figure 4-1: Top view BET-Control-01a showing cracking pattern. a) 0 hours b) 4.5 hours c) 6 hours See Appendix B for photos between 0-6 hours.

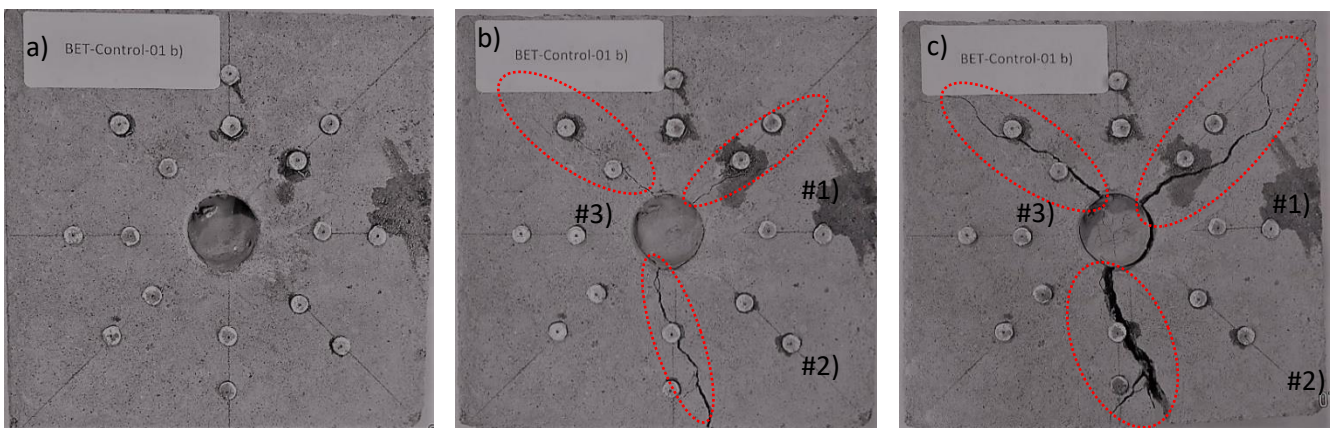


Figure 4-2: Top view BET-Control-01b showing cracking pattern. a) 0 hours b) 4.5 hours c) 6 hours See Appendix B for photos between 0-6 hours.

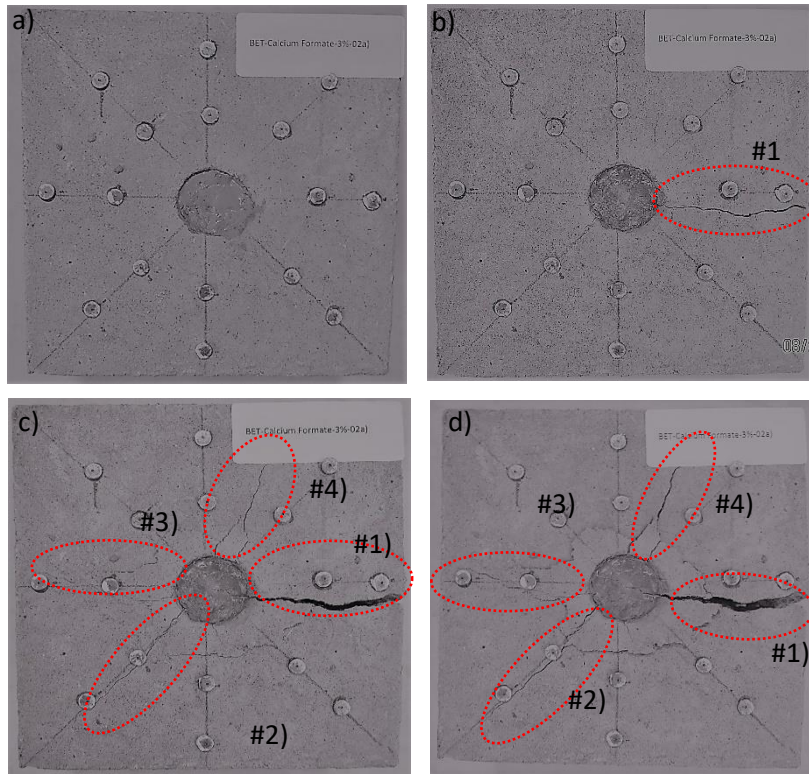


Figure 4-3: Top view of BET- Ca(HCOO)₂-3%-02a showing cracking pattern. a) 0 hours
 b) 4 hours c) 5 hours d) 6 hours (See Appendix B for results between 0-6 hours)

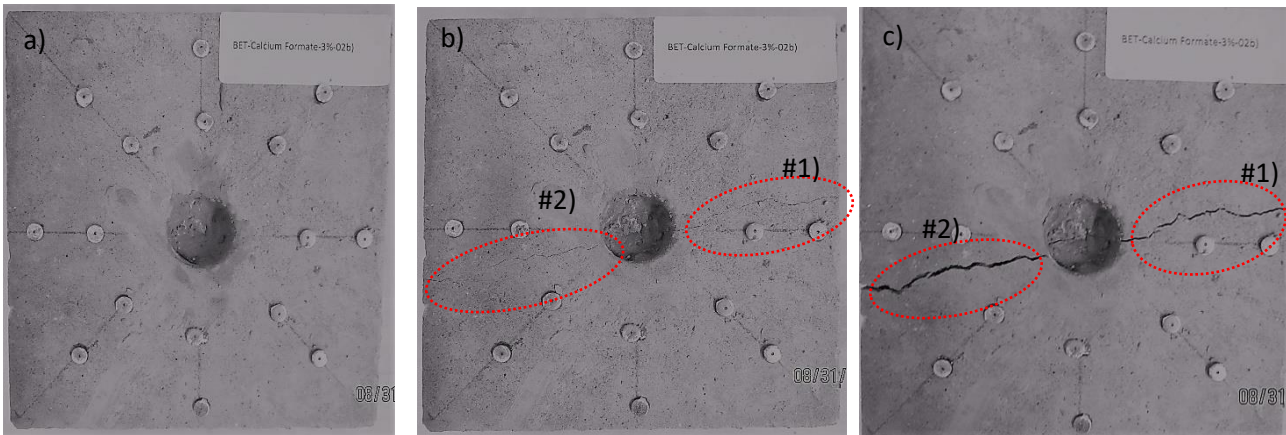


Figure 4-4: Top view of BET- Ca(HCOO)₂-3%-02b showing cracking pattern. a) 0 hours
 b) 4 hours c) 5 hours d) 6 hours (See Appendix B for results between 0-6 hours)

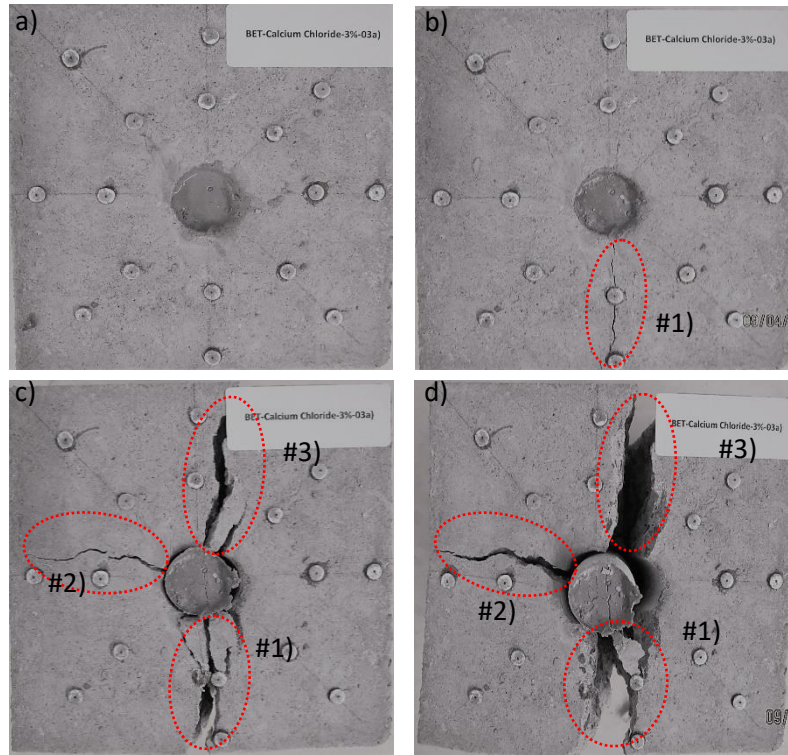


Figure 4-5: Top view of BET- CaCl_2 -3%-03a showing cracking pattern. a) 0 hours b) 4 hours c) 5 hours d) 6 hours (See Appendix B for results between 0-6 hours)

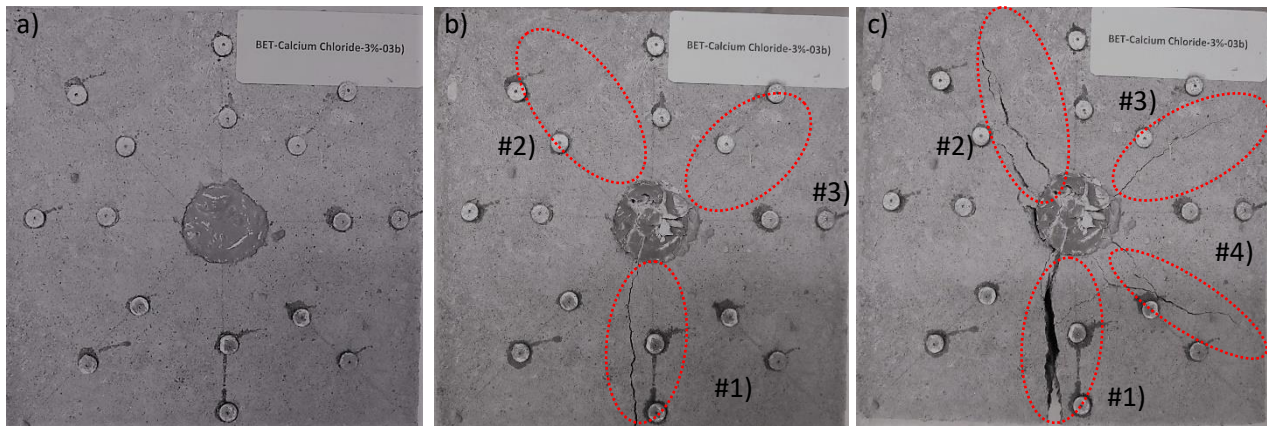


Figure 4-6: Top view of BET- CaCl_2 -3%-03b showing cracking pattern. a) 0 hours b) 4 hours c) 5 hours d) 6 hours (See Appendix B for results between 0-6 hours)

4.2 Discussion

4.2.1 Test #1

A typical presentation of the development of expansive pressures as a function of time is shown in the following figures. As shown in Figure 4-7, the control (pure Betonamit) will be used as the frame of reference to assess the change in the expansive rate with the addition of sodium chloride, calcium chloride and calcium formate. In Figure 4-7, the development of expansive pressure of the control sample is shown where a pressure of 10.35MPa is achieved in 3 hours and 23MPa after 6 hours. The following discussion focuses on the acceleration effects of additives on the expansive pressure of Betonamit over a period 6 hours.

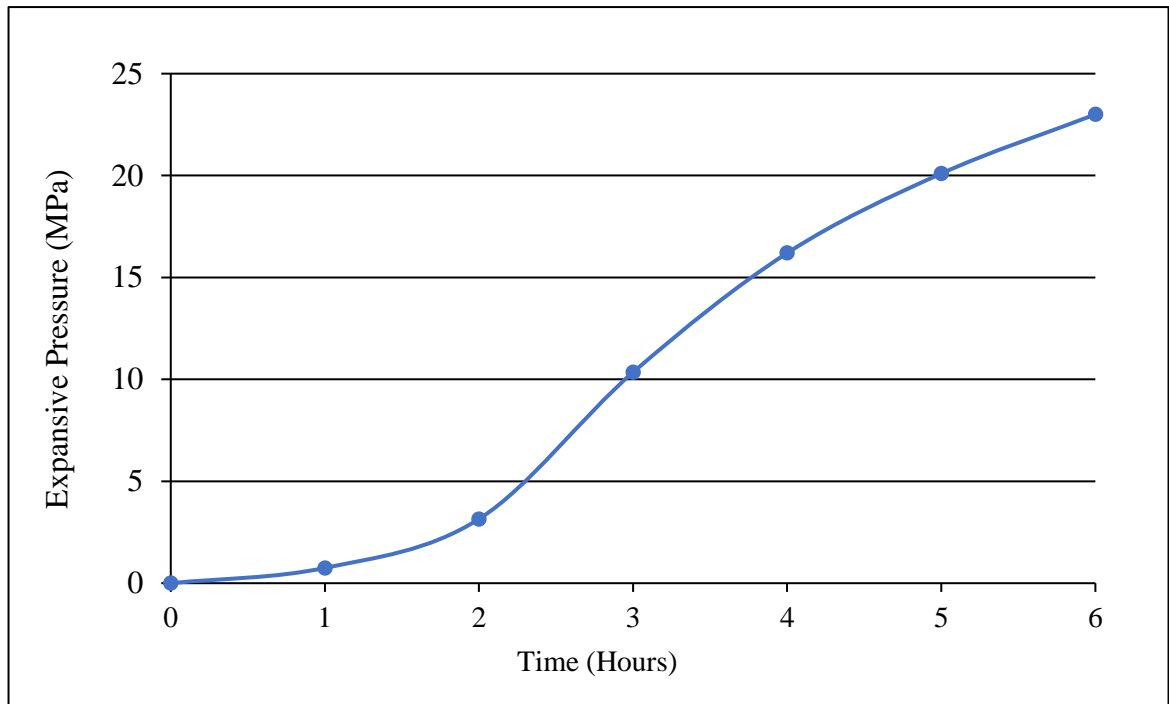


Figure 4-7: Expansive pressure generated by pure SCDA (Betonamit)

4.2.1.1 Sodium Chloride

As discussed in Section 2.12.1, there are several studies that report the effect of sodium chloride as an accelerator. Studies have reported negative effects on the integrity of cement; however, Theoduri and Asambla (2015) reported that the addition of 5% of NaCl BWOW accelerates the dissolution of lime (CaO) which results in the generation of calcium hydroxide. Consequently, various concentration of NaCl were investigated to study its effect on the expansive rate as shown

in Figure 4-8. Evidently, sodium chloride does not provide an increase in pressure but decreases the strength of the SCDA. As shown in Figure 4-8, there is an evident decrease in strength and pressure as the concentration of sodium chloride of increases.

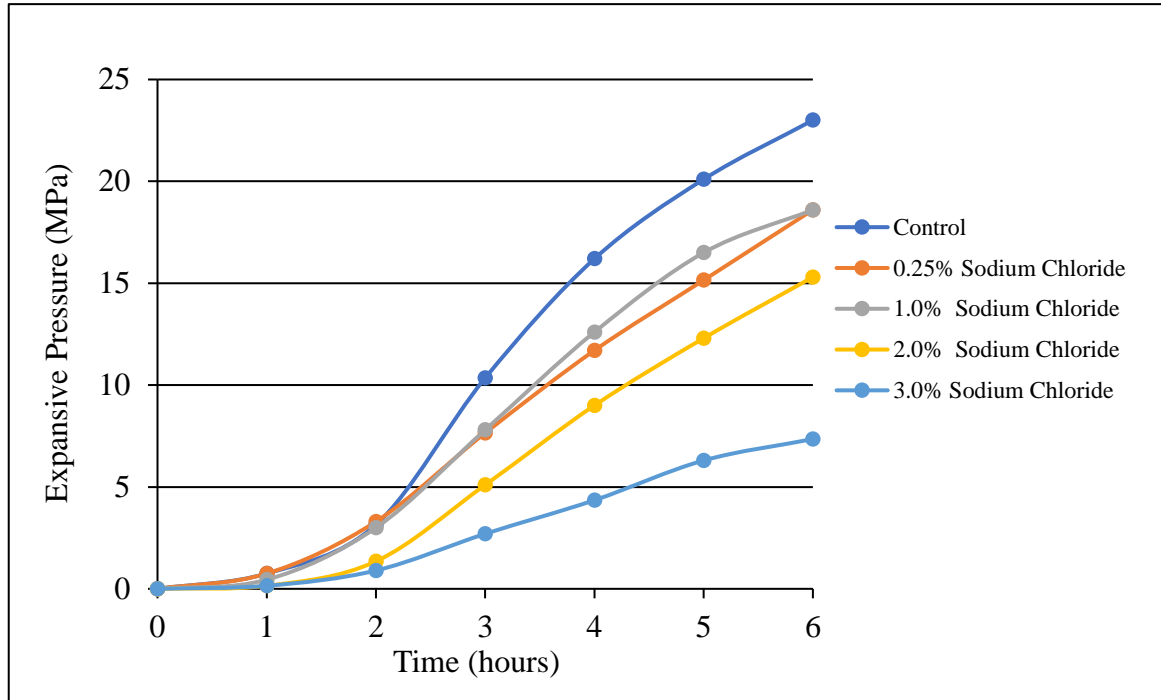


Figure 4-8: Expansive pressure generated by Betonamit and the addition of NaCl By Weight of Cement

4.3.1.2 Calcium Chloride

As discussed in Section 2.12.2, one of the most common accelerators is calcium chloride. Studies have reported positive effect on the formation of calcium hydroxide. Studies conducted by Abdelrazig et al. (1999) concluded that the addition of calcium salts has a pronounced effect on the calcium, hydroxyl and sulphate ion (Ca^{2+} , OH^- , and SO_4^{2-}) concentrations. Other studies show a higher degree of CaO hydration with the addition of 0.75% calcium chloride compared to that of pure Portland Cement. Consequently, various concentrations of CaCl_2 were investigated to study its effect on the expansive rate on Betonamit. As shown in Figure 4-9, the addition of 2-4 % of calcium chloride BWOW show favourable results towards an increase in the rate of pressure compared to that of pure Betonamit. This is in agreement with the findings conducted by Michaux (1989) who reported a concentration of 2-4% of calcium chloride BWOW for increased

compressive strength whereby the strength of cement is determined by the degree of hydration of cement.

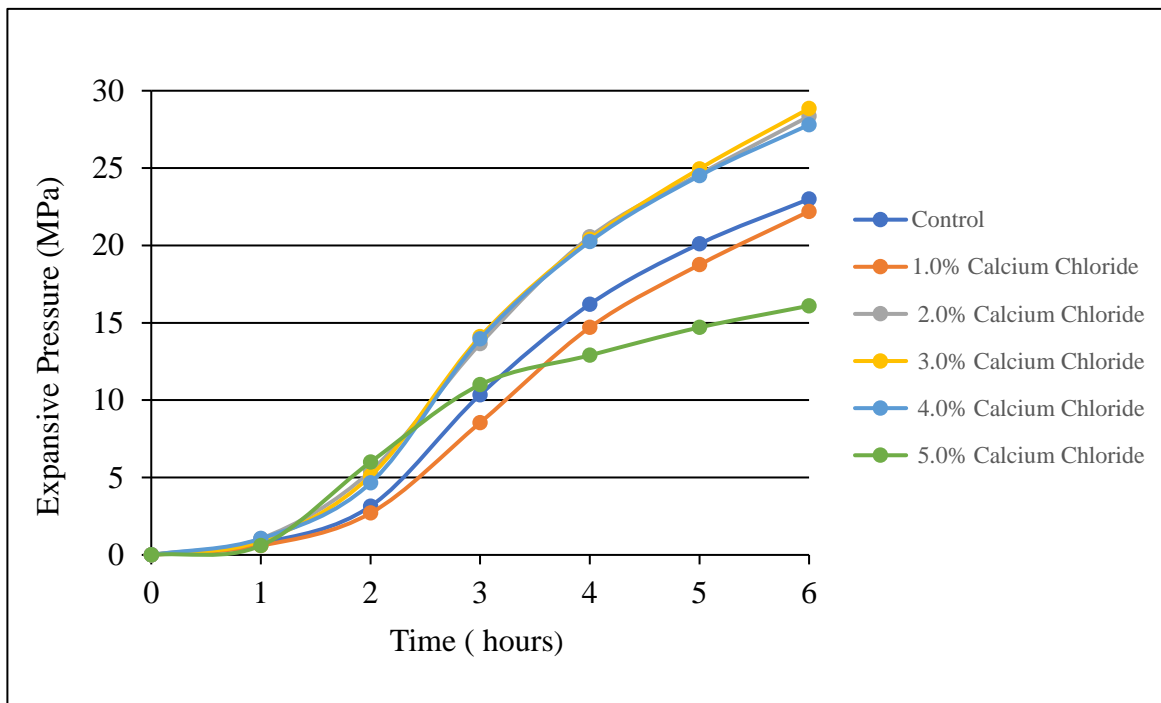


Figure 4-9: Expansive pressure generated by Betonamit and the addition of Calcium chloride By Weight of Water

As shown in Figure 4-10, 3-4% of CaCl_2 BWOW shows a significant increase in pressure in 3 hours. The addition of 2%, 3%, 4% of CaCl_2 BWOW generated a 32%, 36%, and 35% in increase of pressure respectively in 3 hours. As shown in Figure 4-11, the addition of 2%, 3%, and 4% of CaCl_2 BWOW generated 23%, 25%, and 17% increase of pressure respectively in 6 hours. Thus, the concentration of calcium chloride for optimal expansion in 6 hours is 3% of CaCl_2 BWOW.

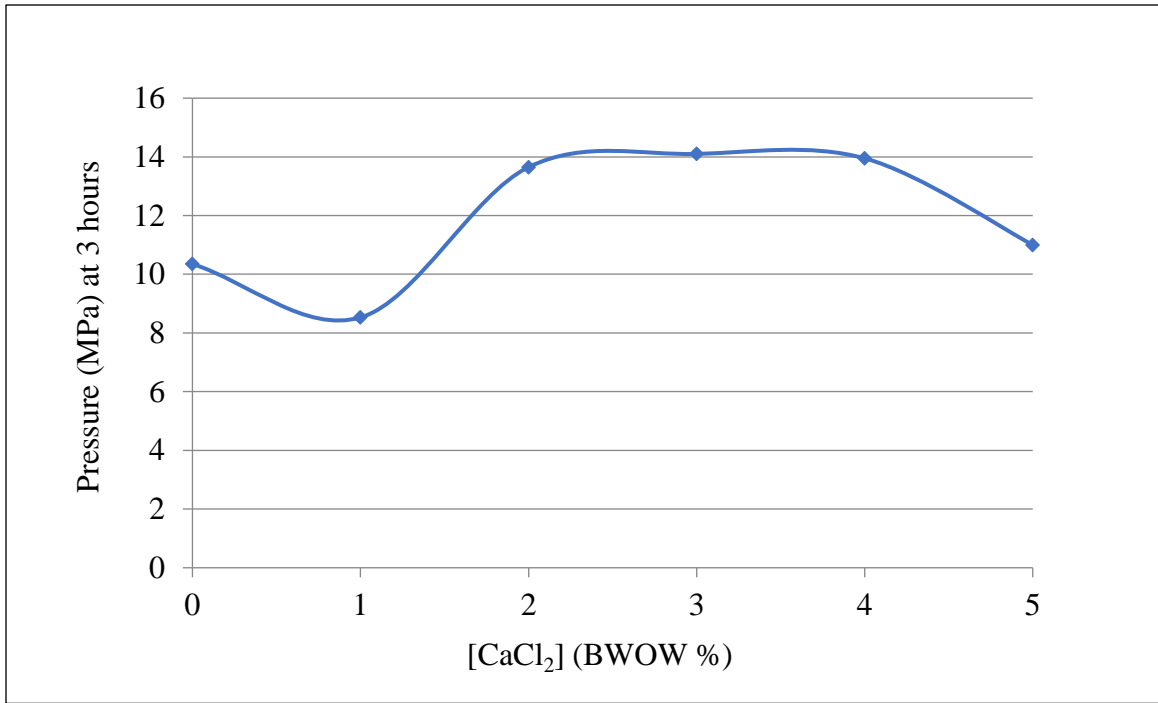


Figure 4-10: Pressure at 3 hours of various concentrations of CaCl₂

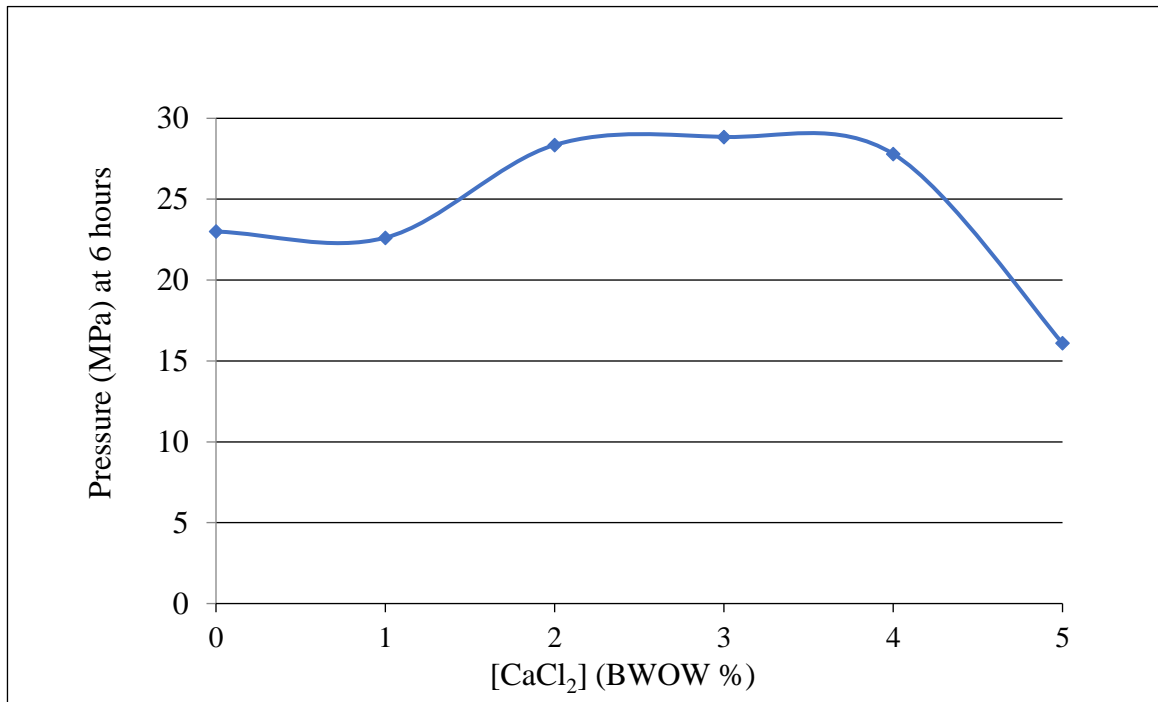


Figure 4-11: Pressure at 6 hours of various concentrations of CaCl₂

4.3.1.3 Calcium Formate

As discussed in Section 2.13.2, calcium formate is another common accelerator for concrete. Evidence suggests that the addition of calcium formate shortens the initial and final setting times and increases the compressive strength of Class G cements. Calcium formate is also shown to activate the liberation of the liberation of $\text{Ca}(\text{OH})_2$, a favourable product for expansion (Heikal,2004). Consequently, various concentrations of Calcium Formate were investigated to study its effect on the expansive rate. As shown in Figure 4-12, the addition of 2-3 % of calcium formate BWOC shows favourable results towards an increase in the rate of pressure compared to that of pure Betonamit. A noticeable decrease is shown with the addition of 4.0% of calcium formate. Evidence suggests that calcium formate has the potential in reducing the time of breakage of SCDA due to its accelerating properties.

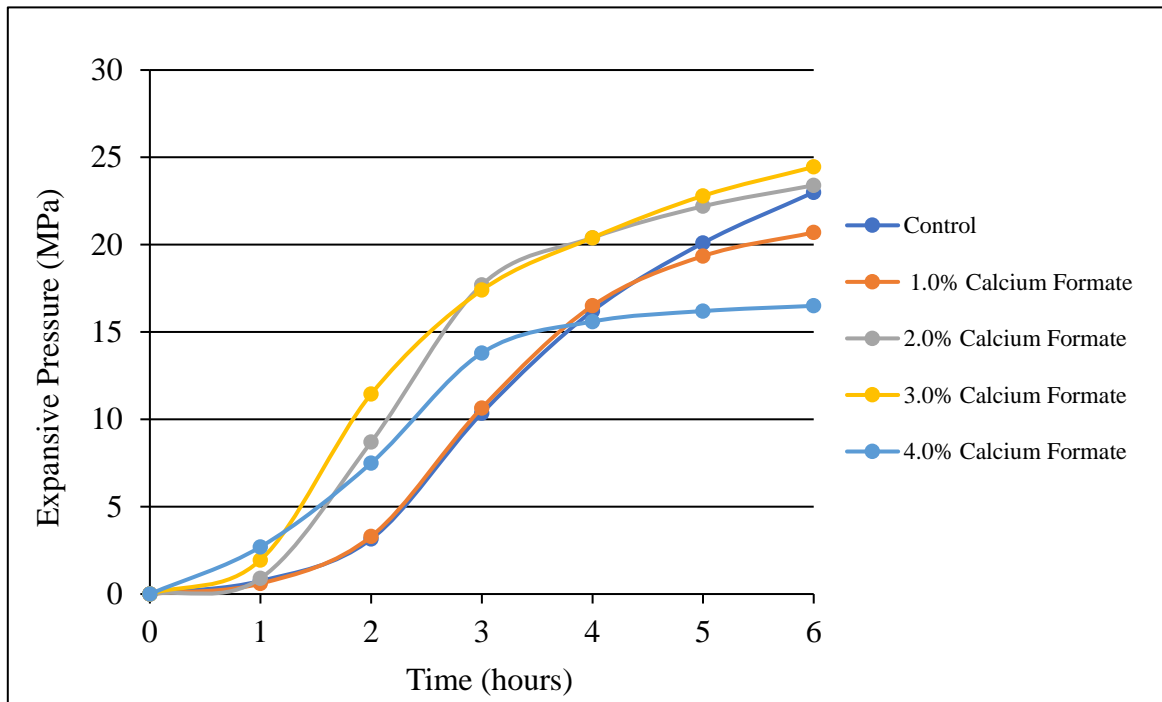


Figure 4-12: Expansive pressure generated by Betonamit and the addition of Calcium formate By Weight of Water

As shown in Figure 4-13, the addition of 2%, 3%, and 4% of calcium formate BWOC generated an 17%, 68%, and 33% in increase of pressure respectively in 3 hours. As shown in Figure 4-14, the addition of 2% and 3% of $\text{Ca}(\text{HCOO})_2$ BWOC generated a 17% and 6 % in increase of pressure respectively in 6 hours. A decrease in strength is evidenced with the addition of 4% and

consequently the SCDA loses its expansive strength. Thus, the concentration of calcium chloride for optimal expansion in 6 hours is 3%.

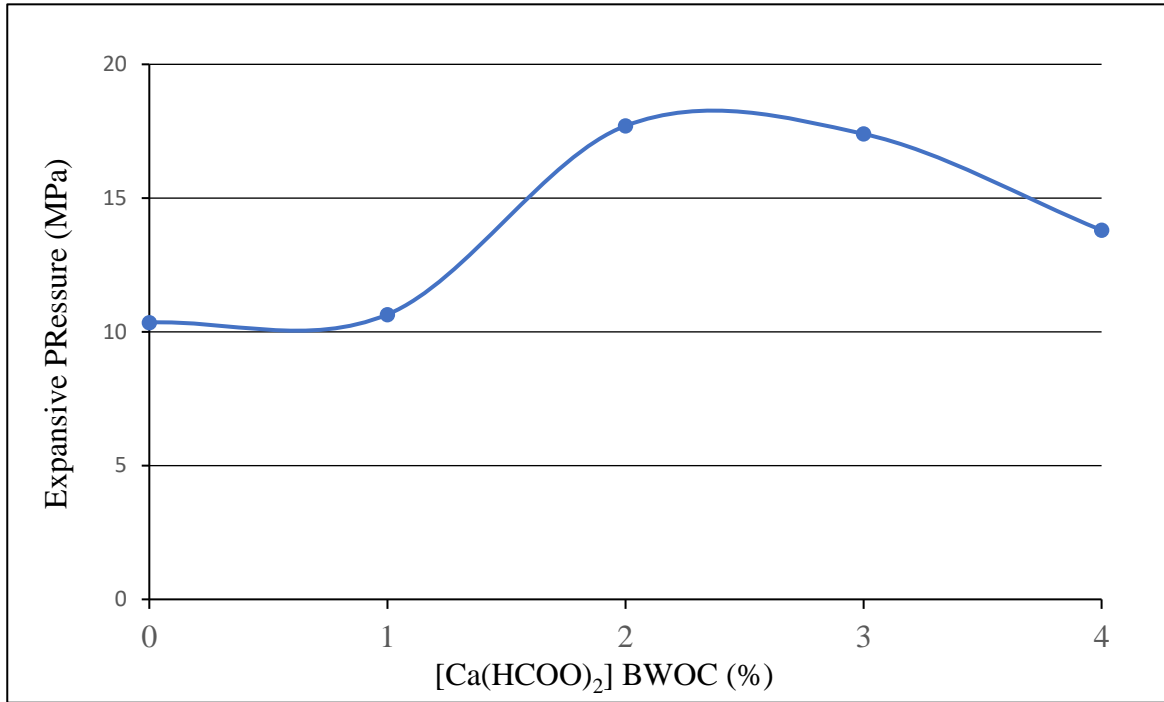


Figure 4-13: Pressure at 3 hours of various concentrations of Ca(HCOO)₂

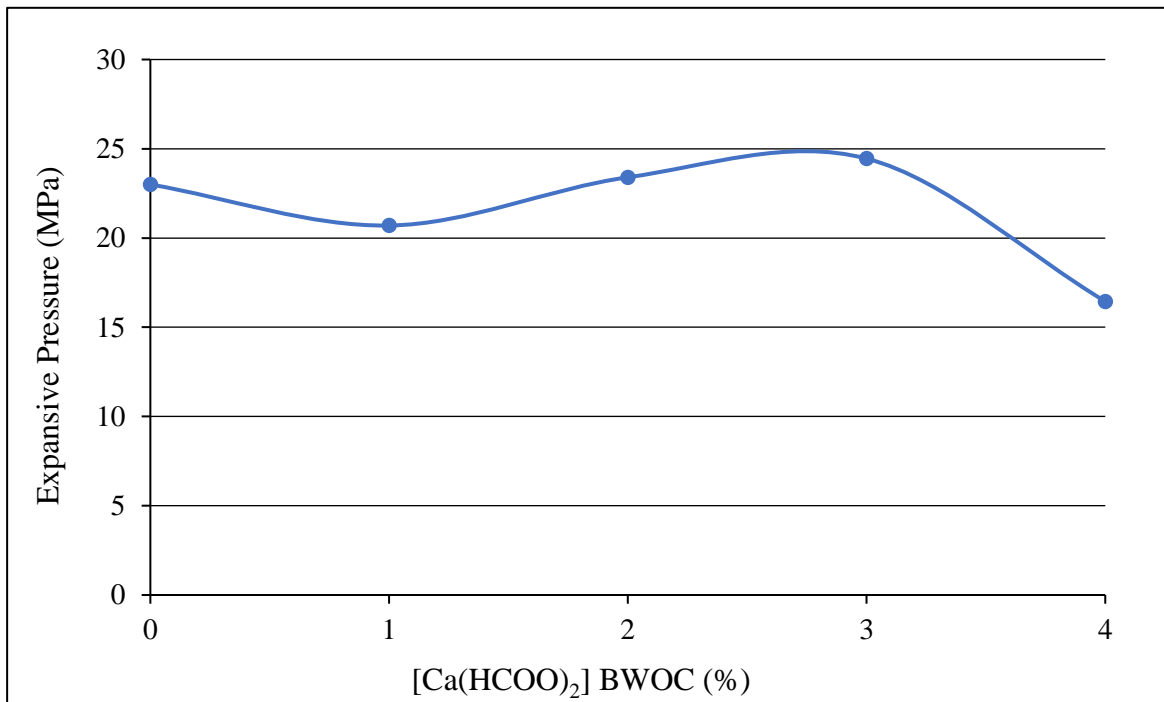


Figure 4-14: Pressure at 6 hours of various concentrations of Ca(HCOO)₂

4.3.1.4 Calcium Chloride vs. $\text{Ca}(\text{HCOO})_2$

Both the addition of 3% calcium chloride BWOW and 3% calcium formate BWOC to Betonamit show accelerating properties. As shown in Figure 4-15, a higher expansive pressure development is exhibited with the addition of 3% calcium formate BWOC between 1-4 hours compared to the control sample and Betonamit + 3% calcium chloride BWOW. There is a pressure increase of 68% at 3 hours with the addition of calcium formate whereas an increase in pressure of 35% with the addition of calcium chloride. The expansive pressure developed with the addition of calcium formate is almost 2 times the magnitude of pressure generated with the addition of calcium chloride in 3 hours. This indicates that earlier hydration occurs with the addition of Calcium Formate compared to calcium chloride. Nonetheless, the addition of 3% calcium chloride BWOW generated a higher expansive pressure at 6 hours compared to the control sample and Betonamit + 3% calcium formate BWOC.

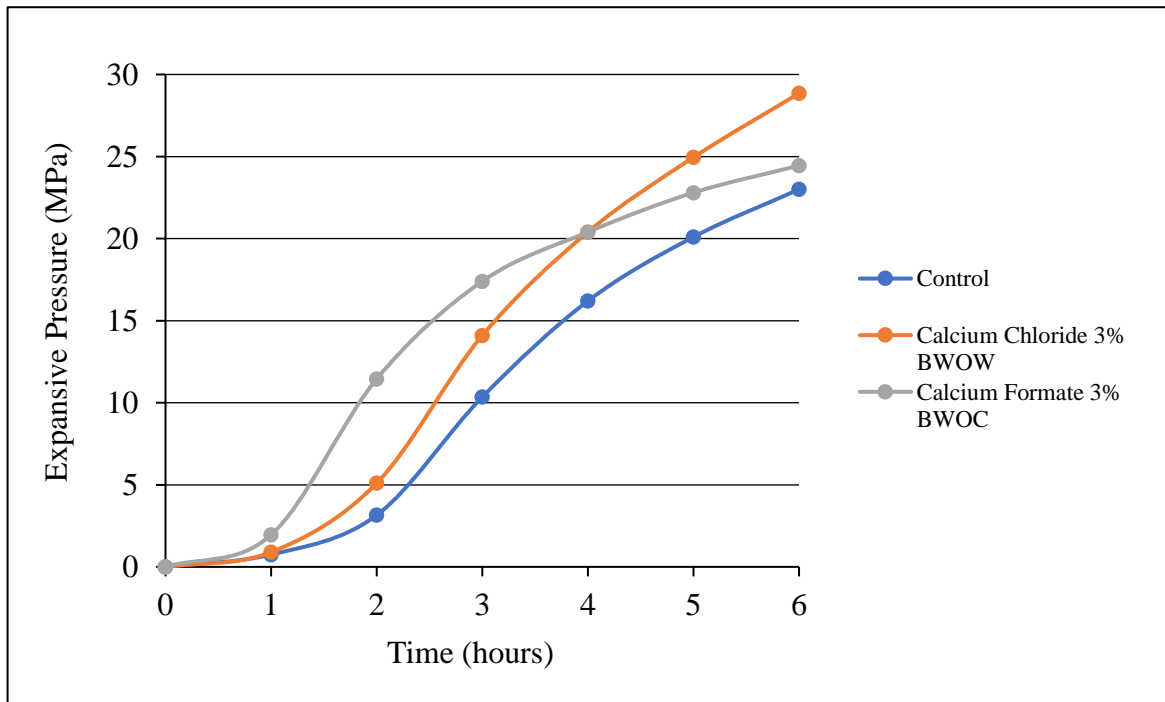


Figure 4-15: Expansive pressure of Betonamit + 3% of CaCl_2 BWOW and Betonamit +3% $\text{Ca}(\text{HCOO})_2$ BWOC

There is a pressure increase of 25% at 6 hours with the addition of calcium formate whereas an increase in pressure of 6% with the addition of calcium chloride. To conclude, both calcium formate and calcium chloride exhibit a higher rate expansive pressure compared to pure Betonamit suggesting that the usage of suitable additives have the potential to reduce time of breakage of hard rock in underground mines.

4.3.2 Test #2

Test #2 is conducted to physically observe the breakage of rock with the addition wt. % admixtures from Test #1 that resulted in the increase in the rate of expansive pressure. The aim of this investigation is to draw a comparison with Test#1 and confirm whether the selected admixtures will create a reduction in time of breakage. The crack growth is monitored over a period of 6 hours by measuring the crack width generated by each fracture. Each of the following figures should be views as a singular test due to the variability in ambient conditions and slight mixing variability.

4.3.2.1 Control

The control, pure Betonamit, will be used as a frame of reference for comparison of time of breakage and crack growth. A consistent fracture is not of interest in investigation but the time of breakage at which the concrete begins to fracture, and the magnitude of crack formation. For the control (pure Betonamit), fracture initiation occurred between 4-5 hours as shown in Figure 4-16- and 4-17. As demonstrated in Table 4-1, the pressure achieved in 4 and 5 hours of pure Betonamit is 16.2 MPa and 20.1MPa respectively possibly indicating the minimum pressure at which a fracture network will be generated assuming that all specimens are homogenous.

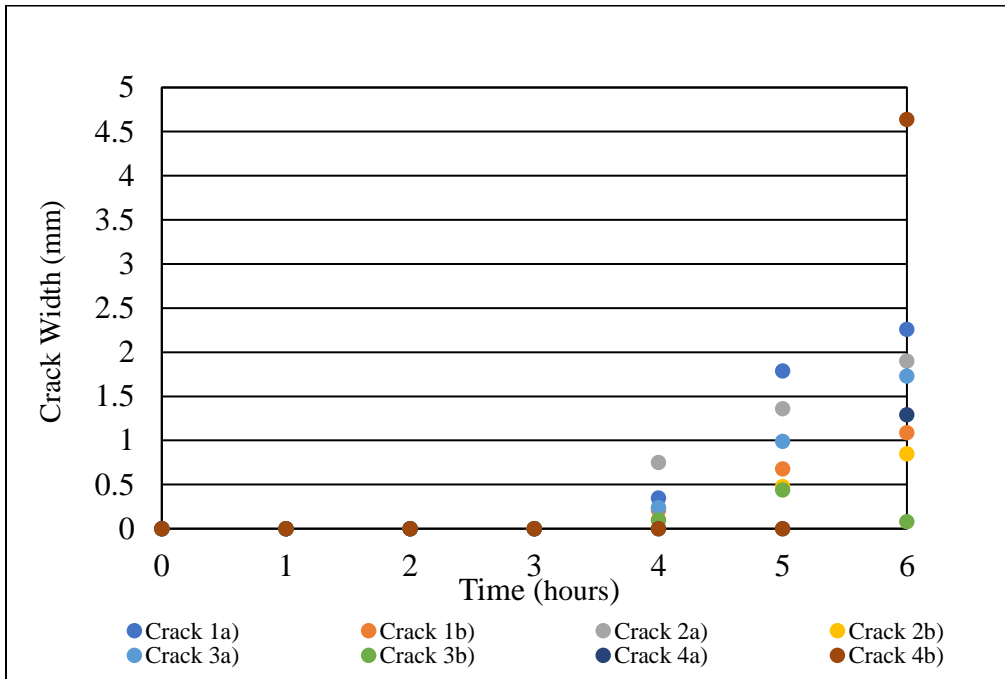


Figure 4-16: BET-Control-01a crack growth over a period of 6 hours

As shown in Figure 4-16 and Figure 4-17, the final magnitude of crack width is similar; however, crack width of 4.64 mm is achieved with BET-control a) in 6 hours while a crack width of 4.86mm is achieved in 6 hours. Thus, a reduction in time of fracture initiation should be at least below 4 hours and the magnitude of cracking should be of notable difference with the modified SCDA.

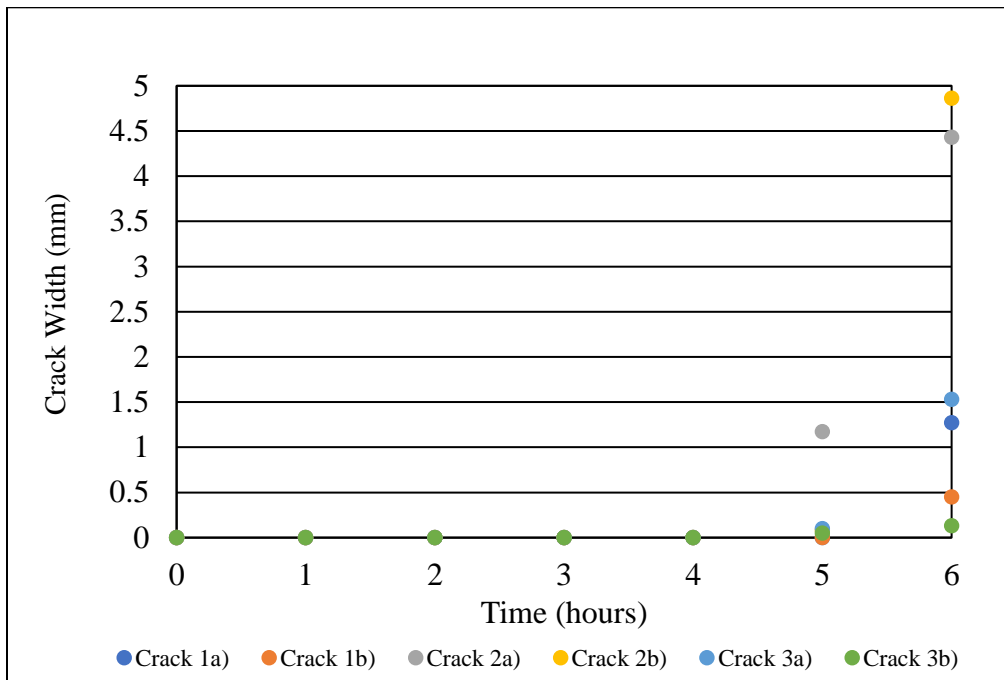


Figure 4-17: BET-Control-01b crack growth over a period of 6 hours

4.3.2.2 Calcium Formate

There was no evidence in time reduction with the addition of Calcium Formate (CF). As shown in Figure 4-18 and 5-19, the initiation of fracture was observed between 4-5 hours showing no noticeable decrease in time of fracture of initiation compared to that of pure Betonamit. As shown in Table 4-1, a pressure of 17.4MPa and 20.4 MPa is achieved in 4 and 5 hours respectively. Compared to that of pure Betonamit, there is no significant increase in pressure between 4-5 hours justifying the parallel in the time of breakage. However, an increase in the degree of fragmentation is observed. As shown in Figure 4-18, and 4-19, a higher degree of fracture generation is demonstrated by a higher crack width at the time of fracture with the addition of Calcium Formate compared to that of pure Betonamit in as shown in Figure 4-16 and 4-17. Thus, calcium formate does not provide much difference in the time of breakage.

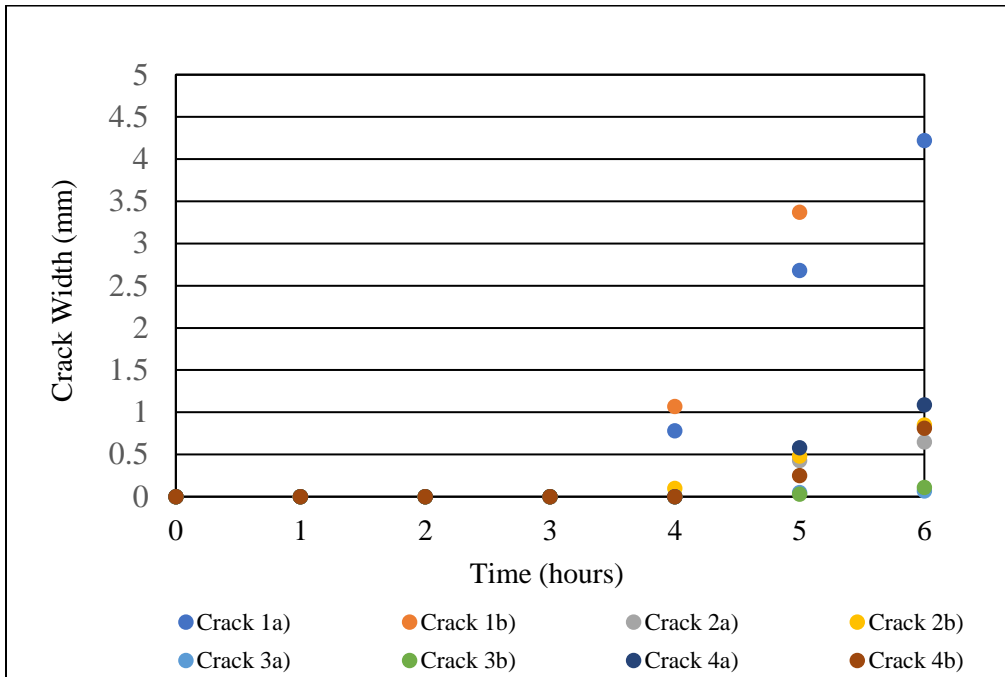


Figure 4-18: BET-Calcium Formate-3%-02a crack growth over a period of 6 hours

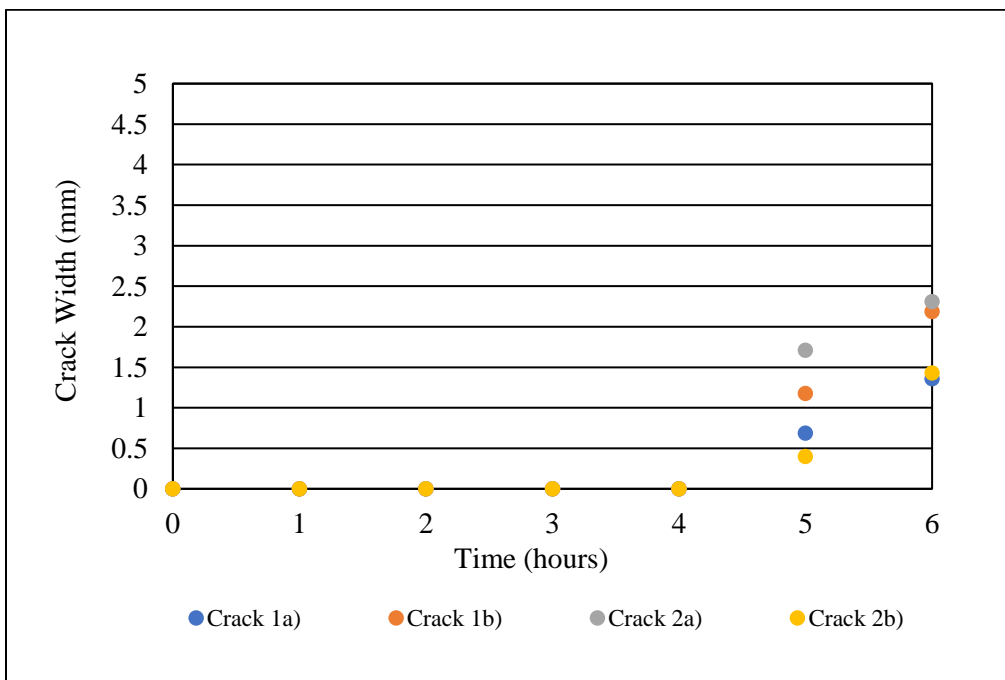


Figure 4-19: BET-Calcium Formate-3%-02b crack growth over a period of 6 hours

4.3.2.3 Calcium Chloride

As shown in Figure 4-5 and 4-6, the initiation of fracture occurred in 3.5 hours for specimen BET-CaCl₂-3%-03a) and 4.5 hours for BET-CaCl₂-3%-03b). The delay in the time of fracture between the duplicates can be explained by the humidity difference when the test was performed such that the BET-CaCl₂-3% 03b) was exposed to 25% humidity as opposed to the consistent 20% humidity measure which may have compromised the SCDA (Refer to Table 3-4). Studies have shown that there is substantial decrease in the rate of hydration of cement when cured in relatively humid conditions causing adverse effect on the curing the cement (Nilsson, 1980). While the control takes 4-5 hours to generate fracture there is still a reduction in the time of breakage for BET-CaCl₂-3% 03b) of about 0.5 hours. This is well in accordance with Figure 4-2 where a pressure of 17.7MPa is achieved in 3.5 hours with the addition of 3% CaCl₂ BWOW and a pressure of 16.2 MPa is achieved in 4 hours with pure Betonamit which is when the time of fracture occurred. However, a conclusive statement on the reduction of time of breakage cannot be made due to a lack of repeatability.

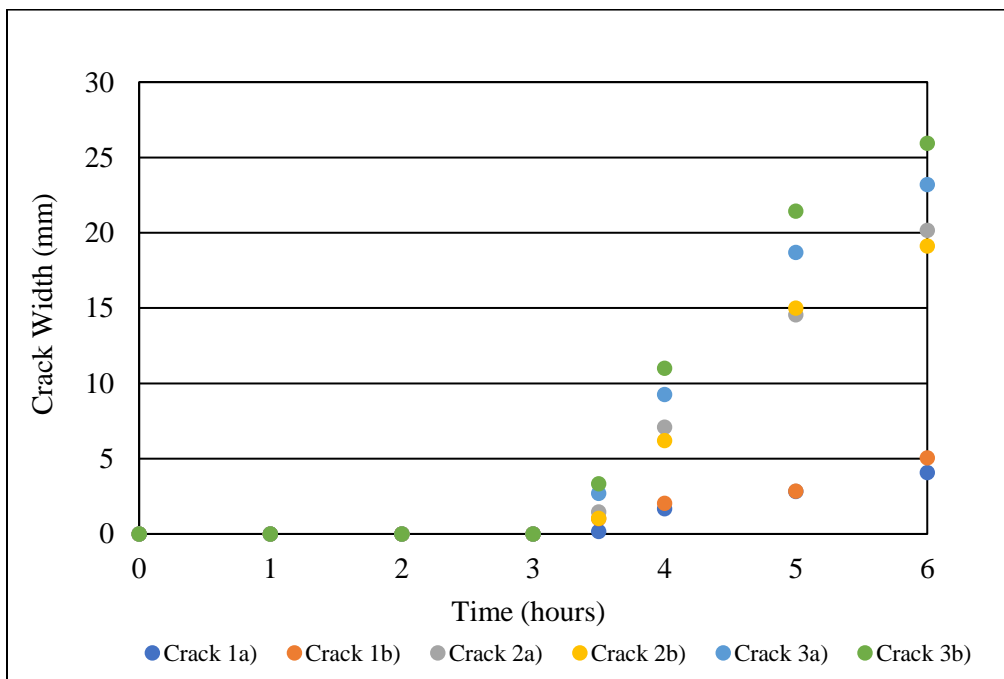


Figure 4-20: BET-Calcium Chloride-3%-03a crack growth over a period of 6 hours

Nonetheless, a higher degree of crack growth is noticed with the addition of 3% CaCl₂ BWOW for both specimens. As shown in Figure 4-20 and 4-21, a crack width of 25.94mm is generated by

BET-Calcium Chloride-3%-03a whereas a crack width of 5.53 mm is generated by BET-Calcium Chloride-3%-03b in 6 hours. While both exhibited a wide gap in the degree of fragmentation compared the control sample, both exhibit a higher degree of fragmentation at the end of 6 hours. This is indicative that more tests are needed to be repeated to duplicate the results obtained by the specimen BET-Calcium Chloride-3%-03a.

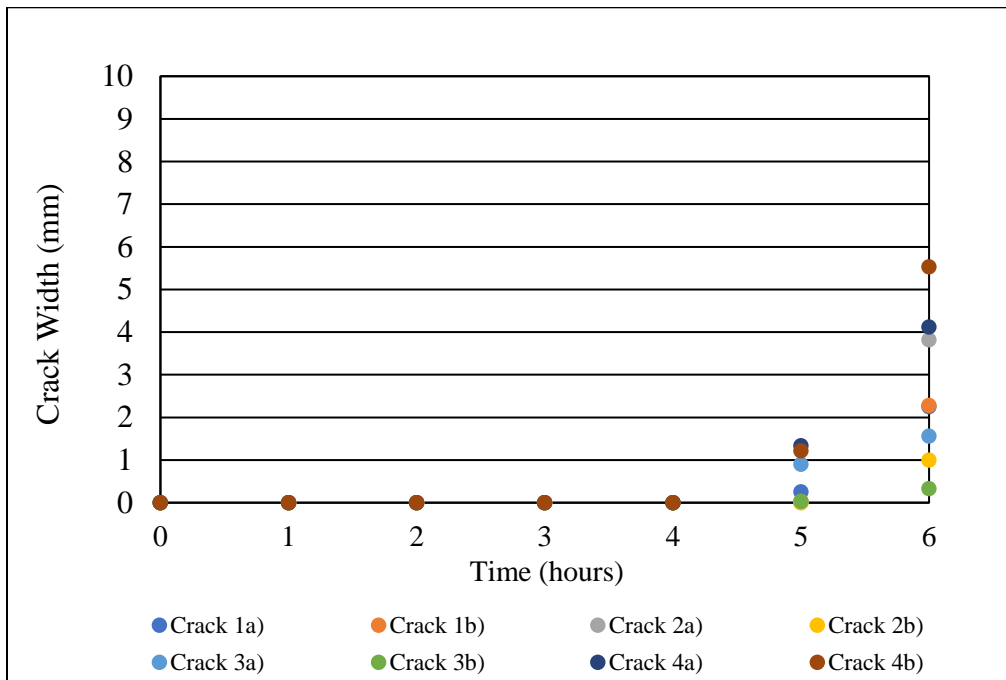


Figure 4-21: BET-Calcium Chloride-3%-03b crack growth over a period of 6 hours

Chapter 5

Conclusion

5.1 Experiment Results

The use of SCDA for the breakage of rock in situ is both novel and unique. Although the base version is already available commercially and is used in construction and demolition industry, it has never been attempted before in underground mine developments. The novelty of this technology lies in the simplicity of its use while offering a safer means for the fragmentation of rock as opposed to blasting. However, due to different confinement (stress) conditions underground, the performance must be enhanced to develop a meaningful effect and feasible method. To enhance the performance of SCDA, it is aimed to improve the rate of expansive pressure generated. This study addresses the time to achieve rock breakage by investigating the effect of accelerators on SCDA in the aim of increasing the rate of pressure and moving one step forward towards the goal of rock fragmentation with SCDA in underground mines. In this thesis, studies have been conducted to find the appropriate concentration of selected admixtures to increase the hydration rate of lime (CaO) and therefore increase the rate expansive pressure of Betonamit; the selected SCDA for this study. The pressure of SCDA and the modified SCDA were monitored over a period of 6 hours to examine the accelerating properties due to the additives selected which included sodium chloride, calcium formate and calcium chloride. This study also examines the time to fracture initiation as well as the degree of fragmentation using optimal concentration of additives for optimal expansion. The following is a list of findings from the studies conducted.

1. The expansive pressure of the control sample in 3 hours and 6 hours are 10.35MPa and 23MPa, respectively.
2. Sodium chloride does not provide an increase in pressure but decreases the strength of the SCDA.
3. The addition of 2-4 % of CaCl₂ BWOW shows an increase in the rate of pressure compared to that of pure Betonamit. The optimal concentration of CaCl₂ BWOW for utmost expansion is 3% where a pressure increase of 36% and 25% is achieved in 3 and 6 hours, respectively.

4. The addition of 2-4 % of $\text{Ca}(\text{HCOO})_2$ BWOC shows an increase in the rate of pressure compared to that of pure Betonamit. The optimal concentration of $\text{Ca}(\text{HCOO})_2$ BWOC for utmost expansion is 3% where CaCl_2 where an increase of 17% and 6% is achieved in 3 and 6 hours, respectively.
5. A higher degree of fragmentation on concrete cubes is achieved with the addition of 3% CaCl_2 BWOW compared to that of pure Betonamit
6. A conclusive statement cannot be made on the time of breakage due to the lack of repeated results. This is due to the variability in humidity conditions and slight variability in the mixing times. The mixing procedure should be carefully monitored.

5.3 Future Testing

Further tests are required to standardize the mixing procedure and preparation of the additive to ensure reliable and repeatable results. Due to different humidity level during the experimentation of Test #2, its effects should be reported. Although SCDA may be used as an alternative method for rock fragmentation, there is lack of research regarding its use in high in-situ stress conditions such as in underground mines. During the fracturing process, there are many factors affecting its volumetric expansion thus making proper quantification of expansive pressure complex. Proper quantification of pressure is necessary for a controllable effective rock fragmentation of rock fragmentation method. Future work would include monitoring the effect of different environmental conditions, pattern design and borehole size for optimal fracture propagation. While SCDA are found to be widely applicable in civil engineering applications, there is a growing interest in investigating its performance under large confining pressure due to in-situ stresses.

5.4 Statement of Contribution

This study examines the expansive pressure of SCDA in attempt to optimize its performance for the potential usage as non-explosive method for breaking rock in underground mines. The use of chemical additives shows promising results in accelerating the rate of expansive pressure compared to that of pure SCDA.

References

Abdelrazig, B. E. I., Bonner, D. G., Nowell, D. V., Dransfield, J. M., & Egan, P. J. (1999). The solution chemistry and early hydration of ordinary portland cement pastes with and without admixtures. *Thermochimica acta*, 340, 417-430.

AEISG, AEISG Code of Practice, Elevated Temperature and Reactive ground, Australian Explosives Industry Safety Group, (2012)

Arshadnejad, S., Goshtasbi, K., & Aghazadeh, J. (2011). A model to determine hole spacing in the rock fracture process by non-explosive expansion material. *International Journal of Minerals, Metallurgy, and Materials*, 18(5), 509.

ASTM, C. 845 Standard: standard specification for expansive hydraulic cement. Annual book of ASTM standards, 390-3

ASTM, C. C39M (2012) Standard test method for compressive strength of cylindrical concrete specimens. *American Society for Testing and Materials, ASTM, West Conshohocken*.

Bentur, A., & Ish-Shalom, M. (1974). Properties of type K expansive cement of pure components II. Proposed mechanism of ettringite formation and expansion in unrestrained paste of pure expansive component. *Cement and concrete research*, 4(5), 709-721

Bensted, J. (1978). Effect of accelerator additives on the early hydration of Portland Cement. *II Cemento*, 75, 13-20.

Bye, G. C. (1999). *Portland cement: composition, production and properties*. Thomas Telford.

C. Gomez, T. Mura, Stresses caused by expansive cement in borehole. *Journal of Engineering Mechanics*, 110, 1001-1005, 1984.

Cody, A. M., Lee, H., Cody, R. D., & Spy, P. G. (2004). The effects of chemical environment on the nucleation, growth, and stability of ettringite $[\text{Ca}_3\text{Al}(\text{OH})_6]_2(\text{SO}_4)_3 \cdot 26\text{H}_2\text{O}$. *Cement and Concrete Research*, 34(5), 869-881.

Cohen, M. D. (1983). Modeling of expansive cements. *Cement and Concrete Research*, 13(4), 519-528.

Cohen, M. D. (1983). Theories of expansion in sulfoaluminate-type expansive cements: schools of thought. *Cement and Concrete Research*, 13(6), 809-818.

El Dessouki, A.; Mitri, H. Rock breakage using expansive cement. *Engineering* 2011, 3, 168.

Farnfield, R.; Wetherelt, A. (2004), After-Blast Fumes from ANFO Mixtures, *Quarry Management*, 31, (2), 11-19.

Folliard, K. J., Ohta, M., Rathje, E., & Collins, P. (1994). Influence of mineral admixtures on expansive cement mortars. *Cement and concrete research*, 24(3), 424-432.

Fu, Y., Gu, P., Xie, P., & Beaudoin, J. J. (1995). Effect of chemical admixtures on the expansion of shrinkage-compensating cement containing a pre-hydrated high alumina cement—based expansive additive. *Cement and concrete research*, 25(1), 29-38

Gambatese, J.A. (2003) “Controlled concrete demolition using expansive cracking agents” *Journal of Construction Engineering and Management*, Vol. 129, pp.98-104

Guo, T., Zhang, S., Ge, H., & Qu, Z. (2015). A Novel" Soundless Cracking Agent Fracturing" for Shale Gas Reservoir Stimulation. *International Journal of Environmental Science and Development*, 6(9), 681.

Han, B., Zhang, L., & Ou, J. (2017). Self-Expanding Concrete. In *Smart and Multifunctional Concrete Toward Sustainable Infrastructures* (pp. 37-53). Springer, Singapore.

Hanif, M. (1997). Deformation behavior of rock around a borehole filled with expansive cement. *Journal of King Abdulaziz University Engineering Sciences*, 9, 93-107.

Hanif, M., Mohammed, N. O. O. R., & AL-MAGHRABI, N. H. (2007). Effective use of expansive cement for the deformation and fracturing of granite. *Gazi University Journal of Science*, 20(1), 1-5

Haque, M. N. (1980). Properties of concrete with and without calcium chloride during drying and wetting. *Cement and Concrete Research*, 10(3), 377-385.

Harada, T.; Idemitsu, T.; Watanabe, A.; Takayama, S.-I. The design method for the demolition of concrete with expansive demolition agents. In *Fracture Concrete and Rock*; Springer: Berlin, Germany, 1989; pp. 47–57.

Heikal, M. (2004). Effect of calcium formate as an accelerator on the physicochemical and mechanical properties of pozzolanic cement pastes. *Cement and Concrete Research*, 34(6), 1051-1056.

Hinze, J., & Brown, J. (1994). Properties of soundless chemical demolition agents. *Journal of construction engineering and management*, 120(4), 816-827

J. Bensted, iL Cemented 1, Plubblicimento, Roma, Italy, 1978, pp-13-20

J.S Lota, J Bensted, P.L, Pratt, Hydration of Class G oil well cement at 20°C and 5°C with calcium formate, Proceedings of 21st International Conference on Cement Microscopy, April 25-29, Las Vegas, Nevada, USA (1999) 160-179

Kishar, E. A., Ahmed, D. A., Mohammed, M. R., & Noury, R. (2013). Effect of calcium chloride on the hydration characteristics of ground clay bricks cement pastes. *Beni-Suef university journal of basic and applied sciences*, 2(1), 20-30.

Labuz, J. F., Shah, S. P., & Dowding, C. H. (1985, April). Experimental analysis of crack propagation in granite. In *International Journal of Rock Mechanics and Mining Sciences & Geomechanics Abstracts* (Vol. 22, No. 2, pp. 85-98). Pergamon

M.Levitt, Precast Concrete, Applied Science Publishers, London 1982.

Mather, B. (1970). *Expansive Cement (C-70-21)*. US Army Engineer Waterways Experiment Station.

Mehta, P. K. (1973). Mechanism of expansion associated with ettringite formation. *Cement and Concrete Research*, 3(1), 1-6.

Michaux, M., Nelson, E., & Vidick, B. (1989). Cement chemistry and additives. *Oilfield Review*, 1(1), 18-25.

- Mikhailov, V., Litver, S., Popov, A., & Popova, V. (1973). *U.S. Patent No. 3,775,143*. Washington, DC: U.S. Patent and Trademark Office.
- Moore, A. E., & Taylor, H. F. W. (1970). Crystal structure of ettringite. *Acta Crystallographica Section B: Structural Crystallography and Crystal Chemistry*, 26(4), 386-393.
- Musunuri, A.; Mitri, H. Laboratory investigation into rock fracturing with expansive cement. *International Journal of Mining and Mineral Engineering* **2009**, 1, 327-345.
- Natanzi, A.S.; Laefer, D.F.; Connolly, L. Cold and moderate ambient temperatures 965 effects on expansive pressure development in soundless chemical demolition agents. 966 *Construction and Building Materials* 2016, 110, 117-127
- Nilsson, L O. (1980). Hygroscopic moisture in concrete - drying, measurement and related material properties, Report, TVBM 1003, Lund Institute of Technology, Lund.
- Opravil, T., Ptáček, P., Šoukal, F., Havlica, J., & Brandštetr, J. (2013). The synthesis and characterization of an expansive admixture for M-type cements I. The influence of free CaO to the formation of ettringite. *Journal of thermal analysis and calorimetry*, 111(1), 517-526.
- Özmen, İ., & Aksoy, E. (2015). Respiratory Emergencies and Management of Mining Accidents. *Turkish thoracic journal*, 16(Suppl 1), S18.
- Ribeiro, M. S. S. (1998). Expansive cement blend for use in shrinkage-compensating mortars. *Materials and Structures*, 31(6), 400-404.
- Sheikh, S. A., Fu, Y., & O'Neill, M. W. (1994). Expansive cement concrete for drilled shafts. *ACI Materials Journal*, 91(3), 237-245.
- Soeda, K., & Harada, T. (1994). The mechanics of expansive pressure generation with expansive demolition agents. *Concrete Library of JSCE*, 23, 121-135.
- Stark, J., & Bollmann, K. (2000). Delayed ettringite formation in concrete. *NORDIC CONCRETE RESEARCH-PUBLICATIONS-*, 23, 4-28.
- Taylor, H.F.W. (1997) *Cement Chemistry*, Thomas Telford, London.

Tenoutasse N, The Hydration Mechanism of C3A and C3S in the Presence of Calcium Chloride and Calcium Sulphate, Proceedings 5th International Symposium on the Chemistry of Cement, Cement Association of Japan, Tokyo, Vol 2, 1969, pp 372-378.

Teodoriu, C.; Asamba, P. Experimental study of salt content effect on class g cement properties with application to well integrity. J. Nat. Gas Sci. Eng. 2015, 24, 324–329

Timoshenko, S., & Goodier, J. N. Theory of elasticity. 1951. New York, 412, 108.

Zhou, X.; Lin, X.; Huo, M.; Zhang, Y. The hydration of saline oil-well cement. Cem. Concr. Res. 1996, 26, 1753–1759

Websites:

<http://www.betonamit.com/technical-manual/> Betonamit technical manual - non-explosive cracking agent (2016) (8 April)

<http://www.dexpan.com/dexpan-non-explosive-controlled-demolition-agent-silent-cracking-breaking.aspx> Archer USA. (Oct 5, 2016)

<http://www.ecobust.com/> Ecobust. (Apr 8, 2016)

<http://www.expando.com.au/what-is-expando> Expando, expansive mortar, non explosive demolition agent used for rock, concrete breaking. (Apr 8, 2016)

http://www.taiheiyom.co.jp/english/product/productSubtop_4/product_4/productEntrye023.html Bristar (for general purpose/bulk type) | non-explosive demolition agent | taiheiyom materials corporation. (8 Apr 2016)

Appendix I : Table of Data Findings

Table I-1: Strain Values (Refer to Table 3-1 for specimen specifications)

Time (min)	S41-BET-01a		S41-BET-01b		Average Pressure (MPa)
	Microstrain($\mu\epsilon$)	Pressure (MPa)	Microstrain($\mu\epsilon$)	Pressure (MPa)	
0	0	0	0	0	0
15	0	0	1.00E-06	0.3	0.15
30	1.00E-06	0.3	2.00E-06	0.6	0.45
45	1.00E-06	0.3	2.00E-06	0.6	0.45
60	2.00E-06	0.6	3.00E-06	0.9	0.75
75	2.00E-06	0.6	4.00E-06	1.2	0.9
90	2.00E-06	0.6	7.00E-06	2.1	1.35
105	5.00E-06	1.5	1.00E-05	3	2.25
120	8.00E-06	2.4	1.30E-05	3.9	3.15
135	1.40E-05	4.2	1.70E-05	5.1	4.65
150	2.10E-05	6.3	2.20E-05	6.6	6.45
165	2.90E-05	8.7	2.70E-05	8.1	8.4
180	3.70E-05	11.1	3.20E-05	9.6	10.35
195	4.20E-05	12.6	3.70E-05	11.1	11.85
210	4.80E-05	14.4	4.00E-05	12.3	13.35
225	5.40E-05	16.2	4.50E-05	13.5	14.85
240	5.90E-05	17.7	4.90E-05	14.7	16.2
255	6.30E-05	18.9	5.20E-05	15.6	17.25
270	6.60E-05	19.8	5.40E-05	16.2	18
285	7.00E-05	21	5.80E-05	17.4	19.2
300	7.30E-05	21.9	6.10E-05	18.3	20.1
315	7.50E-05	22.5	6.30E-05	18.9	20.7
330	7.70E-05	23.1	6.70E-05	20.1	21.6
345	7.90E-05	23.7	6.90E-05	20.7	22.2
360	8.20E-05	24.6	7.10E-05	21.3	23

Table I-2: Strain Values (Refer to Table 3-2 for specimen specifications)

Time (min)	S41-BET-NaCl-01a		S41-BET-NaCl-01b		Average Pressure (MPa)
	Microstrain($\mu\epsilon$)	Pressure (MPa)	Microstrain($\mu\epsilon$)	Pressure (MPa)	
0	0	0	0	0	0
15	1.00E-06	0.3	1.00E-06	0.3	0.3
30	1.00E-06	0.3	1.00E-06	0.3	0.3
45	2.00E-06	0.6	2.00E-06	0.6	0.6
60	3.00E-06	0.9	3.00E-06	0.9	0.9
75	5.00E-06	1.8	5.00E-06	1.8	1.8
90	7.00E-06	2.1	7.00E-06	2.3	2.2
105	1.00E-05	3	1.00E-05	3	3
120	1.30E-05	3.9	1.30E-05	3.9	3.9
135	1.60E-06	4.8	1.60E-06	4.8	4.8
150	2.00E-06	6	2.00E-06	6	6
165	2.40E-06	7.2	2.40E-06	7.2	7.2
180	2.80E-05	8.4	2.80E-05	8.4	8.4
195	3.20E-05	9.6	3.20E-05	9.6	9.6
210	3.40E-06	10.5	3.40E-06	10.2	10.35
225	3.70E-06	11.4	3.70E-06	11.1	11.25
240	4.20E-05	12.6	4.20E-05	12.6	12.6
255	4.50E-05	13.5	4.50E-05	13.5	13.5
270	4.80E-05	14.4	4.80E-05	14.4	14.4
285	5.10E-05	15.3	5.10E-05	15.3	15.3
300	5.40E-05	16.2	5.40E-05	16.2	16.2
315	5.70E-05	17.1	5.70E-05	17.1	17.1
330	6.00E-05	18	6.00E-05	18	18
345	6.30E-05	18.9	6.30E-05	18.9	18.9
360	6.60E-05	19.8	6.60E-05	19.8	19.8

Table I-3: Strain Values (Refer to Table 3-2 for specimen specifications)

Time (min)	S41-BET-NaCl-02a		S41-BET-NaCl-02b		Average Pressure (MPa)
	Microstrain($\mu\epsilon$)	Pressure (MPa)	Microstrain($\mu\epsilon$)	Pressure (MPa)	
0	0	0	0	0	0
15	0.00E+00	0	0.00E+00	0	0
30	0.00E+00	0	0.00E+00	0	0
45	1.00E-06	0.3	0.00E+00	0	0.15
60	2.00E-06	0.6	1.00E-06	0.3	0.45
75	3.00E-06	0.9	3.00E-06	0.9	0.9
90	4.00E-06	1.2	5.00E-06	1.5	1.35
105	7.00E-06	2.1	7.00E-06	2.1	2.1
120	1.00E-05	3	1.00E-05	3	3
135	1.40E-05	4.2	1.30E-06	3.9	4.05
150	1.80E-05	5.4	1.80E-05	5.4	5.4
165	2.20E-05	6.6	2.20E-05	6.6	6.6
180	2.60E-05	7.8	2.60E-05	7.8	7.8
195	3.10E-05	9.3	3.00E-06	8	8.65
210	3.40E-05	10.2	3.40E-05	10.2	10.2
225	3.80E-05	11.4	3.80E-05	11.4	11.4
240	4.20E-05	12.6	4.10E-05	12.6	12.6
255	4.50E-05	13.5	4.50E-05	13.8	13.65
270	4.90E-05	14.7	4.90E-05	15	14.85
285	5.10E-05	15.3	5.10E-05	15.9	15.6
300	5.40E-05	16.2	5.40E-05	16.8	16.5
315	5.60E-05	16.8	5.60E-05	17.4	17.1
330	5.80E-05	17.4	5.80E-05	17.7	17.55
345	6.00E-05	18	6.00E-05	18	18
360	6.20E-05	18.6	6.20E-05	18.6	18.6

Table I-4: Strain Values (Refer to Table 3-2 for specimen specifications)

Time (min)	S41-BET-NaCl-03a		S41-BET-NaCl-03b		Average Pressure (MPa)
	Microstrain($\mu\epsilon$)	Pressure (MPa)	Microstrain($\mu\epsilon$)	Pressure (MPa)	
0	0	0	0	0	0
15	0.00E+00	0	0.00E+00	0	0
30	0.00E+00	0	0.00E+00	0	0
45	1.00E-06	0.3	0.00E+00	0	0.15
60	2.00E-06	0.6	0.00E+00	0	0.3
75	2.00E-06	0.6	0.00E+00	0	0.3
90	3.00E-06	0.9	0.00E+00	0	0.45
105	5.00E-06	1.5	1.00E-06	0.3	0.9
120	8.00E-06	2.4	2.00E-06	0.6	1.5
135	1.10E-05	3.3	5.00E-06	1.5	2.4
150	1.40E-05	4.2	8.00E-06	2.3	3.25
165	1.70E-05	5.1	1.20E-05	3.2	4.15
180	2.00E-05	6	1.50E-05	4.1	5.05
195	2.30E-05	6.9	1.80E-05	5	5.95
210	2.70E-05	8.1	2.10E-05	5.9	7
225	3.00E-05	9	2.40E-05	6.8	7.9
240	3.30E-05	9.9	2.70E-05	7.7	8.8
255	3.60E-05	10.8	3.00E-05	8.6	9.7
270	3.90E-05	11.7	3.30E-05	9.5	10.6
285	4.10E-05	12.3	3.60E-05	10.4	11.35
300	4.30E-05	12.9	3.90E-05	11.3	12.1
315	4.60E-05	13.8	4.20E-05	12.2	13
330	4.80E-05	14.4	4.50E-05	13.1	13.75
345	5.10E-05	15.3	4.80E-05	14	14.65
360	5.30E-05	15.9	5.10E-05	14.9	15.4

Table I-5: Strain Values (Refer to Table 3-2 for specimen specifications)

Time (min)	S41-BET-NaCl-04a		S41-BET-NaCl-04b		Average Pressure (MPa)
	Microstrain($\mu\epsilon$)	Pressure (MPa)	Microstrain($\mu\epsilon$)	Pressure (MPa)	
0	0	0	0	0	0
15	0.00E+00	0	0.00E+00	0	0
30	0.00E+00	0	0.00E+00	0	0
45	0.00E+00	0	0.00E+00	0	0
60	0.00E+00	0	0.00E+00	0	0.15
75	0.00E+00	0	1.00E-06	0.3	0.15
90	1.00E-06	0.3	1.00E-06	0.3	0.3
105	2.00E-06	0.6	1.00E-06	0.3	0.6
120	3.00E-06	0.9	2.00E-06	0.6	0.9
135	4.00E-06	1.2	3.00E-06	0.9	1.2
150	6.00E-06	1.8	5.00E-06	1.5	1.8
165	7.00E-06	2.1	6.00E-06	1.8	1.95
180	9.00E-06	2.7	8.00E-06	2.4	2.7
195	1.00E-05	3	1.00E-05	3	3
210	1.20E-05	3.6	1.10E-06	3.3	3.6
225	1.30E-05	3.9	1.30E-05	3.9	3.9
240	1.50E-05	4.5	1.60E-05	4.8	4.35
255	1.70E-05	5.1	1.80E-05	5.4	5.1
270	1.90E-05	5.7	2.00E-05	6	5.7
285	2.00E-05	6	2.10E-05	6.3	6
300	2.10E-05	6.3	2.20E-05	6.6	6.3
315	2.20E-05	6.6	2.30E-05	6.9	6.6
330	2.30E-05	6.9	2.40E-05	7.2	6.9
345	2.40E-05	7.2	2.50E-05	7.5	7.2
360	2.50E-05	7.5	2.60E-05	7.8	7.35

Table I-6: Strain Values (Refer to Table 3-3 for specimen specifications)

Time (min)	S41-BET-CaCl ₂ -01a		S41-BET-CaCl ₂ -01b		Average Pressure (MPa)
	Microstrain($\mu\epsilon$)	Pressure (MPa)	Microstrain($\mu\epsilon$)	Pressure (MPa)	
0	0	0	0	0	0
15	0.00E+00	0	0.00E+00	0	0
30	0.00E+00	0	0.00E+00	0	0
45	1.00E-06	0.3	1.00E-06	0.3	0.3
60	2.00E-06	0.6	2.00E-06	0.6	0.6
75	3.00E-06	0.9	2.00E-06	0.6	0.75
90	4.00E-06	1.2	4.00E-06	1.2	1.2
105	6.00E-06	1.8	6.00E-06	1.8	1.8
120	9.00E-06	2.7	8.00E-06	2.7	2.7
135	1.40E-05	4.2	1.40E-05	4.2	4.2
150	1.80E-05	5.4	1.80E-05	5.4	5.4
165	2.40E-05	7.2	2.40E-05	7.2	7.2
180	2.90E-05	8.7	2.80E-05	8.4	8.55
195	3.60E-05	10.2	3.60E-05	10.2	10.2
210	4.00E-05	12	4.00E-05	12	12
225	4.40E-05	13.2	4.40E-05	13.2	13.2
240	4.90E-05	14.7	4.90E-05	14.7	14.7
255	5.20E-05	15.6	5.20E-05	15.6	15.6
270	5.50E-05	16.5	5.60E-06	16.8	16.65
285	5.90E-05	17.7	5.90E-05	17.7	17.7
300	6.20E-05	18.6	6.30E-05	18.9	18.75
315	6.50E-05	19.5	6.50E-05	19.5	19.5
330	6.80E-05	20.4	6.80E-05	20.4	20.4
345	7.20E-05	21.6	7.20E-05	21.6	21.6
360	7.50E-05	22.5	7.30E-05	21.9	22.2

Table I-7. Strain Values (Refer to Table 3-3 for specimen specifications)

Time (min)	S41-BET-CaCl ₂ -02a		S41-BET-CaCl ₂ -02b		Average Pressure (MPa)
	Microstrain($\mu\epsilon$)	Pressure (MPa)	Microstrain($\mu\epsilon$)	Pressure (MPa)	
0	0	0	0	0	0
15	1.00E-06	0.3	0	0	0.15
30	2.00E-06	0.6	0	0.3	0.45
45	3.00E-06	0.9	2.00E-06	0.6	0.75
60	4.00E-06	1.2	3.00E-06	0.9	1.05
75	5.00E-06	1.5	4.00E-06	1.2	1.35
90	9.00E-06	2.7	8.00E-06	2.4	2.55
105	1.30E-05	3.9	1.20E-05	3.6	3.75
120	1.90E-05	5.7	1.70E-05	5.1	5.4
135	2.60E-05	7.8	2.30E-05	6.9	7.35
150	3.20E-05	9.6	3.00E-06	9	9.3
165	4.00E-05	12	3.60E-05	10.8	11.4
180	4.70E-05	14.1	4.40E-05	13.2	13.65
195	5.20E-05	15.6	5.00E-05	15	15.3
210	5.80E-05	17.4	5.60E-05	16.8	17.1
225	6.40E-05	19.2	6.20E-05	18.6	18.9
240	6.90E-05	20.7	6.80E-05	20.4	20.55
255	7.20E-05	21.6	7.00E-05	21	21.3
270	7.70E-05	23.1	7.30E-05	21.9	22.5
285	8.00E-05	24	7.60E-05	22.8	23.4
300	8.40E-05	25.2	8.00E-05	24	24.6
315	8.70E-05	26.1	8.30E-05	24.9	25.5
330	9.00E-05	27	8.70E+07	26.1	26.55
345	9.30E-05	27.9	9.00E-05	27	27.45
360	9.60E-05	28.8	9.30E-05	27.9	28.35

Table I-8: Strain Values (Refer to Table 3-3 for specimen specifications)

Time (min)	S41-BET-CaCl ₂ -03a		S41-BET-CaCl ₂ -03b		Average Pressure (MPa)
	Microstrain($\mu\epsilon$)	Pressure (MPa)	Microstrain($\mu\epsilon$)	Pressure (MPa)	
0	0	0	0	0.0	0
15	1.00E-06	0.3	0	0.0	0.15
30	1.00E-06	0.3	0	0.0	0.15
45	2.00E-06	0.6	1.00E-06	0.3	0.45
60	4.00E-06	1.2	2.00E-06	0.6	0.9
75	5.00E-06	1.5	3.00E-06	0.9	1.2
90	8.00E-06	2.4	6.00E-06	1.8	2.1
105	1.30E-05	3.9	1.10E-05	3.3	3.6
120	1.80E-05	5.4	1.60E-05	4.8	5.1
135	2.50E-05	7.5	2.10E-05	6.3	6.9
150	3.20E-05	9.9	2.80E-05	8.4	9.15
165	4.20E-05	12.6	3.80E-05	11.4	12
180	4.80E-05	14.4	4.60E-05	13.8	14.1
195	5.40E-05	16.2	5.20E-05	16.2	16.2
210	5.90E-05	17.7	5.70E-05	17.7	17.7
225	6.40E-05	19.2	6.10E-05	18.9	19.05
240	6.90E-05	20.7	6.50E-05	20.1	20.4
255	7.20E-05	21.6	7.00E-05	21.6	21.6
270	7.60E-05	22.8	7.30E-05	22.5	22.65
285	7.90E-05	23.7	7.60E-05	23.5	23.6
300	8.40E-05	25.2	8.00E-05	24.7	24.95
315	8.70E-05	26.1	8.30E-05	25.9	26
330	9.00E-05	27	8.60E-05	26.8	26.9
345	9.30E-05	27.9	8.90E-05	27.7	27.8
360	9.60E-05	28.8	9.20E-05	28.9	28.85

Table I-9: Strain Values (Refer to Table 3-3 for specimen specifications)

Time (min)	S41-BET-CaCl ₂ -04a		S41-BET-CaCl ₂ -04b		Average Pressure (MPa)
	Microstrain($\mu\epsilon$)	Pressure (MPa)	Microstrain($\mu\epsilon$)	Pressure (MPa)	
0	0	0	0	0.0	0
15	1.00E-06	0.3	0.00E+00	0.0	0.15
30	1.00E-06	0.3	0.00E+00	0.0	0.15
45	2.00E-06	0.6	1.00E-06	0.3	0.45
60	4.00E-06	1.2	3.00E-06	0.9	1.05
75	5.00E-06	1.5	4.00E-06	1.2	1.35
90	8.00E-06	2.4	7.00E-07	2.1	2.4
105	1.30E-05	3.9	1.20E-05	3.6	3.9
120	1.80E-05	5.4	1.50E-05	4.5	4.65
135	2.50E-05	7.5	2.20E-05	6.6	7.2
150	3.20E-05	9.9	2.80E-05	8.4	9
165	4.20E-05	12.6	3.60E-05	10.8	11.7
180	4.80E-05	14.4	4.50E-05	13.5	13.95
195	5.40E-05	16.2	5.30E-05	15.9	16.35
210	5.90E-05	17.7	5.70E-06	17.1	17.55
225	6.40E-05	19.2	6.30E-05	18.9	19.2
240	6.90E-05	20.7	6.60E-05	19.8	20.25
255	7.20E-05	21.6	7.00E-05	21.0	21.45
270	7.60E-05	22.8	7.30E-05	21.9	22.35
285	7.90E-05	23.7	7.60E-05	22.8	23.25
300	8.40E-05	25.2	7.90E-05	23.8	24.5
315	8.70E-05	26.1	8.30E-05	25.0	25.55
330	9.00E-05	27	8.70E-05	26.2	26.6
345	9.30E-05	27.9	9.00E-05	27.1	27.5
360	9.60E-05	28.8	9.10E-05	27.4	27.8

Table I-10: Strain Values (Refer to Table 3-3 for specimen specifications)

Time (min)	S41-BET-CaCl ₂ -05a		S41-BET-CaCl ₂ -05b		Average Pressure (MPa)
	Microstrain($\mu\epsilon$)	Pressure (MPa)	Microstrain($\mu\epsilon$)	Pressure (MPa)	
0	0	0	0	0	0
15	0.00E+00	0.3	0.00E+00	0	0.15
30	0.00E+00	0.3	0.00E+00	0.3	0.3
45	1.00E-06	0.6	1.00E-06	0.6	0.6
60	2.00E-06	1.2	3.00E-06	1.2	1.2
75	4.00E-06	1.5	7.00E-06	2.4	1.95
90	9.00E-06	2.7	1.20E-05	3.6	3.15
105	1.80E-05	4.2	1.90E-05	5.7	4.95
120	3.00E-05	4.8	2.90E-06	8.7	6.75
135	4.00E-05	7.8	3.90E-05	11.7	9.75
150	5.20E-05	9.6	5.20E-05	15.6	12.6
165	5.90E-05	12.6	6.00E-05	18	15.3
180	6.40E-05	14.4	6.50E-05	19.5	16.95
195	6.90E-05	16.8	7.00E-05	21	18.9
210	7.30E-05	18	7.30E-05	21.9	19.95
225	7.50E-05	19.5	7.50E-05	22.5	21
240	7.80E-05	20.7	7.80E-05	23.1	21.9
255	8.00E-05	21.9	8.00E-05	24	22.95
270	8.20E-05	22.8	8.20E-05	24.6	23.7
285	8.30E-05	23.7	8.30E-05	24.9	24.3
300	8.60E-05	25.2	8.60E-05	25.8	25.5
315	8.80E-05	26.1	8.80E-05	26.4	26.25
330	9.00E-05	27	9.00E-05	27	27
345	9.20E-05	27.9	9.20E-05	27.6	27.75
360	9.40E-05	28.2	9.40E-05	28.2	28.2

Table I-11: Strain Values (Refer to Table 3-4 for specimen specifications)

Time (min)	S41-BET-Ca(HCOO) ₂ -01a		S41-BET-Ca(HCOO) ₂ -01b		Average Pressure (MPa)
	Microstrain($\mu\epsilon$)	Pressure (MPa)	Microstrain($\mu\epsilon$)	Pressure (MPa)	
0	0	0	0	0	0
15	0.00E+00	0	0.00E+00	0	0
30	0.00E+00	0	0.00E+00	0	0
45	1.00E-06	0.3	1.00E-03	0.3	0.3
60	2.00E-06	0.6	2.00E-06	0.6	0.6
75	3.00E-06	0.9	3.00E-06	0.9	0.9
90	6.00E-06	1.8	4.00E-06	1.2	1.5
105	9.00E-06	2.7	6.00E-06	1.8	2.25
120	1.40E-05	4.2	8.00E-06	2.4	3.3
135	2.10E-05	6.3	1.20E-05	4.2	5.25
150	3.00E-05	9	1.70E-05	5.1	7.05
165	3.80E-05	11.4	2.10E-05	6.3	8.85
180	4.50E-05	13.5	2.60E-05	7.8	10.65
195	5.30E-05	15.9	3.00E-05	9	12.45
210	5.90E-05	17.7	3.50E-05	10.5	14.1
225	6.20E-05	18.6	4.00E-05	12	15.3
240	6.60E-05	19.8	4.40E-05	13.2	16.5
255	6.90E-05	20.7	4.80E-05	14.4	17.55
270	7.20E-05	21.6	5.00E-05	15	18.3
285	7.40E-05	22.2	5.20E-05	15.6	18.9
300	7.50E-05	22.5	5.40E-05	16.2	19.35
315	7.60E-05	22.8	5.60E-05	16.8	19.8
330	7.70E-05	23.1	5.70E-05	17.1	20.1
345	7.80E-05	23.4	5.80E-05	17.4	20.4
360	7.90E-05	23.7	5.90E-05	17.7	20.7

Table I-12. Strain Values (Refer to Table 3-4 for specimen specifications)

Time (min)	S41-BET-Ca(HCOO) ₂ -02a		S41-BET-Ca(HCOO) ₂ -02b		Average Pressure (MPa)
	Microstrain(μ ϵ)	Pressure (MPa)	Microstrain(μ ϵ)	Pressure (MPa)	
0	0	0	0	0	0
15	0.00E+00	0	0.00E+00	0	0
30	0.00E+00	0	0.00E+00	0	0
45	0.00E+00	0	0.00E+00	0	0
60	0.00E+00	0	0.00E+00	0	0
75	0.00E+00	0	0.00E+00	0	0
90	0.00E+00	0	1.00E-06	0.3	0.15
105	1.00E-06	0.3	4.00E-06	1.2	0.75
120	3.00E-06	0.9	6.00E-06	1.8	1.35
135	4.00E-06	1.2	1.00E-05	3	2.1
150	6.00E-06	1.8	1.50E-05	4.5	3.15
165	7.00E-06	2.1	2.20E-05	6.6	4.35
180	1.00E-05	3	2.70E-05	8.1	5.55
195	1.10E-05	3.3	3.10E-05	9.3	6.3
210	1.30E-05	3.9	3.50E-05	10.5	7.2
225	1.60E-05	4.8	3.90E-05	11.7	8.25
240	1.80E-05	5.4	4.10E-05	12.3	8.85
255	2.10E-05	6.3	4.40E-05	13.2	9.75
270	2.40E-05	7.2	4.60E-05	13.8	10.5
285	2.60E-05	7.8	4.70E-05	14.1	10.95
300	2.90E-05	8.4	4.80E-05	14.4	11.4
315	3.00E-05	8.7	4.90E-05	14.7	11.7
330	3.10E-05	9	5.00E-05	15	12
345	3.20E-05	9.3	5.10E-05	15.3	12.3
360	3.30E-05	9.6	5.20E-05	15.6	12.6

Table I-13: Strain Values (Refer to Table 3-4 for specimen specifications)

Time (min)	S41-BET-Ca(HCOO) ₂ -03a		S41-BET-Ca(HCOO) ₂ -03b		Average Pressure (MPa)
	Microstrain($\mu\epsilon$)	Pressure (MPa)	Microstrain($\mu\epsilon$)	Pressure (MPa)	
0	0	0	0	0	0
15	0.00E+00	0	0.00E+00	0	0
30	0.00E+00	0	0.00E+00	0	0
45	0.00E+00	0	1.00E-06	0	0
60	0.00E+00	0	3.00E-06	0.9	0.45
75	0.00E+00	0	6.00E-06	1.8	0.9
90	0.00E+00	0	9.00E-06	2.7	1.35
105	2.00E-06	0.6	1.90E-05	5.7	3.15
120	6.00E-06	1.8	2.90E-05	8.7	5.25
135	1.20E-05	3.6	3.90E-05	11.7	7.65
150	1.60E-05	4.8	4.70E-05	14.1	9.45
165	1.80E-05	5.4	5.50E-05	16.5	10.95
180	2.20E-05	6.6	5.90E-05	17.7	12.15
195	2.40E-05	7.2	6.10E-05	18.3	12.75
210	2.80E-05	8.4	6.40E-05	19.2	13.8
225	2.90E-05	8.7	6.60E-05	19.8	14.25
240	3.40E-05	10.2	6.80E-05	20.4	15.3
255	3.50E-05	10.5	7.00E-05	21	15.75
270	3.80E-05	11.4	7.20E-05	21.6	16.5
285	4.00E-05	12	7.30E-05	21.9	16.95
300	4.10E-05	12.3	7.40E-05	22.2	17.25
315	4.30E-05	12.9	7.50E-05	22.5	17.7
330	4.30E-05	12.9	7.60E-05	22.8	17.85
345	4.50E-05	13.5	7.70E-05	23.1	18.3
360	4.60E-05	13.8	7.80E-05	23.4	18.6

Table I-14: Strain Values (Refer to Table 3-4 for specimen specifications)

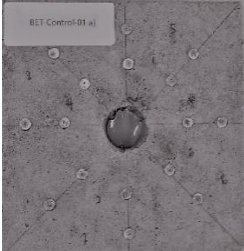
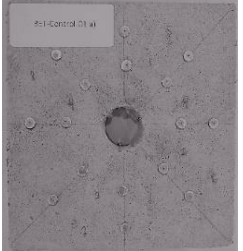
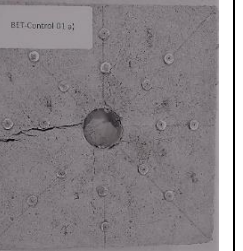
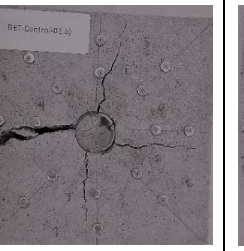
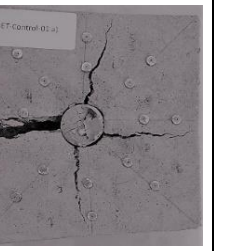
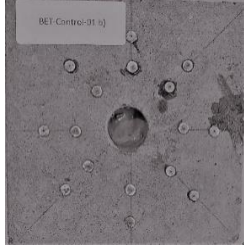
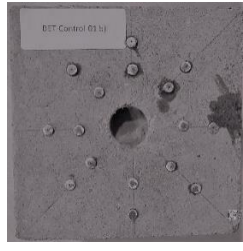
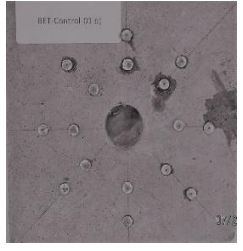
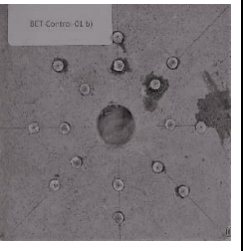
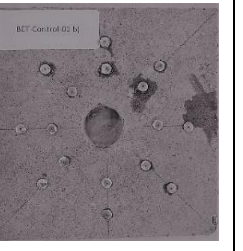
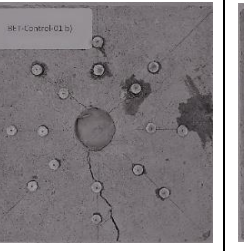
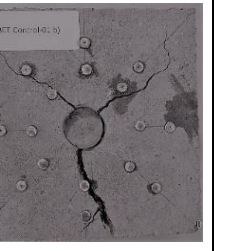
Time (min)	S41-BET-Ca(HCOO) ₂ -04a		S41-BET-Ca(HCOO) ₂ -04b		Average Pressure (MPa)
	Microstrain(μ ϵ)	Pressure (MPa)	Microstrain(μ ϵ)	Pressure (MPa)	
0	0	0	0	0.0	0
15	0.00E+00	0	0.00E+00	0.0	0
30	2.00E-06	0.6	1.00E-06	0.3	0.45
45	4.00E-06	1.2	3.00E-06	0.9	1.05
60	7.00E-06	2.1	6.00E-06	1.8	1.95
75	1.30E-05	3.9	1.20E-05	3.6	3.75
90	2.10E-05	6.3	2.00E-05	6.0	6.15
105	3.00E-05	8.8	2.80E-05	8.4	8.6
120	3.90E-05	11.5	3.80E-05	11.4	11.45
135	4.60E-05	13.5	4.60E-05	13.8	13.65
150	5.00E-05	14.7	5.00E-05	15.0	14.85
165	5.50E-05	16.2	5.40E-05	16.2	16.2
180	5.90E-05	17.4	5.80E-05	17.4	17.4
195	6.30E-05	18.6	6.10E-05	18.3	18.45
210	6.50E-05	19.2	6.40E-05	19.2	19.2
225	6.70E-05	19.8	6.70E-06	20.1	19.95
240	6.90E-05	20.4	6.80E-05	20.4	20.4
255	7.10E-05	21	7.00E-05	21.0	21
270	7.40E-05	21.9	7.20E-05	21.6	21.75
285	7.50E-05	22.2	7.40E-05	22.2	22.2
300	7.70E-05	22.8	7.60E-05	22.8	22.8
315	7.90E-05	23.4	7.80E-05	23.4	23.4
330	8.00E-05	23.7	8.00E-05	24.0	23.85
345	8.10E-05	24	8.10E-05	24.3	24.15
360	8.20E-05	24.3	8.20E-05	24.6	24.45

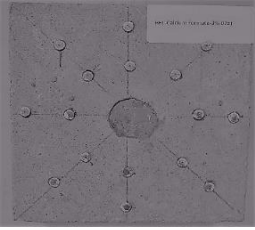
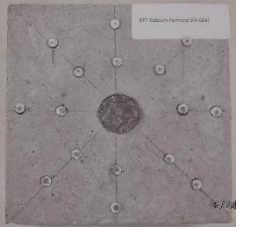
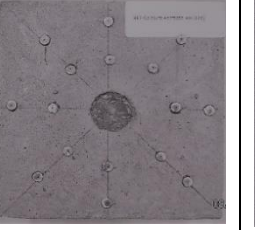
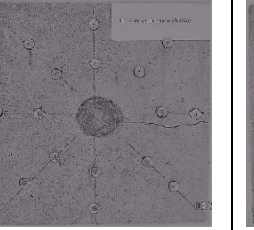
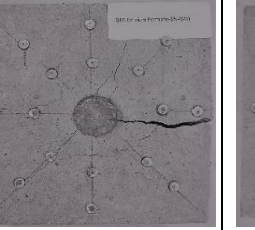
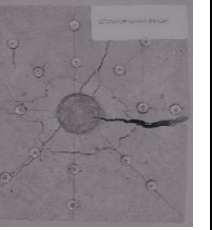
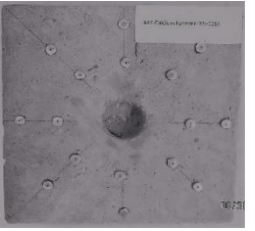
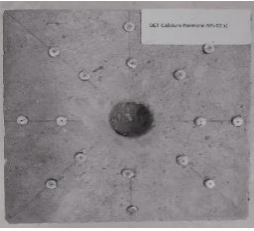
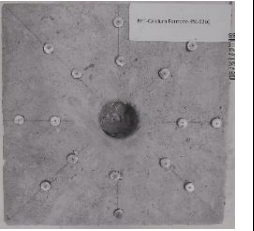
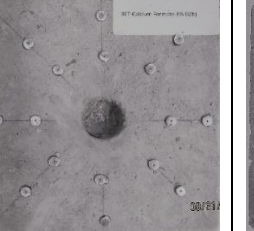
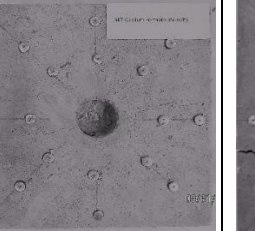
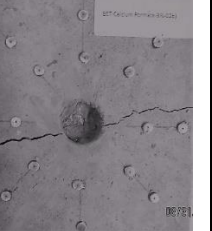
Table I-15: Strain Values (Refer to Table 3-4 for specimen specifications)

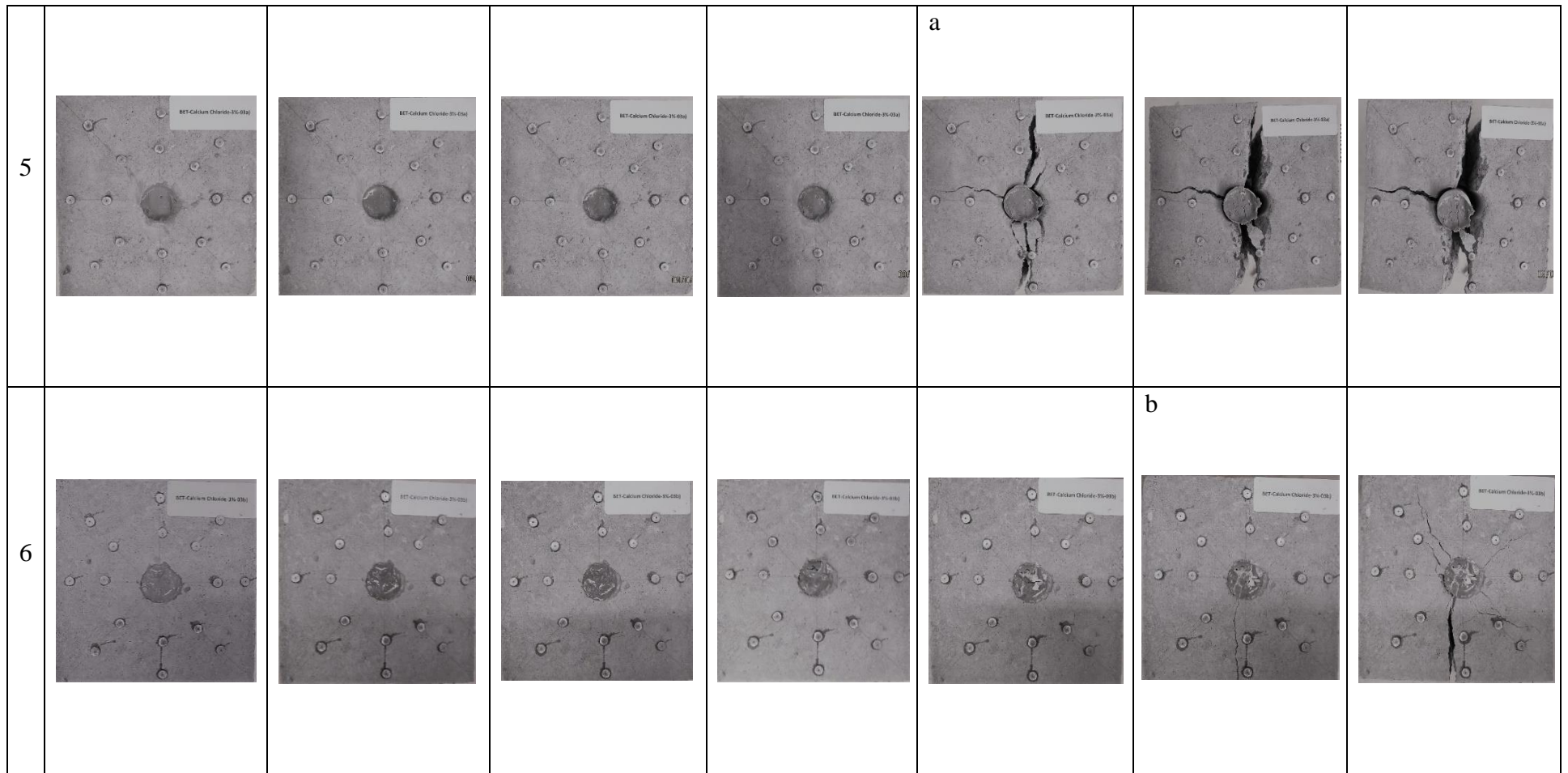
Time (min)	S41-BET-Ca(HCOO) ₂ -05a)		S41-BET-Ca(HCOO) ₂ -045b)		Average Pressure (MPa)
	Microstrain($\mu\epsilon$)	Pressure (MPa)	Microstrain($\mu\epsilon$)	Pressure (MPa)	
0	0	0	0	0.0	0.0
15	0.00E+00	0	0.00E+00	0.0	0.0
30	2.00E-06	0.6	3.00E-06	0.9	0.9
45	6.00E-06	1.8	6.00E-06	1.8	1.8
60	1.00E-05	3	9.00E-06	2.7	2.7
75	1.40E-05	4.2	1.30E-06	3.9	3.9
90	1.90E-05	5.7	1.70E-06	5.1	5.1
105	2.40E-05	7.2	2.10E-05	6.3	6.3
120	2.80E-05	8.4	2.50E-05	7.5	7.5
135	3.30E-05	9.9	3.00E-05	9.0	9.0
150	4.40E-05	13.2	3.80E-05	11.4	11.4
165	4.90E-05	14.7	4.40E-05	13.2	13.2
180	5.30E-05	15.9	4.60E-05	13.8	13.8
195	5.50E-05	16.5	4.80E-05	14.4	14.4
210	5.80E-05	17.4	5.00E-05	15.0	15.0
225	5.90E-05	17.7	5.10E-05	15.3	15.3
240	5.90E-05	17.7	5.20E-05	15.6	15.6
255	5.90E-05	17.7	5.30E-05	15.9	15.9
270	6.00E-05	18	5.40E-05	16.2	16.2
285	6.10E-05	18.3	5.40E-05	16.2	16.2
300	6.10E-05	18.3	5.40E-05	16.2	16.2
315	6.30E-05	18.9	5.50E-05	16.5	16.5
330	6.30E-05	18.9	5.50E-05	16.5	16.5
345	6.40E-05	19.2	5.50E-05	16.5	16.5
360	6.40E-05	19.2	5.50E-05	16.5	16.5

Appendix II: Qualitative Results

Table II-1: Concrete Photos (Refer to Table 3-5 for specimen specifications)

		Time (hours)						
S		0	1	2	3	4	5	6
1								
2								

3							
4							



1 BET-Control-01a

S: Specimen

2 BET-Control-01b

3 Photo at 3.5 hours- BET- CaCl_2 -3%-03a

4 Photo at 4.5 hours- BET- CaCl_2 -3%-03b

5 Photo at 3.5 hours- BET- $\text{Ca}(\text{HCOO})_2$ -3%-02a

6 Photo at 4.5 hours- BET- $\text{Ca}(\text{HCOO})_2$ -3%-02b

^a Photo at 3.5 hours

^b Photo at 4.5 hours